

Winter 2016

# Modeling the Effects of Forecasted Climate Change and Glacier Recession on Late Summer Streamflow in the Upper Nooksack River Basin

Ryan D. Murphy

*Western Washington University*, [murphyhydro@gmail.com](mailto:murphyhydro@gmail.com)

Follow this and additional works at: <https://cedar.wwu.edu/wwuet>

 Part of the [Geology Commons](#)

---

## Recommended Citation

Murphy, Ryan D., "Modeling the Effects of Forecasted Climate Change and Glacier Recession on Late Summer Streamflow in the Upper Nooksack River Basin" (2016). *WWU Graduate School Collection*. 461.  
<https://cedar.wwu.edu/wwuet/461>

This Masters Thesis is brought to you for free and open access by the WWU Graduate and Undergraduate Scholarship at Western CEDAR. It has been accepted for inclusion in WWU Graduate School Collection by an authorized administrator of Western CEDAR. For more information, please contact [westerncedar@wwu.edu](mailto:westerncedar@wwu.edu).

**MODELING THE EFFECTS OF FORECASTED  
CLIMATE CHANGE AND GLACIER RECESSION ON  
LATE SUMMER STREAMFLOW  
IN THE UPPER NOOKSACK RIVER BASIN**

BY  
Ryan D. Murphy

Accepted in Partial Completion  
Of the Requirements for the Degree  
Master of Science  
Geology

Kathleen L. Kitto, Dean of the Graduate School

**ADVISORY COMMITTEE**

Chair, Dr. Robert Mitchell

Dr. Douglas Clark

Dr. Christina Bandaragoda

## **MASTER'S THESIS**

In presenting this thesis in partial fulfillment of the requirements for a master's degree at Western Washington University, I grant to Western Washington University the non-exclusive royalty-free right to archive, reproduce, distribute, and display the thesis in any and all forms, including electronic format, via any digital library mechanisms maintained by WWU.

I represent and warrant this is my original work, and does not infringe or violate any rights of others. I warrant that I have obtained written permissions from the owner of any third party copyrighted material included in these files.

I acknowledge that I retain ownership rights to the copyright of this work, including but not limited to the right to use all or part of this work in future works, such as articles or books.

Library users are granted permission for individual, research and non-commercial reproduction of this work for educational purposes only.

Any further digital posting of this document requires specific permission from the author. Any copying or publication of this thesis for commercial purposes, or for financial gain, is not allowed without my written permission.

Ryan D. Murphy  
February 9, 2016

**MODELING THE EFFECTS OF FORECASTED  
CLIMATE CHANGE AND GLACIER RECESSION ON  
LATE SUMMER STREAMFLOW  
IN THE UPPER NOOKSACK RIVER BASIN**

A Thesis  
Presented to  
The Faculty of  
Western Washington University

In partial Fulfillment  
Of the Requirements for the Degree  
Master of Science

By  
Ryan D. Murphy  
February 2016

## **Abstract**

Like many watersheds in the North Cascades range of Washington State, USA, streamflow in the Nooksack River is strongly influenced by precipitation and snowmelt in the spring and glacial ice melt in the warmer summer months. With a maritime climate and high relief containing approximately 34 km<sup>2</sup> of glacial ice, the streamflow response in the Nooksack River basin is sensitive to increases in temperature. Climate projections from global climate models (GCMs) for the 21<sup>st</sup> Century indicate increases in temperature with variable changes to precipitation. The watershed is a valuable freshwater resource for regional municipalities, industry, and agriculture, and provides critical habitat for endangered salmon species. Thus, understanding the impacts of forecasted climate change is critical for water resources planning purposes. I apply publically available statistically derived 1/16 degree gridded surface climate data along with the Distributed Hydrology Soil Vegetation Model (DHSVM) with newly developed coupled dynamic glacier model to simulate hydrologic and glacial processes through the end of the 21<sup>st</sup> Century.

Simulation results project median winter streamflows to more than double by 2075 due to more precipitation falling as rain rather than snow, and median summer flows to decrease by more than half with a general shift in peak snowmelt derived spring flows toward earlier in the spring. Glaciers are projected to retreat significantly with smaller glaciers disappearing entirely. Ice melt contribution to streamflow is likely to play an important role in sustaining summer baseflows in the Nooksack River. Glacier melt derived streamflow is projected to increase throughout the first half of the 21<sup>st</sup> century and decrease in the latter half after glacier ice volume decreases substantially.

## **Acknowledgements**

Funding for this project was provided by the Nooksack Indian Tribe and the geology department at Western Washington University. I gratefully acknowledge the University of Colorado and the University of Idaho for the publically available meteorological and climatological datasets as well as the University of Washington for allowing me to use their hydrological model in this study. I am grateful for the enthusiastic support of the WWU geology department and my thesis committee. I would like to thank Bob Mitchell, my advisor and thesis committee chair, for all of his help and support throughout the entire graduate school process. I would also like to thank Christina Bandaragoda for all of her assistance with the modeling efforts and for providing such helpful feedback. Thank you to Doug Clark for valuable feedback, particularly with regard to the glacier component of this project. I would like to thank Oliver Grah of the Nooksack Indian Tribe for his oversight and support during this project. I extend a further thank you to researchers at University of Washington including Erkan Istanbuluoglu who provided access to computational resources and his research group; Chris Frans who played an integral part in the development and implementation of the model used throughout this project, and helped with much of the data processing for the meteorological inputs; and Matt Stumbaugh who provided assistance with climatological resources.

## Table of Contents

<b>Abstract</b> .....	iv
<b>Acknowledgements</b> .....	v
<b>List of Tables</b> .....	vii
<b>List of Figures</b> .....	viii
<b>1.0 Introduction</b> .....	1
<b>2.0 Methods</b> .....	5
2.1 <i>Model Setup</i> .....	5
2.2 <i>Calibration and Validation</i> .....	6
2.2.1 <i>Streamflow and Snow Water Equivalent (SWE) Calibration</i> .....	6
2.2.2 <i>Dynamic Glacier Model Setup and Calibration</i> .....	8
2.3 <i>Future Hydrologic Modeling Simulations and Predictions</i> .....	10
<b>3.0 Results</b> .....	11
3.1 <i>Model Calibration</i> .....	11
3.1.1 <i>Snow Water Equivalent</i> .....	13
3.1.2 <i>Historic Glacier Extent</i> .....	13
3.1.3 <i>Streamflow Calibration</i> .....	15
3.2 <i>Historic Glacier Melt</i> .....	16
3.3 <i>Hydrologic Modeling throughout the 21<sup>st</sup> Century</i> .....	17
3.3.1 <i>Snow Water Equivalent</i> .....	17
3.3.2 <i>Glacier Recession and Ice-melt Derived Streamflow</i> .....	18
3.3.3. <i>Streamflow</i> .....	19
<b>4.0 Discussion</b> .....	22
<b>5.0 Conclusion</b> .....	30
<b>6.0 References</b> .....	32
<b>7.0 Tables</b> .....	39
<b>8.0 Figures</b> .....	48
<b>9.0 Appendix A. DHSVM Setup</b> .....	68
<b>10.0 Appendix B. Glacier Model Setup</b> .....	84
<b>11.0 Appendix C. MACA Downscaling Methodology</b> .....	93
<b>12.0 Appendix D. Collaboration and Deliverables to Funding Agencies</b> .....	95

## List of Tables

<b>Table 1.</b> List of GCMs used for future scenario simulations in the Nooksack River basin....	39
<b>Table 2.</b> Forecasted changes (°C) in monthly temperatures.....	40
<b>Table 3.</b> Final calibrated temperature lapse rates used in modeling. ....	41
<b>Table 4.</b> Calibrated DHSVM constants and parameters. ....	42
<b>Table 5.</b> Glacier area and volume errors for the upper Nooksack River Basin.....	43
<b>Table 6.</b> Streamflow calibration statistics. ....	44
<b>Table 7.</b> Modeled changes in future glacier melt magnitude. ....	45
<b>Table 8.</b> Percent of total projected streamflow derived from glacier melt.....	46
<b>Table 9.</b> Projected steamflow magnitude changes in the Nooksack River basin. ....	47



## List of Figures

<b>Figure 1.</b> Nooksack River basin study area map.....	48
<b>Figure 2.</b> Elevation bands for the upper Nooksack River Basin. ....	49
<b>Figure 3.</b> Dynamics ice model processes. ....	50
<b>Figure 4.</b> Meteorological forcing locations throughout the Nooksack River basin. ....	51
<b>Figure 5.</b> Boxplots comparing median monthly Livneh meteorological grid temperatures to observed SNOTEL site temperatures before and after bias correction.....	52
<b>Figure 6.</b> Modeled versus observed daily snow water equivalent (SWE) at three Nooksack River basin SNOTEL stations for water years 2003-2010. ....	53
<b>Figure 7.</b> Modeled versus observed glacier ice extent for the Middle Fork basin for years 1950 and 2009.....	54
<b>Figure 8.</b> Modeled versus observed glacier ice extent for the North Fork basin for years 1950 and 2009.....	55
<b>Figure 9.</b> Simulated and observed annual glacier mass balance for the Sholes Glacier. ....	56
<b>Figure 10.</b> Hydrograph of observed versus calibrated modeled daily streamflow. ....	57
<b>Figure 11.</b> Hydrograph of observed versus calibrated modeled monthly streamflow. ....	58
<b>Figure 12.</b> Modeled versus observed cumulative streamflow over a 10-year calibration/validation period. ....	59
<b>Figure 13.</b> Modeled historic glacier ice melt. ....	60
<b>Figure 14.</b> Modeled future basin SWE for the North, Middle, and South Fork basins. ....	61
<b>Figure 15.</b> Projected glacier change throughout the 21st Century. ....	62
<b>Figure 16.</b> Projected glacier ice melt throughout the 21st Century. ....	63
<b>Figure 17.</b> Modeled future daily median streamflow for the North, Middle, and South Fork basins.....	64
<b>Figure 18.</b> Modeled future daily median streamflow for the North Cedarville Nooksack River gauge location. ....	65
<b>Figure 19.</b> Comparison of modeled historical Middle Fork glacier area changes to Pacific Decadal Oscillation and El Nino Southern Oscillation indexes. ....	66
<b>Figure 20.</b> Modeled future median daily SWE at the SNOTEL gauge locations. ....	67

## 1.0 Introduction

The Nooksack River drains an approximately 2000 km<sup>2</sup> watershed in the North Cascade Mountains in Washington State, USA and serves as a valuable fresh-water resource for commercial, municipal, industrial, irrigation, and domestic uses as well as for fish habitat (Figure 1). The headwaters of the Nooksack River are in high elevation regions near the flanks of Mt. Baker that receive significant winter snowfall and contain a high concentration of glaciers (about 34 km<sup>2</sup>). Historically, streamflow in the Nooksack River basin has been regulated by fall and winter rainfall, and the timing of spring snowmelt and late summer glacier melt. Because of its importance as a resource, water managers and stakeholders have grown concerned over the effects that climate variability and change might have on the region's snowpack and glacier recession and hence, the timing, magnitude, and quality of streamflow in the Nooksack River.

The Nooksack River basin is a transient rain-snow basin due to the maritime climate of the Pacific Northwest (PNW), making it susceptible to impacts from climate change as snowpack is reduced with warming temperatures (Elsner et al., 2010; Mantua et al., 2010; Mauger et al., 2015). The upper sub-basins of the Nooksack River, and the focus of this study, include the North, Middle, and South forks. Each of the three sub-basins differs in relief and the amount of high versus low elevation area, which has a considerable effect on hydrology (Figure 2). In the North and Middle forks, much of the spring and early summer flows are supplied by snowmelt, whereas significant portions of late summer flows are supplied by glacier melt (Bach, 2002; Dickerson-Lange and Mitchell, 2013; Grah and Beaulieu, 2013). The lower elevation South Fork basin, with no glaciated area, is snowmelt

and rain dominated. Nooksack River annual discharge averages approximately 110 cubic meters per second (cms) but can reach as high as 1600 cms during floods (USGS, 2013). Streamflow typically falls below 30 cms in the late summer months as the snowpack and precipitation inputs diminish. During these warm late summer months, the contribution of glacier ice melt becomes increasingly important.

Topographic relief in the Nooksack basin rises from sea level to over 3000 m in the Cascade foothills and mountains (peak elevation 3286 m at Mount Baker), which has a large influence on weather patterns and precipitation distributions due to orographic effects (Dickerson-Lange and Mitchell, 2013). Additionally, the annual variability in temperature and precipitation is strongly influenced by climate events such as the Pacific Decadal Oscillation and El Nino Southern Oscillations, making the PNW a complex and unique meteorological system (Mantua and Hare, 2002; Deser et al., 2012). Observed mean annual PNW temperatures have increased 0.6°-0.8°C since the early 20<sup>th</sup> Century (Abatzoglou et al., 2014). Precipitation for the same time period has also increased overall, but the trends are small when compared to natural variability (Mote et al., 2014). However, assessing local historic changes specific to the Nooksack River basin is difficult because meteorological coverage is sparse, with the nearest long-term weather station located outside of the basin in Clearbrook, WA (Figure 1).

Climate projections for the PNW suggest increased annual temperatures and seasonal changes in precipitation with an increase during the winter months and a decrease during the summer months (Elsner, et al., 2010; Hamlet et al., 2010a; Mote and Salathe Jr, 2010; Vano et al., 2010; Abatzoglou et al., 2014; Tohver et al., 2014). Average annual temperatures are forecast to increase 3.3-9.7°C by 2070 to 2099 compared to the period 1970-1999 (Mote et

al., 2014). Previous Nooksack River basin modeling has predicted a decrease in mean monthly snow water equivalent (SWE) of 33% to 45% at higher elevations, an increase in winter streamflows of 34% to 60%, and a projected decrease in summer streamflow of 22% to 35% by 2050 (Dickerson-Lange and Mitchell, 2013). These findings are consistent with other studies throughout the PNW (e.g., Mote et al., 2005; Vano et al., 2010; Hamlet et al., 2013; Tohver et al., 2014) and suggest that the region could experience the decline and eventual disappearance of a springtime snowmelt peak.

With 12 significant glaciers, Mount Baker has one of the largest networks of glaciers in the North Cascades (Pelto and Brown, 2012). Glacier mass balance studies in the Nooksack River Basin and throughout the PNW have shown significant historical retreat of glaciers and retreat is expected to continue as the climate warms (Fountain et al., 1997; Bidlake et al., 2002; Palmer, 2007; Moore et al., 2009; Riedel and Larrabee, 2011; Pelto and Brown, 2012; Stocker et al., 2013). With potentially less snowpack and warmer temperatures, continued glacial recession will likely have adverse long-term effects on the late summer stream flows in the Nooksack River (Donnell, 2007; Grah and Beaulieu, 2013).

In this study, I use the Distributed Hydrology Soil Vegetation Model (DHSVM; Wigmosta et al., 1994) along with a newly coupled dynamic glacier model (Clarke et al., 2015) to assess the impacts of climate change and glacier recession on streamflow within the Nooksack River Basin. I emphasize late summer months, when precipitation inputs are minimal and glacier melt is a significant contributor to streamflow. The DHSVM allows for a high resolution physically based representation of the watershed and takes into account spatial heterogeneity. This grid based distributed hydrology model has been used extensively in the PNW (e.g., Alila and Beckers, 2001; Donnell, 2007; Cuo et al., 2009; Dickerson-

Lange and Mitchell, 2013). The glacier dynamics component of the model simulates glacier flow, melt, and ice volume changes and incorporates them into watershed processes by using mass and energy fluxes between the atmosphere and land surface estimated by the DHSVM at each model cell (Figure 3; Naz et al., 2014; Clarke et al., 2015). In earlier work, ice was treated as static and melted in situ; whereas the dynamic glacier model expands our understanding of glacier contributions to watershed hydrology by simulating changes in glacier area and ice flow downhill using topographic gradients (Figure 2).

Because of the lack of historical weather stations in the Nooksack River basin, I employ a publically available statistically extrapolated historical meteorological 1/16 degree grid (Livneh et al., 2013, 2015) to calibrate the model along with observed streamflow, snow-water equivalents, and observed glacier areal extents. I project future Nooksack basin processes with the calibrated DHSVM forced with publically available 1/16 degree statistically downscaled future climate datasets from global climate models (GCMs) of the Coupled Model Intercomparison Project Phase 5 (CMIP5) that have been downscaled by the Multivariate Adapted Constructed Analogs method (MACA; Abatzoglou and Brown, 2012) using the Livneh historical grid as a training dataset. The gridded meteorological inputs allow control over the local variation and weather patterns in the Nooksack River basin and more efficient downscaling processing, which typically is cumbersome and time-consuming when downscaling to watershed-scale resolution (e.g., Hamlet et al., 2010b). I simulate snowpack, glacial recession, and streamflow evolution for the North, Middle, and South forks of the Nooksack River basin from 1950 to 2099 and project future trends at 30-year climate intervals surrounding the years 2025, 2050, and 2075.

## 2.0 Methods

### 2.1 Model Setup

The DHSVM is a physically based, spatially distributed hydrology model that requires explicit physical characteristics of the watershed, including topography, land cover, soil type, soil thickness, and a streamflow network. The digital inputs were acquired from publically available sources (e.g., USGS, NLCD, STATSGO, and GLIMS) and processed in ArcGIS into 50 m grids (Appendix A). Separate watershed boundaries and digital datasets were created for each sub-basin (North, Middle, and South forks of the Nooksack River basin) to better capture the local variability.

Meteorological inputs for the DHSVM include temperature ( $^{\circ}\text{C}$ ), relative humidity (%), precipitation (m), wind speed (m/s), and incoming shortwave and longwave radiation ( $\text{W}/\text{m}^2$ ). Because of the lack of consistent historical meteorological observations in the Nooksack River basin, I chose to force the model during calibration with a publically available statistically derived meteorological grid (Livneh et al., 2013, 2015). The Livneh grid utilizes precipitation and minimum and maximum temperature data collected from 1915-2011 throughout the contiguous United States from approximately 20,000 National Climate Data Center (NCDC) cooperative observer weather stations and statistically interpolates those data to form a continuous  $1/16$  degree ( $\sim 6$  km) resolution grid. Monthly precipitation estimates from the Parameter-Elevation Regressions on Independent Slopes Model (PRISM; Daly et al., 1994) are incorporated into the Livneh grid to further account for spatial variability. Only stations with a minimum of 20 years of valid data are used in the interpolation. Center points of each Livneh grid cell were used as meteorological input

locations for the DHSVM (Figure 4). The daily Livneh meteorological gridded time series were disaggregated into 3-hour timesteps using the variable infiltration capacity model (VIC; Liang et al., 1994) which employs the MTCLIM scheme for downscaling meteorological forcings (Bohn et al., 2013) to better capture sub-daily fluctuations in radiation inputs.

The DHSVM has flexibility in how the user defines lapse rates for both temperature and precipitation. Rather than using a single temperature lapse rate for the entire basin, I adjusted the lapse rate on a monthly basis. To better capture the influence of complex topographic variability on precipitation, the DHSVM was set up to calculate precipitation lapse rates based on elevation and the magnitudes of precipitation represented by monthly PRISM 30-year precipitation normal grids (1981-2010; PRISM Climate Group, 2014). The manipulation of these precipitation and temperature lapse rates throughout the basin served as additional calibration techniques to improve the model's accuracy.

## *2.2 Calibration and Validation*

### *2.2.1 Streamflow and Snow Water Equivalent (SWE) Calibration*

Calibration and validation of the model included the comparison of modeled streamflow output to historic streamflow observations from USGS gauging stations on the North Fork (12205000), Middle Fork (12208000), South Fork (12209000), and one on the main stem below the confluence of three forks at North Cedarville (12210700; Figure 1). The USGS stream gauge in the Middle Fork is below the City of Bellingham's diversion dam, which periodically diverts water from the Middle Fork to Lake Whatcom via a pipeline (Tracy, 2001). Daily volume estimates of the diverted water (personal communication, Joanie Greenberg) were added to the observed USGS discharge for the calibration period. Modeled

SWE was compared to observed SWE at the Wells Creek (1228 m elevation), Middle Fork Nooksack (1515 m elevation), and Elbow Lake (927 m elevation) NRCS SNOTEL sites in the North, Middle, and South fork basins, respectively (Figure 1). However, since the SNOTEL site measurements only capture meteorology in one small location and are not representative of the entire watershed, SWE measurements were used only as a guide and not as a primary calibration element. As such, I examine SWE results as a basin-wide average. Statistical techniques such as the Nash-Sutcliffe model efficiency coefficient (NSE: Nash and Sutcliffe, 1970) as well as graphical comparisons were used to assess the goodness of fit between the simulated output and the historical observations. When possible, 10-year calibration/validation periods were used to ensure that the model was properly reproducing basin characteristics and its responses to typical meteorological changes, eliminating bias toward anomalous water years. North and Middle fork streamflow was calibrated for water years 2001-2005 and validated for 2006-2010 while South Fork flows were calibrated for water years 1999-2003 and validated for 2004-2008 due to a change in gauging location after water year 2008. Streamflow at the North Cedarville gauge was simulated by adding of the North, Middle, and South fork flow outputs and was calibrated for the water years 2006-2010 (water year 2006 was the first year of consistent record for this gauge). If calibration or validation results from the model were not accurately reproducing the observed data, sensitive parameters that reflected basin characteristics were modified. These sensitive parameters included but were not limited to temperature and precipitation lapse rates, snow and rain temperature thresholds, and soil porosity and lateral conductivity, consistent with other studies of DHSVM parameter sensitivity (Du et al., 2013; Kelleher et al., 2015).



### *2.2.2 Dynamic Glacier Model Setup and Calibration*

The dynamic glacier model requires four main input parameters: 1) glacier domain or the areal extent of ice coverage (including the extent of contiguous ice bodies on both sides of the watershed boundary), 2) bed topography beneath the ice, 3), basin-wide annual mass balance, and 4) ice surface topography (Naz et al., 2014; Appendix B). Domain mask area includes non-glaciated basin area in order to allow for glacier area changes and flow outside of the historically observed ice extent if needed. Glaciers that are adjacent to the basin and glaciers that are at least partially inside of the basin are included, meaning that in some regions the glacier domain extends beyond the area of the watershed mask. This is important as watershed boundaries do not always correspond exactly to glacier flowshed boundaries. Historic observed glacier coverage was obtained through Landsat imagery, GIS land cover layers, and historical USGS topographic maps.

The DEM was assumed to be an adequate representation of basal topography and was thus used as the bed topography elevation input to the dynamic glacier model. Other more complex methods for estimating bed topography have been used in previous studies and require multiple inputs such as thinning rates and distributed mass balances (e.g., Clarke et al., 2013). However, for areas with relatively thin ice coverage (less than 300 m), the effects of using a more complex bed topography compared to using a DEM are minimal, yielding only slight differences in glacier volume and no difference in glacier area (Naz et al., 2014).

The glacier model produces a basin-wide ice mass balance grid which shows the net accumulation or ablation for each 50 m cell, including for non-glaciated areas, for the simulation period (10 years for glacier calibration purposes). A calibrated mass balance field is needed to estimate ice thickness and produce the surface topography field. To calibrate the

mass balance, the glacier model was run under a static mode (i.e., no simulated glacier flow) with a simulated 1000 m thick ice layer over the entire basin. The static and uniform 1000 m ice layer allowed for the estimation of ice change magnitudes for each grid cell throughout the entire basin, thus producing a continuous mass balance grid. A 1000 year spinup period using the mass balance grid was then run to achieve glacier equilibrium conditions. The result of the spinup run was an estimated ice coverage and ice thickness layer based on the mass balance from the static run. If ice coverage did not adequately match historical ice extent observations, model parameters such as temperature lapse rates or snow/rain temperature thresholds were adjusted and the mass balance was recreated using the static model once more, and a new spinup simulation was run. Model parameters were iteratively adjusted until a mass balance that produced reasonable 1950s-scale ice coverage was created. The ice layer was then added to the basin DEM to produce the ice surface topography input needed for the dynamic glacier model.

In this initial application of the coupled hydrology-glacier model in the Nooksack River basin, I calibrated the glacier model based primarily on historical ice extents from 1950 (Raup et al., 2007) and 2009. A 20-year annual mass balance record from the Sholes Glacier in the North Fork basin was compared to modeled mass balance outputs from the Sholes. However, given the short period of observational record and the relatively long model runs, as well as the large spatial distribution of glaciers within the basin, the Sholes mass balance was not used as a primary calibration parameter but was used simply to ensure reasonably realistic mass balance results during calibration runs.

Once the glacier inputs had been produced, the DHSVM-glacier model was run and ice changes were incorporated into the watershed hydrology processes. The coupled model

was run for a 60-yr calibration period from 1950-2010 and simulated glacier changes were compared to observed areal changes. Because of the coupled nature of the model, streamflow and SWE calibration was carried out in concert with glacier calibration. To obtain historic glacier melt contribution to streamflow, the DHSVM was run twice from 1950-2010; once under dynamic glacier conditions and once with all glaciation turned off (i.e., all ice was removed from the basin). The difference in the resulting streamflow between the two runs was then assumed to be the glacier melt contribution to streamflow. With glaciation turned off, the DHSVM assumes that there is no permanent ice anywhere within the watershed. Glaciated areas are replaced by soil type found in the soil coverage input file for that area (usually bedrock for higher elevation areas) and all other parameters remain the same as in the dynamic model run.

### *2.3 Future Hydrologic Modeling Simulations and Predictions*

To capture the variability in possible future climate scenarios, I used the MACA downscaled results from 10 GCMs under two Representative Concentration Pathway (RCP) scenarios (RCP4.5 and RCP8.5; Table 1). Rupp et al. (2013) determined that these 10 GCMs in particular are most suitable for climate prediction in the PNW. The 10 MACA downscaled GCMs indicate an annual temperature increase by 2075 ranging from approximately 2 to 3.4 degrees C for the RCP 4.5 scenario and 2.9 to 4.7 degrees C for the RCP 8.5 scenario in the upper Nooksack Basin (Table 2). MACA climate data are downscaled using the Livneh et al. (2013) observational data as the training dataset (Appendix C). As such, the same Livneh grid point locations (Figure 4) serve as MACA climate forcings locations and the same lapse rates and elevation corrections used in the calibration process for the Livneh grids are applied

to the MACA data. Using the Livneh and MACA datasets ensures that climate corrections to historical periods can be applied to maintain consistency in future prediction.

I simulate hydrology and glacier dynamics in the Nooksack River basin with the calibrated DHSVM model for water years 2010-2099 using 20 MACA climate scenarios as meteorological inputs. For the glaciated Middle and North Fork basins, simulations were performed with and without glaciers for each MACA scenario to estimate the ice melt contribution to streamflow. To project long term trends in hydrologic processes within the basin, I examine 30-year median flows (including glacier melt) and median SWE centered on 2025, 2050, and 2075. Additionally, ice coverage maps were produced at 10-year intervals in order to track glacier changes through time.

### **3.0 Results**

#### *3.1 Model Calibration*

Because of biases to input data, simultaneous calibration of the DHSVM to streamflow, SWE, and glacier extent proved unrealistic without additional tuning and bias corrections. I started the calibration process by correcting the statistically derived, historical Livneh data for observed biases. A cold bias was noted in the Livneh grid when compared to modern PRISM normals (1981-2010). The Livneh grid implemented in this study was developed using a constant temperature lapse rate of minus 6.5 degrees C per km (Livneh et al., 2013). At high elevations in particular, the maximum and minimum monthly Livneh temperatures were significantly lower than those from the PRISM climatology. The cold bias was also apparent when comparing Livneh monthly median temperatures to those at the SNOTEL sites within the appropriate Livneh cells in the upper Nooksack River basin (Figure

5). A delta method correction (e.g., Sperna Weiland et al., 2010; Watanabe et al., 2012) was applied to all Livneh cells within each of the three sub-basins to adjust to the PRISM temperature normals (Chris Frans, personal communication). After the correction, a comparison with SNOTEL observational temperature data from each of the three sub-basins indicated a more realistic representation of monthly temperatures (Figure 5).

A precipitation bias was also identified in the Livneh data; in some locations, lower elevation cells showed a considerably higher precipitation than those at higher elevations. A correction was applied where necessary by incorporating a monthly precipitation correction factor derived using observed precipitation and elevation relationships between the nearby Abbotsford weather station and the basin SNOTEL sites (Figure 1). The precipitation lapse rate between the stations was used to produce a monthly correction scaling factor to adjust Livneh precipitation magnitudes in the South Fork and North Fork basins. In the Middle Fork basin, precipitation correction was not required and uncorrected Livneh data was used for precipitation inputs.

The bias corrections markedly improved the calibration of the model. Additional calibration required the adjustment of the DHSVM parameters, specifically the rain/snow threshold temperatures and the temperature-lapse rate values. Each of the three basins was unique and required different parameter magnitudes and modifications to balance the observed streamflow, SWE, and glacier coverage. The glaciated Middle and North fork basins were more problematic because the glacier coverage was more sensitive to temperature lapse rates than hydrology was. Thus, final calibration required the use of different temperature lapse rates in each basin (Table 3). Peak flows and baseflows were

moderately influenced by soil properties such as thickness, porosity, and lateral hydraulic conductivity. Such model parameters were altered as needed and differed by basin (Table 4).

### *3.1.1 Snow Water Equivalent*

Calibrating SWE to specific SNOTEL observations had mixed results, partly because a SNOTEL site represents a single grid cell in the DHSVM and may not reflect basin-wide snow hydrology. SNOTEL sites have also been shown to produce biased temperature readings in some locations, potentially affecting calibration accuracy (e.g., Oyler et al., 2015). The model reasonably predicted the SWE at the Wells Creek SNOTEL site in the North Fork basin, with most water years matching closely to the observed dataset (Figure 6). The model under-simulated SWE during most years at the SNOTEL sites in the Middle Fork and South Fork basins (Figure 6). While annual magnitudes of SWE were not replicated satisfactorily in the model runs, the temporal distribution of SWE matched the data closely for most water years. Note, however, that the model's success in predicting streamflow, particularly spring and early summer flows, in part validates its ability to capture basin-wide snow accumulation and melt. In the results and discussion, I present SWE changes as a basin-wide average.

### *3.1.2 Historic Glacier Extent*

Initial ice extent (1950) compared well to historical estimates of glacier coverage in both the Middle and North fork basins, with a 14% over-estimation of total modeled ice extent for the North and Middle forks combined (Figures 7 and 8; Table 5). In the Middle Fork, comparisons between observed 2009 ice extent and simulated ice extent after a simulation period from 1950 to 2009 show that the model is producing reasonable ice extent

changes through time, comparable to observed estimates (Figure 7). Simulated 2009 ice extent was greater than the estimated observed extent and contained thin ice coverage in the steep cliff bands of the mountains. The excess thin ice is attributed at least in part to the lack of an avalanching component in the model and the thin ice was left in place to maintain the hydrologic mass balance of the basin.

The North Fork basin, with far more glaciated area than the Middle Fork, had more error associated with both the initial 1950 and 2009 ice coverages (Figure 8). Initial 1950s ice coverage in the higher relief regions of Mount Baker was difficult to reproduce and the final spinup results over-estimated ice extent in the lower tongues of the Roosevelt and Mazama glaciers. During model runs from 1950-2009, over-simulation of ice in the lower reaches of these glacier valleys occurred as well, resulting in too large of a glaciated area. This problem was not able to be corrected without negatively impacting the ice extent in adjacent glaciated areas and was the most pronounced on Mount Baker. Modeled annual mass balance from the Sholes glacier on Mount Baker did, however, compare well with the 20-year observational record (Figure 9; Pelto and Brown, 2012). Glacier area changes on Mount Shuksan more closely matched observational ice coverage changes through 2009. Like in the Middle Fork basin, small patches of excess thin ice were simulated in places where no glaciers exist. The 2009 ice extent error was approximately 46% for the North and Middle fork basins combined (Table 5). While the area was over-estimated during historical runs, the majority of modeled ice volume still remained within the target observed extent (Table 5) indicating that the majority of modeled ice was still being simulated where it should be.

### *3.1.3 Streamflow Calibration*

Calibrated streamflow compared well to all four USGS stream gauges within the upper Nooksack basin. Daily late summer flows were captured well but peak storm flows throughout each water year were generally under-simulated in each of the three basins (Figure 10). Calibration of monthly peak flows varied and the model over-simulated peak magnitudes during some water years and under-simulated during others (Figure 11). The modeled streamflow had Nash-Sutcliffe efficiency scores of greater than 0.5 for daily flows and greater than 0.7 for monthly flows for 10-year calibration/validation periods at their respective USGS gauges (Table 6). Cumulative streamflow calibration success also differed between basins and was heavily influenced by large individual storm events. The model under-simulated cumulative stream discharge by less than 6% at the Middle Fork USGS gauge location and less than 5% in the North Fork basin but over-simulated cumulative stream discharge by less than 4% for the South Fork basin at the end of their respective 10-yr calibration/validation periods (Figure 12 and Table 6). Mean monthly stream discharge error was less than 4% for the North Fork, less than 5% for the Middle Fork, and less than 2% for the South Fork (Table 6).

At the North Cedarville gauge where flows from the three sub-basins are combined, daily and monthly streamflows were simulated with Nash-Sutcliffe efficiency scores of 0.53 and 0.71, respectively (Figures 10 and 11 and Table 6). Peak flows were generally under-simulated while baseflows and recession curves matched well, with the exception of water year 2009 when simulated January and February baseflows were too low. A positive cumulative stream discharge error at the gauge location of 3.6% at the end of the calibration period was obtained, indicating an over-simulation of streamflow volume after the 5-year



period (Figure 12). Mean monthly stream discharge error was less than 5% at the North Cedarville gauge location (Table 6).

### *3.2 Historic Glacier Melt*

Modeled historic glacier melt volumes for the North and Middle fork basins appreciably support streamflow in the late summer months, particularly August and September. The timing of the glacier melt season differs by basin, extending from early May through the end of October for the North Fork and from mid-June through the end of October for the Middle Fork. During many water years, daily late summer glacier melt contribution to streamflow regularly exceeds 1.5 cms in the Middle Fork and 5 cms in the North Fork (Figure 13). Modeled median monthly historical glacier melt reaches approximately 15% of total streamflow for both the North and Middle Fork basins and just above 10% at the North Cedarville location during August and September, although there is large variation throughout the historical simulation period (Figure 13). Monthly median glacier melts can make up as much as 50% of total flows in the Middle Fork and 40% in the North Fork basins. Third quartile melts are approximately 30% of total flow in the Middle Fork and 25% of total flow in the North Fork for the late summer months. It should be noted however, that because peak glacier melt contribution to streamflow occurs at the end of August and beginning of September, monthly averages may dampen the analysis of the total melt flows on daily and weekly timescales.

### *3.3 Hydrologic Modeling throughout the 21<sup>st</sup> Century*

#### *3.3.1 Snow Water Equivalent*

Model results for all three sub-basins forecast a significant basin-wide snowpack SWE decrease in both the RCP 4.5 and 8.5 forcing scenarios as warming occurs (Figure 14). Through 2050, both RCP scenarios show similar SWE magnitudes but toward the second half of the century the RCP 8.5 scenarios result in a significantly lower daily basin-wide average SWE than the RCP 4.5 scenarios. By 2075, Middle Fork ensemble median SWE magnitudes peak at approximately 0.4 m and 0.25 m for RCP 4.5 and 8.5 respectively, significantly lower than the historical modeled median (1950-2010) of approximately 0.8 m. South Fork ensemble median SWE magnitudes at 2075 peak at approximately 0.15 m and just over 0.05 m for RCP 4.5 and 8.5 respectively, also a significant decrease compared to the historical modeled median (1950-2010) of just over 0.4 m. In the North Fork basin, a decrease is projected from the historical modeled peak magnitude of approximately 0.75 m to just under 0.4 m and just over 0.2 m for RCP 4.5 and 8.5 respectively.

In addition to SWE magnitude changes, deviations from the historic timing of snowpack presence and SWE peaks are expected throughout the 21<sup>st</sup> Century in parts of the Nooksack River basin (Figure 14). The timing of peak SWE in the South Fork basin is forecasted to change under both RCP ensembles by the year 2075, when peak magnitudes are expected to shift to the month of February rather than March. The development of a snowpack in the South Fork basin is projected to occur later in the fall and disappear earlier in the spring, leaving the basin snow-free for longer time periods. In the North and Middle Fork basins, however, average elevation is higher and the timing of peak SWE is not expected to change as much. Even under the most aggressive scenarios, some snowpack is

expected to remain in the Middle Fork basin throughout the whole of a normal water year in 2075.

### *3.3.2 Glacier Recession and Ice-melt Derived Streamflow*

Under all future scenarios, large glaciers are modeled to decrease significantly in areal extent and ice thickness while smaller glaciers are likely to disappear completely. Glacier area changes throughout the 21<sup>st</sup> Century are forecasted to be similar in magnitude and timing under both RCP scenarios until the latter half of the century when the two scenarios begin to diverge from one another (Figure 15). Glacier area is forecast to decline steadily under RCP 8.5 throughout the century but the rate of decline lessens near the year 2050 for the RCP 4.5 ensemble. Additionally, a greater variation exists among GCMs under the RCP 4.5 scenario for both the Middle and North Fork basins. Modeled Middle Fork median ensemble ice extent for RCP 8.5 indicates a decrease 87% in the Middle Fork basin by the end of the century. RCP 4.5 is less severe but modeling still forecasts a significant decrease in area of approximately 69% (Figure 15). North Fork median ensemble ice extent is modeled to decrease by approximately 66% and 88% for RCP 4.5 and 8.5 respectively by 2099 (Figure 15).

An increase in temperatures throughout the Nooksack basin is expected to alter the amount of glacier melt that is available to the stream (Figure 16). In both the North and Middle Fork basins, modeled glacier melt contribution to streamflow in the late summer months is estimated to be at a maximum during the first half of the 21<sup>st</sup> Century when the largest surface area of ice is available for melt. During this time, median future ensemble ice melt exceeds modeled historical melt magnitudes under both RCP 4.5 and 8.5 scenarios. At the year 2025, modeled median peak ice melt for late summer months increases from

modeled historical levels by up to 51% for the North Fork and 87% for the Middle Fork (Table 7). The percentage of total streamflow that is derived from glacier melt is projected to approximately double for the Middle Fork and triple for the North Fork during this same time (Table 8). By 2050, peak glacier ice melt is forecast to be less than at 2025 with peak median magnitudes between 15-37% higher than historical levels for the Middle Fork and between 14-20% lower for the North Fork. By 2075, ice melt is projected to be at approximately half of historical levels throughout both basins and at the North Cedarville gauge with little difference between RCP 4.5 and 8.5. The percentage of total streamflow derived from ice melt is projected to decrease to levels similar to 1950-2010 by the second half of the century. Timing of peak glacier ice melt is not forecast to change. A change in the timing of the onset of annual glacier melt is projected, however, with little to no estimated ice melt contribution to streamflow during the months of May or June by 2075 throughout the Nooksack River basin. The glacier melt estimates, particularly for the early decades of the 21<sup>st</sup> Century are subject to error because the 2009 glacier ice extent was overestimated during historical model runs. Thus, glacier ice melt contribution to streamflow for the early decades of the future simulations is likely to be lower than the modeling projects.

### *3.3.3. Streamflow*

Modeled results using 10 GCMs and RCP.45 and RCP 8.5 forcing scenarios within each of the three Nooksack sub-basins indicate similar trends throughout the 21<sup>st</sup> Century with a general decrease in spring and summer flows and an increase in winter flows. Spring peak flows are predicted to occur earlier in the water year by as much as two months in parts of the upper Nooksack River basin, although peak spring melt varies by location in both magnitude and timing.

Middle Fork Nooksack River modeling results through the end of the 21<sup>st</sup> Century indicate a decrease in median daily spring streamflow magnitudes, although the timing of this peak remains unchanged (Figure 17). An increase in winter flows and a decrease in summertime flows are projected throughout the 21<sup>st</sup> Century and become more significant toward the end of the century for both the RCP 4.5 and 8.5 scenarios. The RCP scenarios deviate little from one another until the latter half of the century when winter and summer flow changes between the two become more pronounced. The largest changes are projected to occur within the months of January, July, and August with a forecasted increase from historical winter flows by as much as 93% and 127% for RCP 4.5 and 8.5 scenarios respectively by 2075 (Table 9). Middle Fork summer flows are modeled to decrease by as much as 52% and 65% for RCP 4.5 and 8.5 respectively by 2075.

South Fork Nooksack River modeling results through the end of the 21<sup>st</sup> Century indicate a decrease in median peak spring snowmelt derived streamflow magnitudes as well as a shift in the timing of spring snowmelt runoff to earlier in the water year by as much as two months (Figure 17). Like in the Middle Fork, an increase in winter flows and a decrease in summertime flows are projected throughout the 21<sup>st</sup> Century and become more significant toward the end of the century for both the RCP 4.5 and 8.5 scenarios. South Fork summer flows by 2025 are projected to decline by a greater percentage than in the North and Middle Fork basins. By 2075, the largest changes are projected to occur within the months of January and July with a forecasted increase in winter flows by as much as 82% and 112% for RCP 4.5 and 8.5 scenarios (Table 9). Summer flows by the year 2075 are projected to decrease by as much as 65% and 76% for RCP scenarios 4.5 and 8.5, respectively.

Future model projections indicate more substantial changes in the North Fork Nooksack River basin than in the Middle or South Fork basins as much of the area transitions from snow dominated to rain dominated. While winter flows are expected to increase and summer flows are expected to decrease, like in the other basins, the magnitude of change is higher by the latter half of the century (Figure 17). Median January forecasts indicate streamflow increases by as much as a 161% and 253% for RCP 4.5 and 8.5 respectively (Table 9). Summer median flow decreases for the month of July are projected to be -62% and -77% for RCP 4.5 and 8.5 respectively. Like in the Middle and South Fork basins, the two RCP scenarios are similar until 2075 when they begin to diverge.

Modeled streamflow projections at the North Cedarville gauge location, which encompass the flows from each of the three sub-basins, indicate similar trends with a decrease in winter flows and an increase in summer flows and little difference between RCP scenarios until 2075 (Figure 18). Snowmelt derived flows, which historically peaked during the months of May and June, show little to no shift in timing for RCP 4.5 by 2075 but a slight shift earlier in the season for RCP 8.5 by 2075. Modeling indicates an increase in median daily streamflow for the month of January by as much as 85% and 119% for RCP 4.5 and 8.5 respectively (Table 9). Summer median flows are projected to decrease the most in July by 59% and 72% for RCP 4.5 and 8.5.

Peak discharge events, such as those from winter storms, are forecasted with lower confidence than median streamflows and baseflows. Observed historical streamflows above certain thresholds are difficult to capture through instrumentation and are predicted based solely on a rating curve and gauge height. Moreover, because modeled daily rainfall magnitudes are disaggregated into 3-hour time steps, high intensity storms responsible for

peaks are dampened. Because of these factors that lead to uncertainty in peak flow magnitudes, calibration of the DHSVM focused on the timing of storm events rather than achieving the exact magnitude. Forecasted high flow events should therefore be treated with caution and used only as a guide of trend.

#### **4.0 Discussion**

Changes in temperature and precipitation in recent decades have affected glaciers on a global scale and throughout western North America, leading to a general decline in total glacier area (Moore and Demuth, 2001; Lemke et al., 2007; Moore et al., 2009; Bolch et al., 2010; Pelto and Brown, 2012; Gardner et al., 2013; Hartmann et al., 2013; Clarke et al., 2015). Long term field monitoring within the North Cascades has shown a significant decrease in the net mass balance of all benchmark glaciers studied (Bidlake et al., 2010; Riedel and Larrabee, 2011). Included among these is the South Cascade Glacier which has been monitored since 1958 and showed a net decrease in area from 2.71 km<sup>2</sup> to approximately 1.73 km<sup>2</sup> by 2007 with continued retreat since then (Bidlake et al 2010). Other regional studies, however, have noted variable changes in North Cascades glacier area since the mid-1900s with periods of advance as well as periods of retreat (Pelto and Brown., 2012; O'Neal et al., 2015). Pelto and Hedlund (2001) found that nearly half of the glaciers within the North Cascades advanced from the 1950s through the 1970s while others retreated. The relationship between large-scale climate events such as the PDO and ENSO have been noted in previous studies (Moore and Demuth, 2001; Josberger et al., 2007), suggesting that these interdecadal climate events have a regional effect on glacier size. In the application of the calibrated dynamic glacier model in the DHSVM, I found cycles of advance and retreat

within the Nooksack basin, including a rapid advance through the 1950s and another advance in the 1970s with a period of retreat in between. However, when compared to time series of the Pacific Decadal Oscillation and the El Nino Southern Oscillation, there is very little relationship between the timing of warm cycles (positive index) and modeled glacier retreat or cold cycles (negative index) and modeled glacier growth (Figure 19).

Although the glacial model simulated historical advances and retreats, the final calibration of glacier extent, especially in the North Fork basin, did not match the observed extent in some locations because the model simulated ice in areas where there should be no ice (Figure 10 and Figure 11). Extra ice development was in part due to the limited control of the temperature and precipitation interpolations at high elevations in complex terrains, particularly on Mount Baker. This led to the simulation of thick ice tongues in the lower valleys flanking Mount Baker. Thin ice development was also noted in areas between glaciers and could be due in part to the lack of an avalanche simulator in the glacier dynamics model that would transport snow from steep cliff areas to the valleys and glaciers below. In reality, snow accumulates on steep cliff areas but generally avalanches to the valley floor before enough snow is able to accumulate and reach the density of ice (e.g., Elder et al., 1991). The thin ice layers were kept in the calibrated version in an effort to preserve the hydrologic mass balance within the watershed but likely were a contributing factor in the variability seen in modeled historical ice extent, particularly during early timesteps of the simulation period (i.e., the 1950s) when the thin ice layer initially formed.

Like other glacier change modeling studies (Radić et al., 2013; Naz et al, 2014; Clarke et al., 2015), I relied on estimated historical ice extent for glacier spinup and calibrations and assumed that historical observations of areal ice extent were accurate and



were a representation of equilibrium conditions. I used glacier areal changes through time to assess the model's effectiveness at simulating dynamic glacier processes. In reality, estimating ice coverage from datasets such as satellite imagery is difficult because ice-bedrock boundaries cannot always be readily identified remotely. Other sources for observed glacier extent included digitized glacier outlines from 1:100,000 and 1:24,000 scale USGS topographic maps. Due to the small scale of these maps, there is error associated with the historical glacier locations and therefore is error in the initial and calibrated ice coverages used in the model.

In all of the future modeling results, I find that projected median changes under RCP 4.5 and 8.5 scenarios are similar to one another through the first half of the 21<sup>st</sup> Century and then deviate beyond 2050. This pattern is due to the time lag response in the mitigation narratives imposed in the RCP 4.5 scenario in the GCMs (e.g., Hansen et al., 2005). Even with the decrease in anthropogenic greenhouse gas emissions proposed under the RCP 4.5 scenario, atmospheric conditions do not stabilize and reach equilibrium until decades after mitigation measures are executed. Thus, the hydrological effects of emissions mitigation scenarios are likely to be felt more in the long-term rather than in the immediate future.

Glaciers throughout the Nooksack River basin, based on DHSVM-glacier modeling, are forecasted to recede by nearly 90% throughout the 21<sup>st</sup> Century with smaller glaciers disappearing entirely by 2100, even under RCP 4.5 climate scenarios (Figure 15). Stahl et al. (2008) found that even once temperatures and atmospheric conditions have become more stable, glaciers may still take decades to reach a new equilibrium and will continue to melt until that happens. Thus, even under future scenarios which incorporate emissions mitigation strategies and less aggressive warming such as RCP 4.5, glaciers are expected to show

significant retreat through the end of the century. In British Columbia, Canada, Clarke et al. (2015) projects similar trends in glacier retreat, with near total glacier loss in many places for the RCP 8.5 scenario by 2100 and little difference between RCP scenarios until after 2050. Similarly, Radić et al. (2013) model an average decrease in glacier area of greater than 75% in Western Canada and the United States under 14 CMIP5 GCMs and the RCP 4.5 scenario. My simulated changes in glacial recession through time are largely dependent on changes in ice thickness, which is difficult to properly estimate using modeling alone. I used a DEM to approximate ice thickness which has limitations, and without proper thickness, ice volume cannot be accurately established (Naz et al., 2014). However, since most historic areal extent changes through time matched observations, I assumed the estimated modeled ice thickness to be reasonable.

With a potential reduction in glacier area and volume projected throughout the 21<sup>st</sup> Century under all future scenarios, the ice available (or lack therein) for melt will ultimately affect streamflow. I project median monthly glacier melt and its contribution to streamflow to be at its highest in the first half of the 21<sup>st</sup> century when warmer temperatures and an earlier spring snowmelt will leave the glaciated areas exposed to atmospheric heat inputs for longer periods of time (Table 7). At 2025, modeling results indicate not only an increase in median ice melt magnitude but also an approximate doubling in the proportion of total streamflow derived from glacial melt for the Middle Fork, and a tripling for the North Fork during the summer months (Table 8). The larger increase in the streamflow melt component for the North Fork is likely due to the melting of excess ice that was over-simulated during historical model simulations. By 2075, the total magnitude of melt will be significantly lower than historical levels due to the reduction in glacial area. However, the proportion of total

streamflow derived from ice melt is projected to be similar to historical levels because of an overall reduction in streamflow due to less snowmelt and lower summer precipitation.

Similar trends in glacier melt discharge magnitudes have been noted in other glacier change studies in Western North America (Nolin et al., 2010; Clarke et al., 2015). For the first part of the 21<sup>st</sup> Century, glaciated basins such as the Middle Fork and North Fork will likely show less of a dramatic decrease in summer streamflows due to the increased rate of glacier melt, which partially compensates for the reduction in snowmelt. This is evident when comparing projected summer streamflow changes of the non-glaciated South Fork basin to the glaciated Middle and North Fork basins (Table 9).

Modeling results project a significant decrease in basin average SWE in the Nooksack River basin as temperatures warm throughout the 21<sup>st</sup> Century (Figures 14). These trends are consistent with Dickerson-Lange and Mitchell (2013) in the Nooksack River basin, and other regional modeling studies in the PNW (e.g., Hamlet et al., 2005; Mote et al., 2005; Mote et al., 2008; Adam et al., 2009). Our modeling results indicate a large decrease in median SWE magnitude as soon as 2025 for both RCP 4.5 and 8.5 scenarios, especially in the South Fork basin where peak elevations are lower (~ 2000 m) and only about 25% of the basin is above 1000 m (Figure 2). The large decrease so early in the century is attributed to the transient nature of the low to mid elevation parts of the basin which are more sensitive to small changes in temperatures, and shift from being snow dominated to rain dominated (Elsner et al., 2010). Modeled SWE trends in the South Fork basin also show a much faster rate of decline through the end of the century and a shift in annual peak SWE to earlier in the season (Figure 14). The shift in the annual SWE peak is not as evident in the Middle and North Fork

basins, which have more northerly exposed aspects and higher percentages of areas with elevations between 1000 m and 3000 m (Figure 2).

The projected decrease in snowpack and changes in glacier melt magnitudes significantly affect the timing and magnitude of streamflow in the Nooksack River. My results reflect the general streamflow trends observed in other local and regional studies (e.g., Stahl et al., 2008; Vano et al., 2010; Dickerson-Lange and Mitchell, 2013; Hamlet et al., 2013) which forecast a decrease in summer streamflows and an increase in winter flows when higher relief areas transition to being rain-dominated. Winter runoff will increase as the snow-line increases in elevation leaving more basin area snow-free and exposed to rainfall, thus increasing the flood risk during the wetter months (Tohver et al., 2014). While the overall amount of annual precipitation is not projected to change drastically from modern magnitudes in the PNW, warmer temperatures will reduce the basin-wide SWE available for spring and early summer snowmelt (Vano et al, 2010). I project spring peak runoff, which is primarily due to snowmelt, to occur earlier in the water year and to be substantially lower (Figure 17 and Figure 18) if temperatures are similar to those forecast in the more aggressive climate models. The hydrograph is likely to shift from a bimodal distribution to a more unimodal distribution, as is characteristic of rain-dominated systems (Figure 17 and 18). Other modeling studies in the PNW have projected similar changes in the timing of peak snowmelt runoff (Barnett et al., 2004; Vano et al., 2010; Dickerson-Lange and Mitchell, 2013), which has the potential to greatly impact water resources in the drier summer months and threaten valuable stream habitat.

The DHSVM-glacier model did well at reproducing hydrological processes in low- to mid-elevation areas which make up the majority of the basin (Figure 2), but was less

effective at higher elevations. This affected the results of glaciation, basin average snowpack SWE, and streamflow in areas of the Nooksack River basin at high elevation. The reasonable simulation of glacier mass balance on the Sholes glacier (Figure 12), which has its highest point at approximately 2100 m, shows the ability of the DHSVM-glacier model to simulate ice mass changes effectively where meteorology and snowpack evolution is reproduced realistically. At higher elevations, however, snowpack was found to be melting at too slow a rate or not at all during summer months which led to the production of too much ice on parts of Mount Baker. While some snowpack does exist on Mount Baker year-round, basin average SWE should realistically be lower during late summer months (Figure 14). The excess summer snow also accounts for the lack of change in seasonal timing of peak SWE for the North and Middle forks. If projections are compared to historical modeled magnitudes at the SNOTEL sites, a clear shift in peak SWE timing to earlier in the season can be seen (Figure 20). Additionally, this excess snowpack on Mount Baker is likely responsible for the lack of a shift in the spring snowmelt runoff peak for the Middle Fork and the minimal change seen in the North Fork. The Middle and North forks contain a larger proportion of total basin area at high elevation and are therefore more heavily influenced by the larger high-elevation summer snowpack. The complexities of the Mount Baker climate system with its high relief and maritime weather events made controlling and refining modeled temperature lapse rates at high elevations difficult. Attempts to alter lapse rates included manually changing monthly temperature lapse rates at individual high elevation Livneh grid cells nodes. However, the alteration of monthly temperature lapse rates from their final calibrated values led to poor model performance with respect to streamflow.

As with all modeling studies, there are uncertainties. I relied on statistically extrapolated daily meteorology grids (Livneh et al., 2013) to force the model during calibration. Although this method allowed for complete meteorological coverage of the study area, it required bias corrections and lapse rate adjustments, and was disaggregated in to 3-hour timesteps in order to capture sub-daily snowpack and ice changes. Disaggregation introduces error which can be propagated through the modeling process (e.g., Margulius and Entekhabi, 2001). Disaggregation also takes daily precipitation data and averages it over 3-hr timesteps making streamflows during observed high intensity storm events difficult to replicate. Although this may be problematic when assessing storm effects, it is less of an issue when examining seasonal trends in snowpack evolution and long-term glacial dynamics and melt.

Additional uncertainties come from the GCM climate forecasts since they make generalizations about many climate parameters and are at a coarse resolution relative to a 2000 km<sup>2</sup> watershed. The parameterization of finer scale processes undoubtedly introduces assumptions that do not hold true in the natural climate system and are not necessarily consistent between GCMs (Stainforth et al., 2007; Stocker et al., 2013). Recent studies have noted the variability among GCMs as a large source of uncertainty in the forecasting of glacial and hydrological changes (Barnett et al., 2005; Radić et al., 2013; Clarke et al., 2015). I found this to hold true and assumed ensemble medians to be the best representative projection of changes in hydrologic and glacial processes. Moreover, I used GMCs downscaled to the Nooksack basin using the MACA method, which is better at reproducing historical weather parameters than other commonly used downscaling techniques (Abatzoglou and Brown, 2012). However, because it relies on historical weather grids as the

training dataset, historical weather patterns and weather event regularity are assumed to remain consistent throughout the future. Bias behavior in the forcing data is also assumed to remain unchanged through time. Future work should focus on improving the spatial distribution of predictions of mountain glaciers in the Nooksack River basin by further refining lapse rates and other climate parameters.

## **5.0 Conclusion**

Climate studies have revealed changes to Earth's dynamic climate system and have projected changes and variability to continue into the foreseeable future. Changing climate conditions have the potential to alter dramatically the hydrology of much of the world with increasing temperatures, variable precipitation, reduced snowpacks, and glacial recession. Shifts in the hydrologic cycle will almost certainly affect water resources that are critical to individuals, communities, and natural habitats. In the PNW, where snowpack and glaciers are currently responsible for much of the summertime streamflow, understanding the potential effects of climate change is necessary.

Through the use of the DHSVM and dynamic glacier model forced with downscaled gridded future GCMs, I quantified trends in basin snowpack, streamflow, glacier recession, and glacier melt contribution to streamflow in the Nooksack River basin throughout the 21<sup>st</sup> Century. A projected decrease in summer streamflows and an increase in winter flows as snowpack and glacier ice volume is decreased have the potential to strain water resources and valuable fish spawning habitat. Glaciers have historically provided a natural water storage buffer to support late summer baseflows but with a reduction in glacier volume, the water available during warmer months will be reduced. In the face of such changes, improved

water resource conservation and planning may become imperative to protect our natural resources.



## 6.0 References

- Abatzoglou, J.T., and Brown, T.J., 2012, A comparison of statistical downscaling methods suited for wildfire applications: *International Journal of Climatology*, v. 32, p. 772–780, doi: 10.1002/joc.2312.
- Abatzoglou, J.T., Rupp, D.E., and Mote, P.W., 2014, Seasonal Climate Variability and Change in the Pacific Northwest of the United States: *Journal of Climate*, v. 27, p. 2125–2142, doi: 10.1175/JCLI-D-13-00218.1.
- Adam, J.C., Hamlet, A.F., and Lettenmaier, D.P., 2009, Implications of global climate change for snowmelt hydrology in the twenty-first century: *Hydrological Processes*, v. 23, p. 962–972.
- Alila, Y., and Beckers, J., 2001, Using numerical modelling to address hydrologic forest management issues in British Columbia: *Hydrological Processes*, v. 15, p. 3371–3387, doi: 10.1002/hyp.1038.
- Bach, A., 2002, Snowshed Contributions to the Nooksack River Watershed, North Cascades Range, Washington: *Geographical Review*, v. 92, p. 192–212, doi: 10.1111/j.1931-0846.2002.tb00004.x.
- Bandaragoda, C., J. Greenberg, M. Dumas and Gill, P., 2012. Lower Nooksack Water Budget Overview. In Bandaragoda, C., J. Greenberg, M. Dumas and P. Gill, (eds). Lower Nooksack Water Budget, (pp. 3-35 ). Whatcom County, WA: WRIA 1 Joint Board.
- Barnett, T., Malone, R., Pennell, W., Stammer, D., Semtner, B., and Washington, W., 2004, The effects of climate change on water resources in the west: introduction and overview: *Climatic Change*, v. 62, p. 1–11.
- Bidlake, W.R., Josberger, E.G., and Savoca, M.E., 2002, Water, ice, and meteorological measurements at South Cascade Glacier, Washington, balance year 2002: U.S. Geological Survey Scientific Investigations Report 2004-5089, 38 p.
- Bohn, T.J., Livneh, B., Oyler, J.W., Running, S.W., Nijssen, B., and Lettenmaier, D.P., 2013, Global evaluation of MTCLIM and related algorithms for forcing of ecological and hydrological models: *Agricultural and Forest Meteorology*, v. 176, p. 38–49.
- Bolch, T., Menounos, B., and Wheate, R., 2010, Landsat-based inventory of glaciers in western Canada, 1985–2005: *Remote Sensing of Environment*, v. 114, p. 127–137, doi: 10.1016/j.rse.2009.08.015.

- Clarke, G.K., Anslow, F., Jarosch, A., Radic, V., Menounos, B., Bolch, T., Berthier, E., and others, 2013, Ice volume and subglacial topography for western Canadian glaciers from mass balance fields, thinning rates, and a bed stress model: *Journal of Climate*, v. 26, p. 4282–4303.
- Clarke, G.K., Jarosch, A.H., Anslow, F.S., Radić, V., and Menounos, B., 2015, Projected deglaciation of western Canada in the twenty-first century: *Nature Geoscience*, v. 8, p. 372–377.
- Cuo, L., Lettenmaier, D.P., Alberti, M., and Richey, J.E., 2009, Effects of a century of land cover and climate change on the hydrology of the Puget Sound basin: *Hydrological Processes*, v. 23, p. 907–933, doi: 10.1002/hyp.7228.
- Daly, C., Neilson, R.P., and Phillips, D.L., 1994, A statistical-topographic model for mapping climatological precipitation over mountainous terrain: *Journal of applied meteorology*, v. 33, p. 140–158.
- Deser, C., Knutti, R., Solomon, S., and Phillips, A.S., 2012, Communication of the role of natural variability in future North American climate: *Nature Climate Change*, v. 2, p. 775–779, doi: 10.1038/nclimate1562.
- Dickerson-Lange, S.E., and Mitchell, R., 2013, Modeling the effects of climate change projections on streamflow in the Nooksack River basin, Northwest Washington: *Hydrological Processes*, doi: 10.1002/hyp.10012.
- Donnell, C.B., 2007, Quantifying the Glacial Meltwater Component of Streamflow in the Middle Fork Nooksack River, Whatcom County, WA, Using a Distributed Hydrology Model: M.S. Thesis, Department of Geology, Western Washington University, Bellingham, WA.
- Du, E., Link, T.E., Gravelle, J.A., and Hubbart, J.A., 2013, Validation and sensitivity test of the distributed hydrology soil-vegetation model (DHSVM) in a forested mountain watershed: *Hydrological Processes*, p. n/a–n/a, doi: 10.1002/hyp.10110.
- Elder, K., Dozier, J., and Michaelsen, J., 1991, Snow accumulation and distribution in an alpine watershed: *Water Resources Research*, v. 27, p. 1541–1552.
- Elsner, M.M., Cuo, L., Voisin, N., Deems, J.S., Hamlet, A.F., Vano, J.A., Mickelson, K.E., Lee, S.-Y., and Lettenmaier, D.P., 2010, Implications of 21st century climate change for the hydrology of Washington State: *Climatic Change*, v. 102, p. 225–260.
- Fountain, A.G., Krimmel, R.M., and Trabant, D.C., 1997, A strategy for monitoring glaciers: U.S. Geological Survey circular, 1132.
- Gardner, A.S., Moholdt, G., Cogley, J.G., Wouters, B., Arendt, A.A., Wahr, J., Berthier, E., Hock, R., Pfeffer, W.T., Kaser, G., and others, 2013, A reconciled estimate of glacier contributions to sea level rise: 2003 to 2009: *science*, v. 340, p. 852–857.

- Grah, O., and Beaulieu, J., 2013, The effect of climate change on glacier ablation and baseflow support in the Nooksack River basin and implications on Pacific salmonid species protection and recovery: *Climatic Change*, v. 120, p. 657–670, doi: 10.1007/s10584-013-0747-y.
- Hamlet, A.F., Carrasco, P., Deems, J., Elsner, M.M., Kamstra, T., Lee, C., Lee, S.Y., Mauger, G., Salathe, E.P., Tohver, I., and others, 2010a, Final Report for the Columbia Basin Climate Change Scenarios Project: University of Washington, Climate Impacts Group, Seattle, Washington, DC.
- Hamlet AF, Salathé EP, Carrasco P. 2010b. Statistical Downscaling Techniques for Global Climate Model Simulations of Temperature and Precipitation with Application to Water Resources Planning Studies. Columbia Basin Climate Change Scenarios Project (PI: Alan F. Hamlet), University of Washington, Seattle, WA; 28pp.
- Hamlet, A.F., Elsner, M.M., Mauger, G.S., Lee, S.-Y., Tohver, I., and Norheim, R.A., 2013, An overview of the Columbia Basin Climate Change Scenarios Project: Approach, methods, and summary of key results: *Atmosphere-ocean*, v. 51, p. 392–415.
- Hansen, J., Nazarenko, L., Ruedy, R., Sato, M., Willis, J., Del Genio, A., Koch, D., Lacis, A., Lo, K., Menon, S., and others, 2005, Earth's Energy Imbalance: Confirmation and Implications: *Science*, v. 308, p. 1431–1435.
- Hartmann, D.L., A.M.G. Klein Tank, M. Rusticucci, L.V. Alexander, S. Brönnimann, Y. Charabi, F.J. Dentener, E.J. Dlugokencky, D.R. Easterling, A. Kaplan, B.J. Soden, P.W. Thorne, M. Wild and P.M. Zhai, 2013: Observations: Atmosphere and Surface. In: *Climate Change 2013: The Physical Science Basis. Contribution of Working Group I to the Fifth Assessment Report of the Intergovernmental Panel on Climate Change* [Stocker, T.F., D. Qin, G.-K. Plattner, M. Tignor, S.K. Allen, J. Boschung, A. Nauels, Y. Xia, V. Bex and P.M. Midgley (eds.)]. Cambridge University Press, Cambridge, United Kingdom and New York, NY, USA.
- Josberger, E.G., Bidlake, W.R., March, R.S., and Kennedy, B.W., 2007, Glacier mass-balance fluctuations in the Pacific Northwest and Alaska, USA: *Annals of Glaciology*, v. 46, p. 291–296.
- Kelleher, C., Wagener, T., and McGlynn, B., 2015, Model-based analysis of the influence of catchment properties on hydrologic partitioning across five mountain headwater subcatchments: *Water Resources Research*, v. 51, p. 4109–4136, doi: 10.1002/2014WR016147.
- Lemke, P., et al., 2007, Observations: Changes in snow, ice and frozen ground, in *Climate Change 2007: The Physical Science Basis: Working Group I Contribution to the Fourth Assessment Report of the International Panel on Climate Change*, edited by S. Solomon et al., pp. 339–383, Cambridge Univ. Press, New York.

- Liang, X., Lettenmaier, D.P., Wood, E.F., and Burges, S.J., 1994, A simple hydrologically based model of land surface water and energy fluxes for general circulation models: *Journal of Geophysical Research: Atmospheres* (1984–2012), v. 99, p. 14415–14428.
- Livneh, B., Bohn, T.J., Pierce, D.W., Munoz-Arriola, F., Nijssen, B., Vose, R., Cayan, D.R., and Brekke, L., 2015, A spatially comprehensive, hydrometeorological data set for Mexico, the U.S., and Southern Canada 1950–2013: *Scientific Data*, v. 2, p. 150042, doi: 10.1038/sdata.2015.42.
- Livneh, B., Rosenberg, E.A., Lin, C., Nijssen, B., Mishra, V., Andreadis, K.M., Maurer, E.P., and Lettenmaier, D.P., 2013, A Long-Term Hydrologically Based Dataset of Land Surface Fluxes and States for the Conterminous United States: Update and Extensions: *Journal of Climate*, v. 26.
- Mantua, N.J., and Hare, S.R., 2002, The Pacific decadal oscillation: *Journal of oceanography*, v. 58, p. 35–44.
- Mantua, N., Tohver, I., and Hamlet, A., 2010, Climate change impacts on streamflow extremes and summertime stream temperature and their possible consequences for freshwater salmon habitat in Washington State: *Climatic Change*, v. 102, p. 187–223.
- Margulis, S.A., and Entekhabi, D., 2001, Temporal disaggregation of satellite-derived monthly precipitation estimates and the resulting propagation of error in partitioning of water at the land surface: *Hydrology and Earth System Science*, v. 5.
- Mauger, G.S., J.H. Casola, H.A. Morgan, R.L. Strauch, B. Jones, B. Curry, T.M. Busch Isaksen, L. Whitely Binder, M.B. Krosby, and A.K. Snover, 2015. State of Knowledge: Climate Change in Puget Sound. Report prepared for the Puget Sound Partnership and the National Oceanic and Atmospheric Administration. Climate Impacts Group, University of Washington, Seattle. doi: 10.7915/CIG93777D
- Moore, R.D., and Demuth, M.N., 2001, Mass balance and streamflow variability at Place Glacier, Canada, in relation to recent climate fluctuations: *Hydrological Processes*, v. 15, p. 3473–3486, doi: 10.1002/hyp.1030.
- Moore, R.D., Fleming, S.W., Menounos, B., Wheate, R., Fountain, A., Stahl, K., Holm, K., and Jakob, M., 2009, Glacier change in western North America: influences on hydrology, geomorphic hazards and water quality: *Hydrological Processes*, v. 23, p. 42.
- Mote, P.W., Hamlet, A.F., Clark, M.P., and Lettenmaier, D.P., 2005, Declining mountain snowpack in western North America.: *Bulletin of the American meteorological Society*, v. 86.
- Mote, P., Hamlet, A., and Salathé, E., 2008, Has spring snowpack declined in the Washington Cascades? *Hydrology and Earth System Sciences*, v. 12, p. 193–206.

- Mote, P.W., and Salathe Jr, E.P., 2010, Future climate in the Pacific Northwest: Climatic Change, v. 102, p. 29–50, doi: 10.1007/s10584-010-9848-z.
- Mote, P., Snover, A.K., Capalbo, S., Eigenbrode, S.D., and Littell, J., 2014, Northwest. Chapter 21 in Climate Change Impacts in the United States: The Third U.S. National Climate Assessment, J. Melillo, Terese (T.C.) Richmond, and G.W. Yohe, Eds.: U.S. Global Change Research Program, v. 16-1 nn.
- Nash, Je., and Sutcliffe, J.V., 1970, River flow forecasting through conceptual models part I—A discussion of principles: Journal of hydrology, v. 10, p. 282–290.
- Naz, B.S., Frans, C.D., Clarke, G.K.C., Burns, P., and Lettenmaier, D.P., 2014, Modeling the effect of glacier recession on streamflow response using a coupled glacio-hydrological model: Hydrol. Earth Syst. Sci., v. 18, p. 787–802, doi: 10.5194/hess-18-787-2014.
- O’Neal, M.A., Hanson, B., Carisio, S., and Satinsky, A., 2015, Detecting recent changes in the areal extent of North Cascades glaciers, USA: Quaternary Research, v. 84, p. 151–158.
- Oyler, J.W., Dobrowski, S.Z., Ballantyne, A.P., Klene, A.E., and Running, S.W., 2015, Artificial amplification of warming trends across the mountains of the western United States: Geophysical Research Letters, v. 42, p. 2014GL062803, doi: 10.1002/2014GL062803.
- Palmer, R.N., 2007, Final Report of the Climate Change Technical Committee. A report prepared by the Climate Change Technical Subcommittee of the Regional Water Supply Planning Process, Seattle, WA: University of Washington, Climate Impacts Group.
- Pelto, M., and Brown, C., 2012, Mass balance loss of Mount Baker, Washington glaciers 1990–2010: Hydrological Processes, v. 26, p. 2601–2607.
- Pelto, M.S., and Hedlund, C., 2001, Terminus behavior and response time of North Cascade glaciers, Washington, U.S.A.: Journal of Glaciology, v. 47, p. 497–506, doi: 10.3189/172756501781832098.
- PRISM Climate Group, 2014, Oregon State University, <http://prism.oregonstate.edu>, created 23 September 2014.
- Radić, V., Bliss, A., Beedlow, A.C., Hock, R., Miles, E., and Cogley, J.G., 2013, Regional and global projections of twenty-first century glacier mass changes in response to climate scenarios from global climate models: Climate Dynamics, v. 42, p. 37–58, doi: 10.1007/s00382-013-1719-7.

- Raup, B., Racoviteanu, A., Khalsa, S.J.S., Helm, C., Armstrong, R., and Arnaud, Y., 2007, The GLIMS geospatial glacier database: A new tool for studying glacier change: *Global and Planetary Change*, v. 56, p. 101–110, doi: 10.1016/j.gloplacha.2006.07.018.
- Riedel, J., and Larrabee, M.A., 2011, North Cascades National Park Complex glacier mass balance monitoring annual report, Water year 2009: North Coast and Cascades Network: Natural Resource Technical Report NPS/NCCN/NRTR—2011.
- Rupp, D.E., Abatzoglou, J.T., Hegewisch, K.C., and Mote, P.W., 2013, Evaluation of CMIP5 20th century climate simulations for the Pacific Northwest USA: *Journal of Geophysical Research: Atmospheres*, v. 118, p. 10–884.
- Salathe Jr, E.P., Leung, L.R., Qian, Y., and Zhang, Y., 2010, Regional climate model projections for the State of Washington: *Climatic Change*, v. 102, p. 51–75.
- Sperna Weiland, F.C., Van Beek, L.P.H., Kwadijk, J.C.J., and Bierkens, M.F.P., 2010, The ability of a GCM-forced hydrological model to reproduce global discharge variability: *Hydrology and Earth System Sciences*, v. 14, p. 1595–1621.
- Stahl, K., Moore, R.D., Shea, J.M., Hutchinson, D., and Cannon, A.J., 2008, Coupled modelling of glacier and streamflow response to future climate scenarios: *Water Resources Research*, v. 44, p. W02422, doi: 10.1029/2007WR005956.
- Stainforth, D.A., Downing, T.E., Washington, R., Lopez, A., and New, M., 2007, Issues in the interpretation of climate model ensembles to inform decisions: *Philosophical transactions. Series A, Mathematical, physical, and engineering sciences*, v. 365, p. 2163–77.
- Stocker, T.F., Qin, D., Plattner, G.-K., Alexander, L.V., Allen, S.K., Bindoff, N.L., Breon, F.-M., Church, J.A., Cubasch, U., Emori, S., Forster, P., Friedlingstein, P., Gillet, N., Gregory, J.M., et al., 2013, Technical Summary. In: *Climate Change 2013: The Physical Science Basis. Contribution of Working Group I to the Fifth Assessment Report of the Intergovernmental Panel on Climate Change* [Stocker, T.F., D. Qin, G.-K. Plattner, M. Tignor, S.K. Allen, J. Boschung, A. Nauels, Y. Xia, V. Bex and P.M. Midgley (eds.)]: Cambridge University Press.
- Tracy, K., 2001, Changes in Mirror Lake, Northwestern Washington, as a Result of the Diversion of Water from the Nooksack River: WWU Masters Thesis Collection, Paper 438.
- Tohver, I.M., Hamlet, A.F., and Lee, S.-Y., 2014, Impacts of 21st-Century Climate Change on Hydrologic Extremes in the Pacific Northwest Region of North America: *JAWRA Journal of the American Water Resources Association*, v. 50, p. 1461–1476.

- United States Geological Survey (USGS). 2013. USGS Water Science Center, Annual Water-Data Reports. Available from: <http://wa.water.usgs.gov/cgi/adr.cgi?12210700> (accessed October 2015)
- Vano, J.A., Voisin, N., Cuo, L., Hamlet, A.F., Elsner, M.M., Palmer, R.N., Polebitski, A., and Lettenmaier, D.P., 2010, Climate change impacts on water management in the Puget Sound region, Washington State, USA: *Climatic Change*, v. 102, p. 261–286, doi: 10.1007/s10584-010-9846-1.
- Watanabe, S., Kanae, S., Seto, S., Yeh, P.J.-F., Hirabayashi, Y., and Oki, T., 2012, Intercomparison of bias-correction methods for monthly temperature and precipitation simulated by multiple climate models: *Journal of Geophysical Research: Atmospheres*, v. 117, p. D23114, doi: 10.1029/2012JD018192.
- Wigmosta, M.S., Vail, L.W., and Lettenmaier, D.P., 1994, A distributed hydrology-vegetation model for complex terrain: *Water resources research*, v. 30, p. 1665–1679.

## 7.0 Tables

**Table 1.** List of GCMs and associated information used to model the effects of forecasted climate change on streamflow in the Nooksack River Basin.

Model Name	Model Country	Model Agency	Ensemble Used	Resolution (lat x long)
<b>bcc-csm1-1-m</b>	China	Beijing Climate Center, China Meteorological Administration	r1i1p1	2.7906 x 2.8125
<b>CanESM2</b>	Canada	Canadian Centre for Climate Modeling and Analysis	r1i1p1	2.7906 x 2.8125
<b>CCSM4</b>	USA	National Center of Atmospheric Research	r6i1p1	0.9424 x 1.25
<b>CNRM-CM5</b>	France	National Centre of Meteorological Research	r1i1p1	1.4008 x 1.40625
<b>CSIRO-Mk3-6-0</b>	Australia	Commonwealth Scientific and Industrial Research Organization/Queensland Climate Change Centre of Excellence	r1i1p1	1.8653 x 1.875
<b>HadGEM2-ES</b>	United Kingdom	Met Office Hadley Center	r1i1p1	1.25 x 1.875
<b>HadGEM2-CC</b>	United Kingdom	Met Office Hadley Center	r1i1p1	1.25 x 1.875
<b>IPSL-CM5A-MR</b>	France	Institut Pierre Simon Laplace	r1i1p1	2.5352 x 2.5
<b>MIROC5</b>	Japan	Atmosphere and Ocean Research Institute (The University of Tokyo), National Institute for Environmental Studies, and Japan Agency for Marine-Earth Science and Technology	r1i1p1	1.4008 x 1.40625
<b>NorESM1-M</b>	Norway	Norwegian Climate Center	r1i1p1	1.8947 x 2.5



**Table 2.** Median forecasted monthly temperature increases (degrees C) for 10 MACA downscaled GCMs under RCP 4.5 and 8.5 scenarios for Mount Baker (white rows) and the low elevation area near the North Cedarville gauge (gray rows) at 2099 compared to the 1950-2010 historical mean. Average monthly and annual temperature increases are shown in bold. The *annual average* value represents the mean annual ensemble temperature increase for both locations.

RCP 4.5														
GCM	Jan	Feb	Mar	Apr	May	Jun	Jul	Aug	Sep	Oct	Nov	Dec	AVG	
bcc-csm1-1-m	2.14	2.46	1.94	1.83	1.66	2.58	2.70	2.69	2.46	1.49	1.93	1.86	2.15	
	2.23	2.48	2.10	2.08	1.67	2.51	2.69	2.72	2.41	1.72	1.83	2.03	2.21	
CanESM2	3.36	3.26	3.55	2.66	1.96	4.50	5.32	4.63	3.56	2.29	1.71	2.24	3.25	
	3.31	3.14	3.50	2.69	1.92	4.34	5.27	4.53	3.62	2.56	1.79	2.32	3.25	
CCSM4	2.81	2.31	1.48	1.79	2.14	2.56	2.70	2.57	2.26	1.74	2.57	2.14	2.26	
	2.89	2.26	1.63	1.97	2.14	2.53	2.73	2.49	2.30	1.99	2.45	2.10	2.29	
CNRM-CM5	2.26	2.51	2.01	2.67	3.21	1.60	2.27	2.67	2.26	1.60	1.90	1.85	2.23	
	2.19	2.50	2.13	2.82	3.06	1.59	2.37	2.64	2.43	1.94	1.95	1.89	2.29	
CSIRO-Mk3-6-0	2.65	2.48	2.44	2.22	1.92	3.34	3.45	4.38	3.24	2.60	2.60	2.22	2.79	
	2.58	2.45	2.50	2.33	1.93	3.33	3.58	4.35	3.24	2.83	2.61	2.24	2.83	
HadGEM2-CC365	2.59	1.68	4.35	3.53	3.27	2.98	3.85	3.81	3.60	2.94	1.72	1.95	3.02	
	2.61	1.60	4.42	4.01	3.06	2.96	3.71	3.79	3.56	3.05	1.73	2.02	3.04	
HadGEM2-ES365	2.50	1.99	4.06	4.27	2.88	3.35	4.06	4.35	3.97	3.54	2.86	1.89	3.31	
	2.54	1.89	4.09	4.89	2.91	3.41	4.00	4.24	4.01	3.83	2.83	1.86	3.38	
IPSL-CM5A-MR	2.08	2.23	2.81	2.44	2.25	2.46	3.70	3.20	3.44	2.31	2.08	3.00	2.67	
	2.09	2.30	2.95	2.55	2.21	2.56	3.71	3.22	3.39	2.56	2.11	3.08	2.73	
MIROC5	2.02	1.67	2.44	1.94	1.53	2.13	2.12	2.97	2.00	1.83	2.31	2.20	2.10	
	1.97	1.71	2.57	2.07	1.55	2.27	2.11	2.90	2.05	2.01	2.38	2.29	2.16	
NorESM1-M	2.94	2.58	2.44	1.71	2.58	3.00	3.25	3.29	2.19	1.88	2.14	1.52	2.46	
	3.11	2.72	2.55	1.94	2.57	3.03	3.33	3.31	2.23	2.16	2.12	1.54	2.55	
Monthly Average	2.54	2.31	2.80	2.62	2.32	2.85	3.35	3.44	2.91	2.34	2.18	2.11		
Annual Average	2.65													
RCP 8.5														
bcc-csm1-1-m	3.40	3.21	2.97	2.64	3.20	3.90	4.52	4.09	3.39	2.64	2.52	2.90	3.28	
	3.53	3.17	3.04	2.84	3.24	3.81	4.52	4.04	3.45	2.86	2.55	3.05	3.34	
CanESM2	5.10	4.51	4.81	3.51	3.06	4.81	7.44	6.82	5.40	3.76	3.04	3.59	4.65	
	5.17	4.49	4.88	3.58	3.13	4.86	7.30	6.74	5.44	3.90	3.15	3.68	4.69	
CCSM4	3.81	3.10	2.15	2.35	2.97	3.31	4.09	4.57	3.40	2.94	3.80	3.75	3.35	
	3.79	3.18	2.37	2.56	2.93	3.46	4.21	4.51	3.48	3.14	3.82	3.71	3.43	
CNRM-CM5	3.42	2.90	3.16	3.75	4.05	3.00	3.99	4.38	3.75	2.23	2.60	2.75	3.33	
	3.40	2.88	3.14	3.84	3.79	2.91	3.99	4.11	3.60	2.43	2.70	2.91	3.31	
CSIRO-Mk3-6-0	3.43	3.08	2.43	2.69	2.84	4.30	5.43	5.19	4.44	3.39	2.87	2.98	3.59	
	3.36	3.15	2.40	2.91	2.87	4.31	5.48	5.22	4.38	3.56	2.92	3.03	3.63	
HadGEM2-CC365	3.60	2.84	6.55	4.79	4.22	4.80	5.88	5.88	5.63	4.73	3.77	3.06	4.65	
	3.64	2.89	6.65	5.37	3.98	4.85	5.79	5.82	5.74	4.99	3.83	3.07	4.72	
HadGEM2-ES365	3.34	3.74	5.96	5.37	3.56	5.42	5.47	5.90	5.39	4.38	3.64	2.88	4.59	
	3.39	3.66	6.17	5.93	3.66	5.25	5.50	5.84	5.37	4.61	3.62	2.91	4.66	
IPSL-CM5A-MR	3.41	3.37	3.53	3.19	3.68	3.92	4.91	5.00	4.93	3.78	3.52	4.39	3.97	
	3.58	3.32	3.64	3.29	3.54	4.03	5.00	5.05	4.92	4.11	3.58	4.47	4.04	
MIROC5	2.71	2.46	2.86	2.44	2.41	3.14	3.71	4.08	3.12	2.77	2.55	2.51	2.90	
	2.68	2.37	2.84	2.55	2.33	3.26	3.77	4.10	3.15	3.02	2.62	2.51	2.93	
NorESM1-M	2.54	2.20	1.81	2.07	3.20	3.95	5.08	4.78	3.96	3.04	2.78	2.35	3.15	
	2.67	2.25	1.98	2.27	3.06	3.93	5.09	4.76	3.91	3.22	2.82	2.35	3.19	
Monthly Average	3.50	3.14	3.67	3.40	3.29	4.06	5.06	5.04	4.34	3.48	3.14	3.14		
Annual Average	3.77													

**Table 3.** Final calibrated monthly temperature lapse rates for the North, Middle, and South Fork basins of the Nooksack River.

<b>Month</b>	<b>Lapse Rate (dec C/km)</b>			
	<b>North Fork (modified cells)</b>	<b>North Fork (all others)</b>	<b>Middle Fork (all cells)</b>	<b>South Fork (all cells)</b>
<i>January</i>	-5	-6	-6	-8.5
<i>February</i>	-6	-7	-7	-8.5
<i>March</i>	-7	-8	-8	-8.5
<i>April</i>	-8	-9	-9	-8.5
<i>May</i>	-9	-9.8	-9.8	-8.5
<i>June</i>	-9	-9.8	-9.8	-8.5
<i>July</i>	-9	-9.8	-9.8	-8.5
<i>August</i>	-9	-9.8	-9.8	-8.5
<i>September</i>	-8	-9	-9	-8.5
<i>October</i>	-7	-8	-8	-8.5
<i>November</i>	-6	-7	-7	-8.5
<i>December</i>	-5	-6	-6	-8.5

**Table 4.** Calibrated constants and parameters for the DHSVM and coupled glacier dynamics model for the North, Middle, and South Fork basins.

Description	Value		
Global Constants			
	North Fork	Middle Fork	South Fork
Ground Roughness (m)	0.02	0.02	0.02
Snow Roughness (m)	0.01	0.01	0.01
Rain Threshold (°C)	-1	0	0.5
Snow Threshold (°C)	1	2	2
Snow Water Capacity	0.07	0.07	0.03
Rain LAI Multiplier	0.0003	0.0003	0.0003
Snow LAI Multiplier	0.0003	0.0003	0.0003
Min Intercepted Snow (m)	0.005	0.005	0.005
Temperature Lapse Rate (°C/m)	VARIABLE	VARIABLE	-0.0085
Glacier Albedo	0.25	0.25	0.32
Maximum Snow Albedo	0.81	0.81	0.81
Soil Parameters			
Loamy Sand			
Lateral Conductivity (m/s)	0.001	0.005	0.001
Exponential Decrease	5	5	3
Porosity	0.42/0.42/0.42	0.42/0.42/0.42	0.42/0.42/0.42
Sandy Loam			
Lateral Conductivity (m/s)	0.005	0.0025	0.0005
Exponential Decrease	5	5	3
Porosity	0.4/0.4/0.4	0.4/0.4/0.4	0.4/0.4/0.4
Silty Loam			
Lateral Conductivity (m/s)	0.0005	0.0005	0.0001
Exponential Decrease	5	5	3
Porosity	0.46/0.46/0.46	0.46/0.46/0.46	0.46/0.46/0.46
Loam			
Lateral Conductivity (m/s)	0.0005	0.0005	0.0001
Exponential Decrease	5	5	3
Porosity	0.43/0.43/0.43	0.43/0.43/0.43	0.43/0.43/0.43
Soil Thickness, Max/Min (m)	3.5/0.76	3.5/0.76	3.5/0.76

**Table 5.** Glacier area and volume errors for the upper Nooksack River Basin for 1950 and 2009 compared to observed areal ice extent.

<b>All Nooksack Glaciers (1950)</b>		
area observed (sq km)	area modeled (sq km)	error (%)
38.37	43.75	14

<b>All Nooksack Glaciers (2009)</b>		
area observed (sq km)	area modeled (sq km)	error (%)
33.6	49.05	46

<b>Modeled Ice Volume (2009)</b>	
Outside Observed Area	Inside Observed Area
31%	69%

**Table 6.** Calibrated model Nash-Sutcliffe efficiency scores, cumulative discharge error, and mean monthly streamflow error at the North Fork, Middle Fork, South Fork, and North Cedarville USGS stream gauge locations. North, Middle, and South Fork statistics represent 10-year calibration and validation periods while the North Cedarville statistics only represent a 5-year simulation due to a limitation of consistent stream gauge data at that location.

	USGS Stream Gauge Location			
	North Fork	Middle Fork	South Fork	North Cedarville
Daily Streamflow (E)	0.63	0.51	0.64	0.53
Monthly Streamflow (E)	0.78	0.74	0.87	0.71
Cumulative Streamflow Error (%)	-4.89	-5.94	3.12	3.61
Mean Monthly Error (%)	-3.77	-4.68	1.87	4.57

**Table 7.** Modeled changes in glacier melt magnitude for the North and Middle Fork basins of the Nooksack River as well as the North Cedarville gauge location for the years 2025, 2050, and 2075. Each percentage refers to a deviation from the historical (1950-2010) monthly median.

	Month	RCP 4.5	RCP 8.5	RCP 4.5	RCP 8.5	RCP 4.5	RCP 8.5
		2025		2050		2075	
North Fork	May	45%	56%	-91%	-91%	-97%	-98%
	Jun	20%	20%	-89%	-89%	-98%	-99%
	Jul	30%	41%	-48%	-39%	-88%	-85%
	Aug	47%	46%	-20%	-14%	-59%	-60%
	Sep	46%	51%	-14%	-10%	-55%	-58%
	Oct	78%	104%	-10%	19%	-46%	-41%
Middle Fork	May	0%	0%	0%	0%	0%	0%
	Jun	435%	462%	-50%	-25%	-73%	-58%
	Jul	28%	33%	-81%	-62%	-98%	-95%
	Aug	78%	87%	15%	37%	-55%	-52%
	Sep	73%	74%	21%	28%	-45%	-51%
	Oct	77%	80%	4%	29%	-56%	-53%
North Cedarville	May	31%	43%	-92%	-92%	-97%	-97%
	Jun	25%	25%	-89%	-88%	-98%	-99%
	Jul	28%	41%	-51%	-41%	-89%	-86%
	Aug	50%	53%	-16%	-5%	-59%	-59%
	Sep	49%	51%	-9%	-4%	-53%	-57%
	Oct	80%	100%	-6%	22%	-46%	-44%

**Table 8.** Modeled percent of monthly median streamflow component derived from glacier ice melt for the North and Middle Fork basins and North Cedarville for historical and RCP 4.5 and 8.5 future scenarios. Historical melt component is a monthly median representing a 60-year simulation period from 1950-2010. Future results represent 30-year medians centered on 2025, 2050, or 2075.

	Month	1950-2010	RCP 4.5	RCP 8.5	RCP 4.5	RCP 8.5	RCP 4.5	RCP 8.5
			2025		2050		2075	
North Fork	May	0%	1%	1%	0%	0%	0%	0%
	Jun	1%	2%	2%	0%	0%	0%	0%
	Jul	4%	12%	13%	7%	9%	2%	4%
	Aug	16%	51%	51%	39%	47%	29%	38%
	Sep	16%	42%	44%	32%	37%	21%	23%
	Oct	2%	8%	9%	4%	5%	2%	2%
Middle Fork	May	0%	0%	0%	0%	0%	0%	0%
	Jun	0%	0%	0%	0%	0%	0%	0%
	Jul	2%	4%	4%	1%	2%	0%	0%
	Aug	12%	25%	27%	22%	28%	12%	17%
	Sep	16%	33%	32%	27%	32%	17%	19%
	Oct	2%	4%	4%	2%	3%	1%	1%
North Cedarville	May	0%	0%	0%	0%	0%	0%	0%
	Jun	1%	1%	1%	0%	0%	0%	0%
	Jul	3%	5%	6%	3%	4%	1%	1%
	Aug	13%	26%	27%	19%	24%	12%	16%
	Sep	13%	23%	23%	17%	20%	10%	12%
	Oct	1%	3%	3%	1%	2%	1%	1%

**Table 9.** Projected changes in streamflow for the North, Middle, and South Fork basins of the Nooksack River for the years 2025, 2050, and 2075. Each percentage refers to a deviation from the historical (1950-2010) monthly median.

	Month	RCP 4.5	RCP 8.5	RCP 4.5	RCP 8.5	RCP 4.5	RCP 8.5
		2025		2050		2075	
North Fork	Oct	-3%	3%	6%	6%	11%	6%
	Nov	25%	30%	42%	52%	59%	78%
	Dec	26%	37%	83%	90%	94%	169%
	Jan	76%	103%	131%	161%	161%	253%
	Feb	53%	59%	85%	93%	118%	176%
	Mar	45%	48%	61%	65%	78%	97%
	Apr	15%	16%	15%	21%	20%	19%
	May	-5%	-5%	-7%	-7%	-13%	-26%
	Jun	-6%	-8%	-16%	-21%	-30%	-49%
	Jul	-32%	-34%	-51%	-59%	-62%	-77%
	Aug	-25%	-25%	-47%	-52%	-63%	-73%
	Sep	-5%	-5%	-27%	-33%	-41%	-50%
Middle Fork	Oct	-9%	-2%	-6%	-8%	0%	9%
	Nov	18%	23%	30%	35%	39%	48%
	Dec	18%	23%	52%	53%	56%	88%
	Jan	46%	60%	85%	97%	93%	127%
	Feb	26%	34%	42%	49%	59%	79%
	Mar	27%	25%	33%	34%	36%	40%
	Apr	-1%	-3%	-7%	-1%	-9%	-16%
	May	-19%	-22%	-30%	-29%	-37%	-44%
	Jun	-16%	-18%	-27%	-29%	-35%	-49%
	Jul	-25%	-26%	-38%	-44%	-47%	-61%
	Aug	-14%	-16%	-35%	-40%	-52%	-65%
	Sep	-13%	-11%	-27%	-34%	-48%	-58%
South Fork	Oct	-13%	-11%	-9%	-17%	-9%	-7%
	Nov	17%	16%	20%	26%	32%	37%
	Dec	14%	16%	42%	41%	42%	69%
	Jan	45%	62%	72%	83%	82%	112%
	Feb	16%	25%	28%	35%	44%	61%
	Mar	24%	23%	29%	31%	30%	33%
	Apr	0%	-3%	-7%	-3%	-11%	-23%
	May	-25%	-28%	-39%	-41%	-50%	-62%
	Jun	-41%	-42%	-54%	-57%	-65%	-75%
	Jul	-40%	-42%	-59%	-66%	-65%	-76%
	Aug	-40%	-41%	-51%	-56%	-57%	-65%
	Sep	-39%	-43%	-47%	-53%	-57%	-64%
North Cedarville	Oct	-13%	-11%	-8%	-14%	-8%	-2%
	Nov	15%	15%	25%	31%	35%	43%
	Dec	15%	18%	44%	43%	44%	76%
	Jan	43%	64%	73%	86%	85%	119%
	Feb	18%	26%	32%	38%	45%	63%
	Mar	21%	20%	26%	28%	29%	33%
	Apr	3%	0%	-2%	2%	-3%	-12%
	May	-16%	-17%	-27%	-27%	-33%	-44%
	Jun	-18%	-19%	-29%	-33%	-40%	-55%
	Jul	-32%	-34%	-48%	-56%	-59%	-72%
	Aug	-25%	-27%	-45%	-49%	-58%	-67%
	Sep	-18%	-17%	-30%	-38%	-44%	-54%



## 8.0 Figures

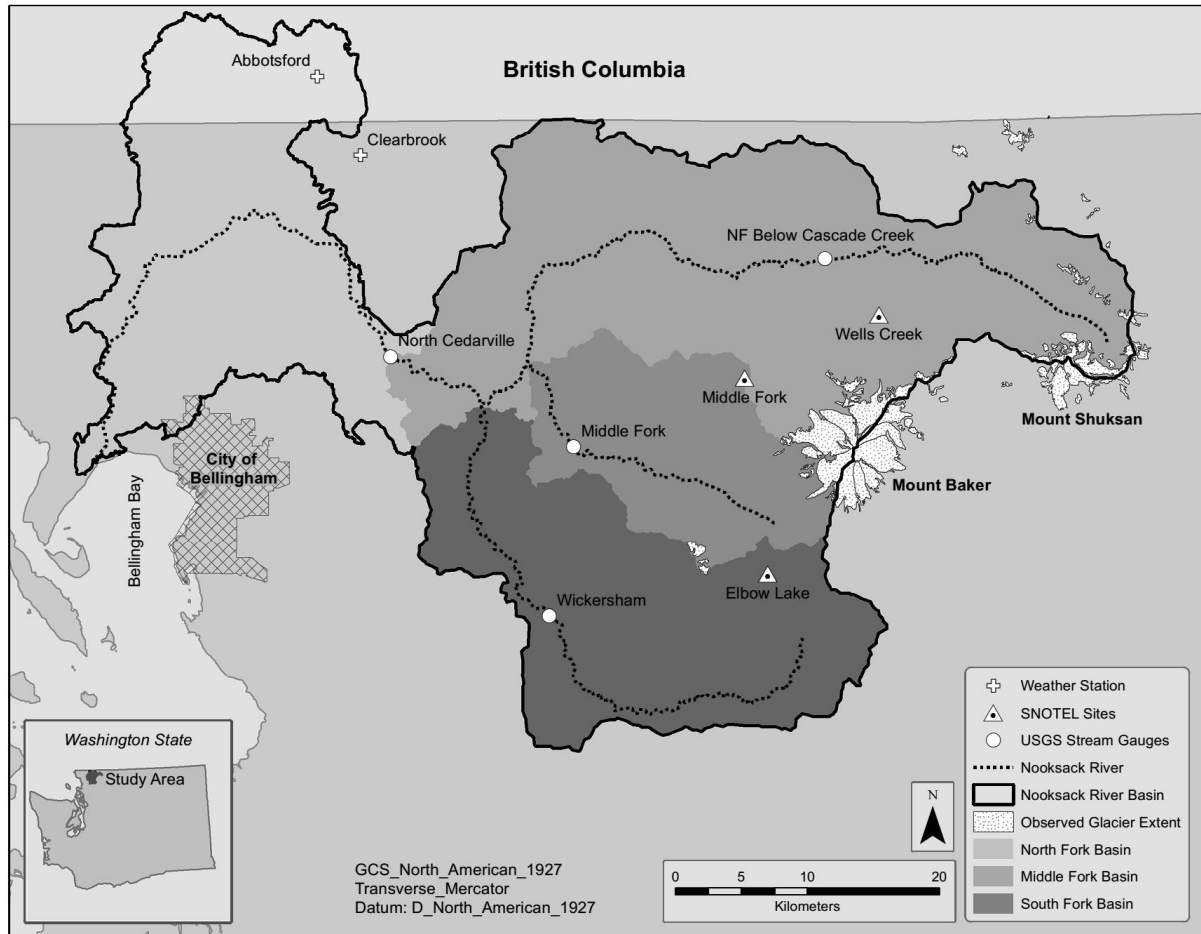


**Figure 1.** The Nooksack River basin located in northwest Washington State. USGS stream gauges are shown with circles. Active SNOTEL stations at Elbow Lake (south fork), Middle Fork (middle fork), and Wells Creek (north fork) are indicated by dotted triangles. Weather stations are indicated by plus signs. The horizontal line across the top of the watershed indicates the United States-Canada border.

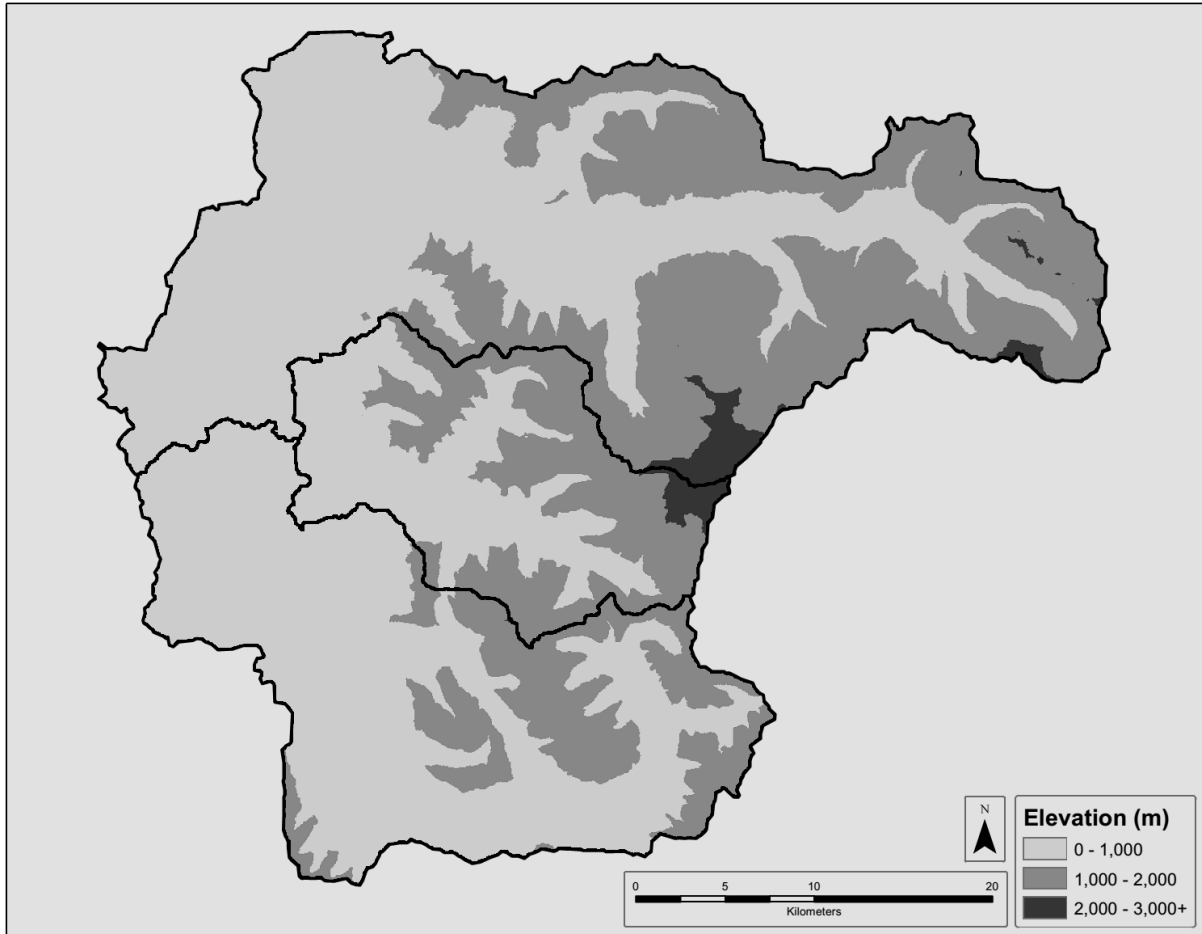


**Figure 2.** Elevation bands for the upper Nooksack River Basin indicating lower elevation (lighter colored) to higher elevation (darker colored) regions. The North, Middle, and South Fork basins are outlined in black.

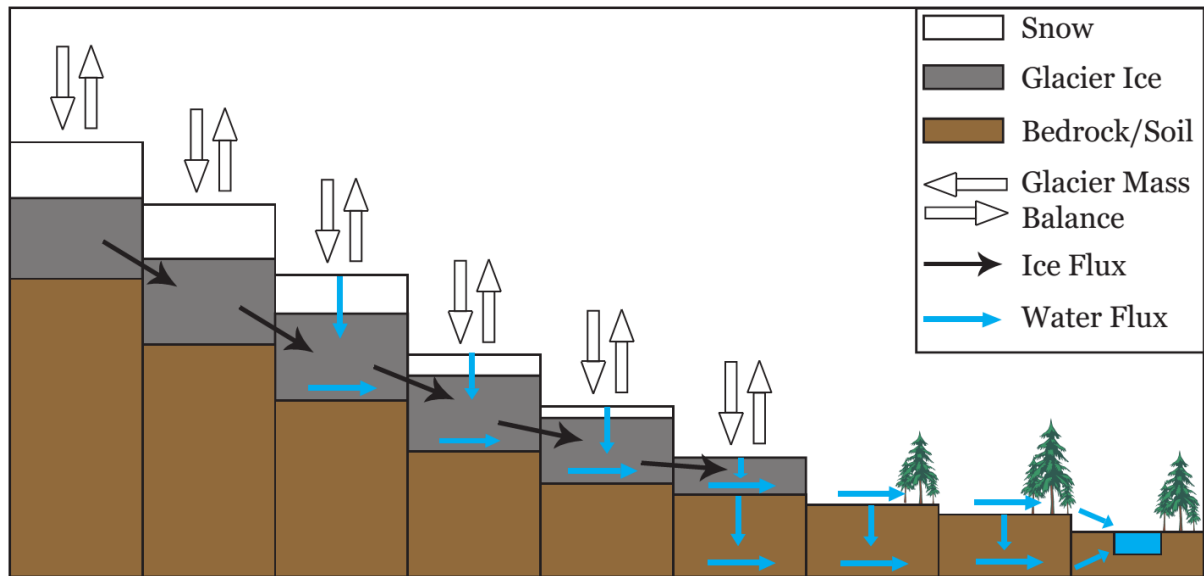


**Figure 3.** Water and ice flux processes and how they are simulated by the coupled DHSVM and glacier dynamics model. Mass and energy fluxes as well as ice and snow-water equivalent determine monthly mass balance for each 50m grid cell (modified from Naz et al., 2014).

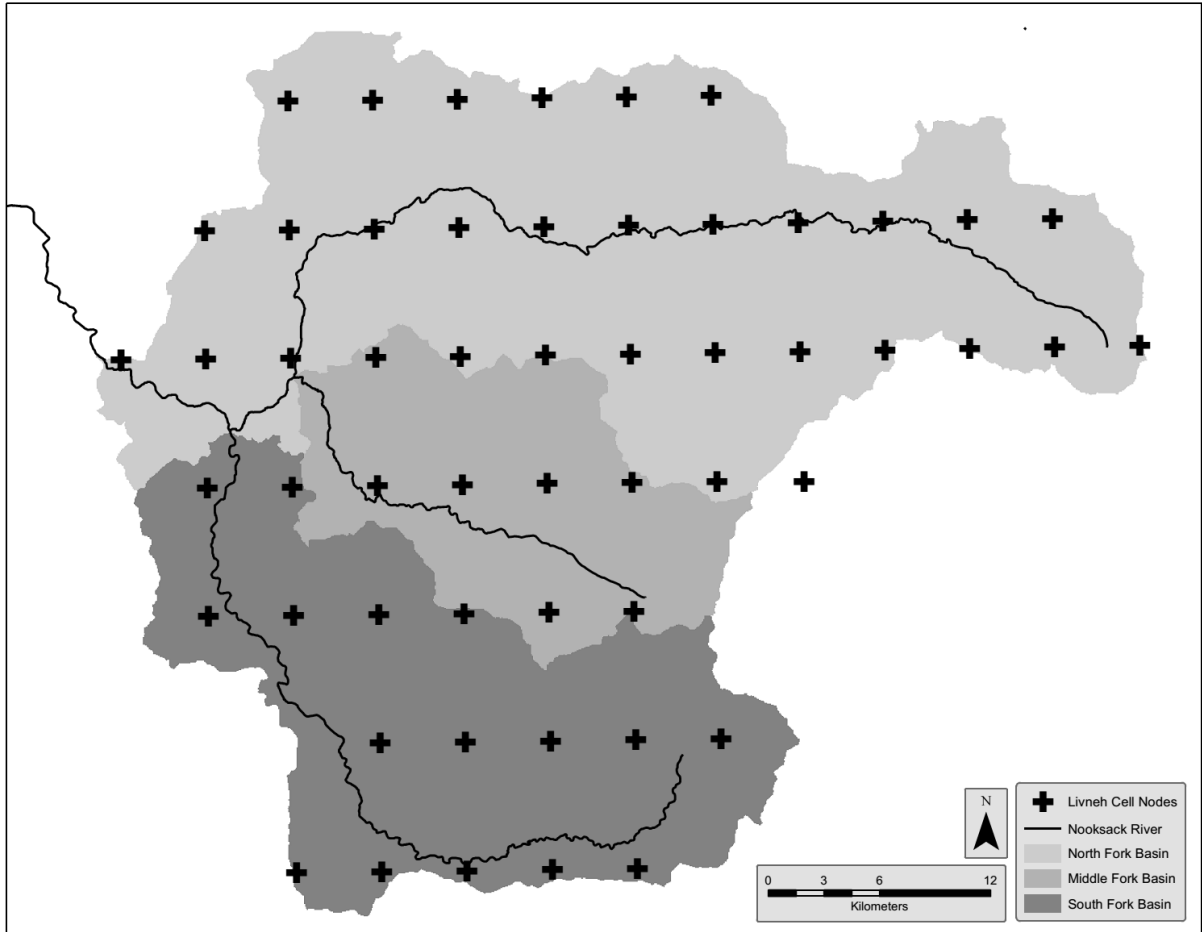


**Figure 4.** Center nodes of 1/16 degree Livneh grid overlain on the upper Nooksack River basin. Grid points are used as the locations for the Livneh meteorology forcing inputs.

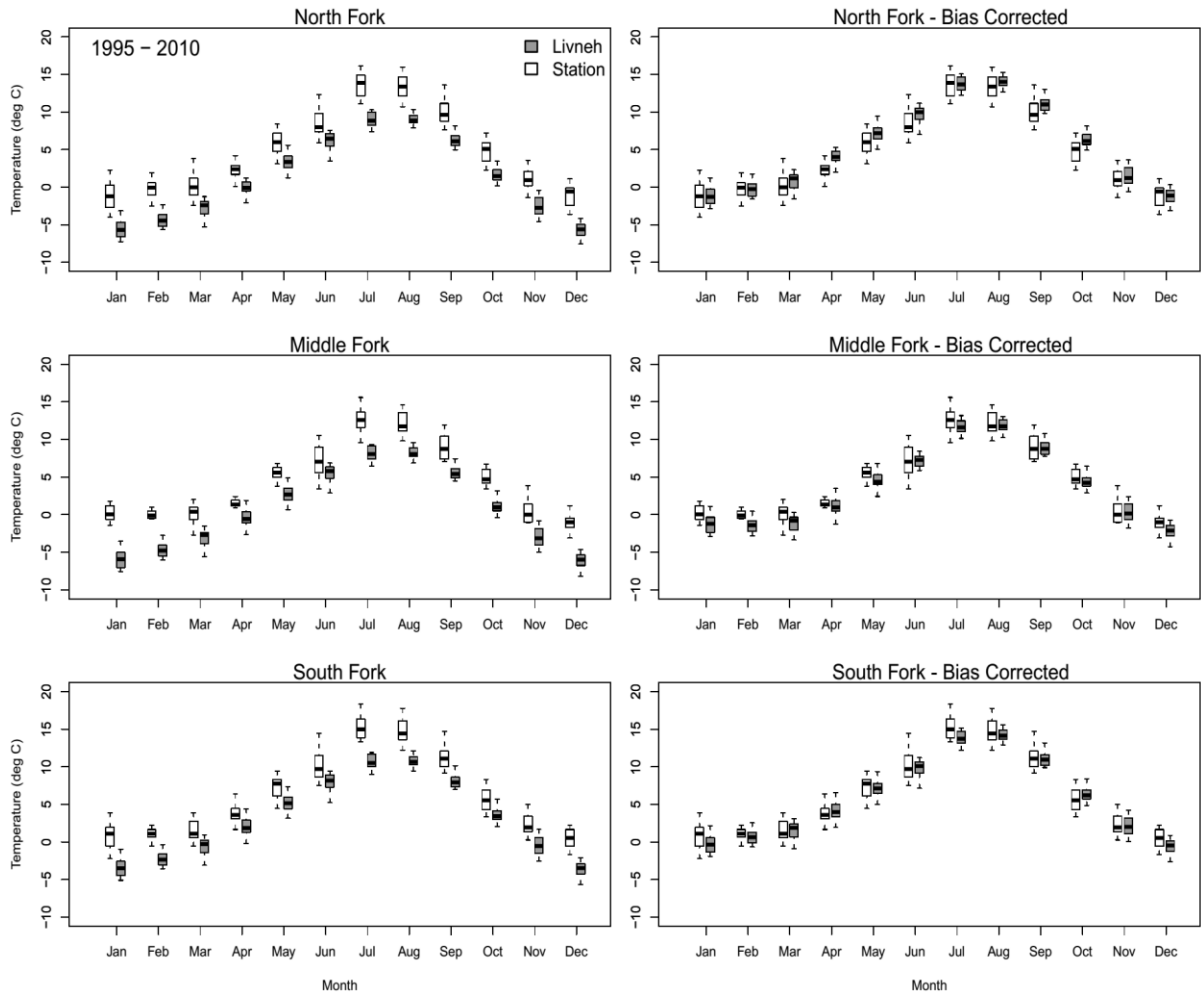


**Figure 5.** Monthly median SNOTEL temperature observations (1995-2010) for the North, Middle, and South Fork basins compared with Livneh temperatures before and after a delta change correction was applied to eliminate a cold bias found when compared to PRISM 30-yr normals (1981-2010). The Middle Fork SNOTEL was not operational prior to water year 2003.

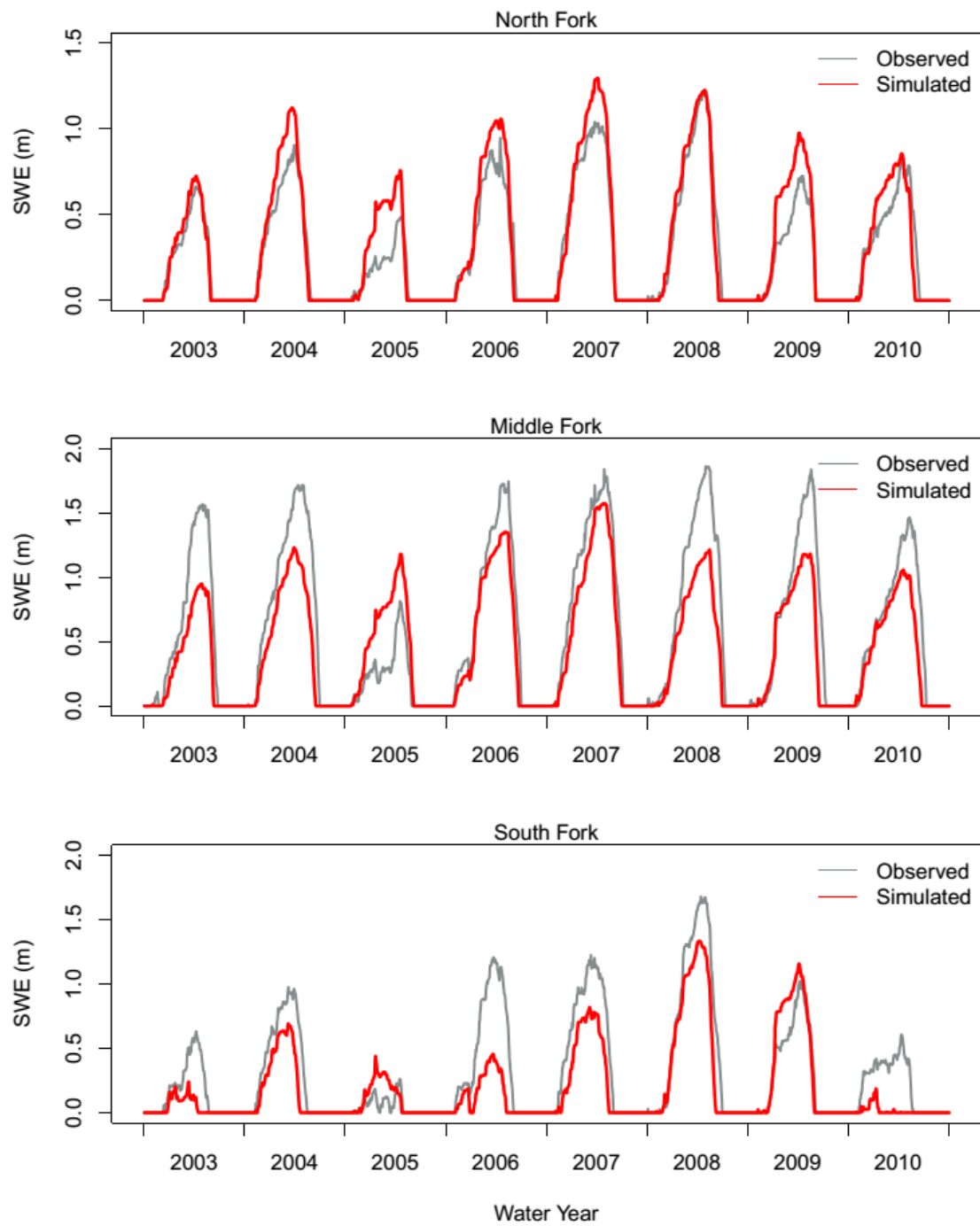


**Figure 6.** Daily SWE calibration results at the Wells Creek (North Fork), Middle Fork, and Elbow Lake (South Fork) SNOTEL site locations.

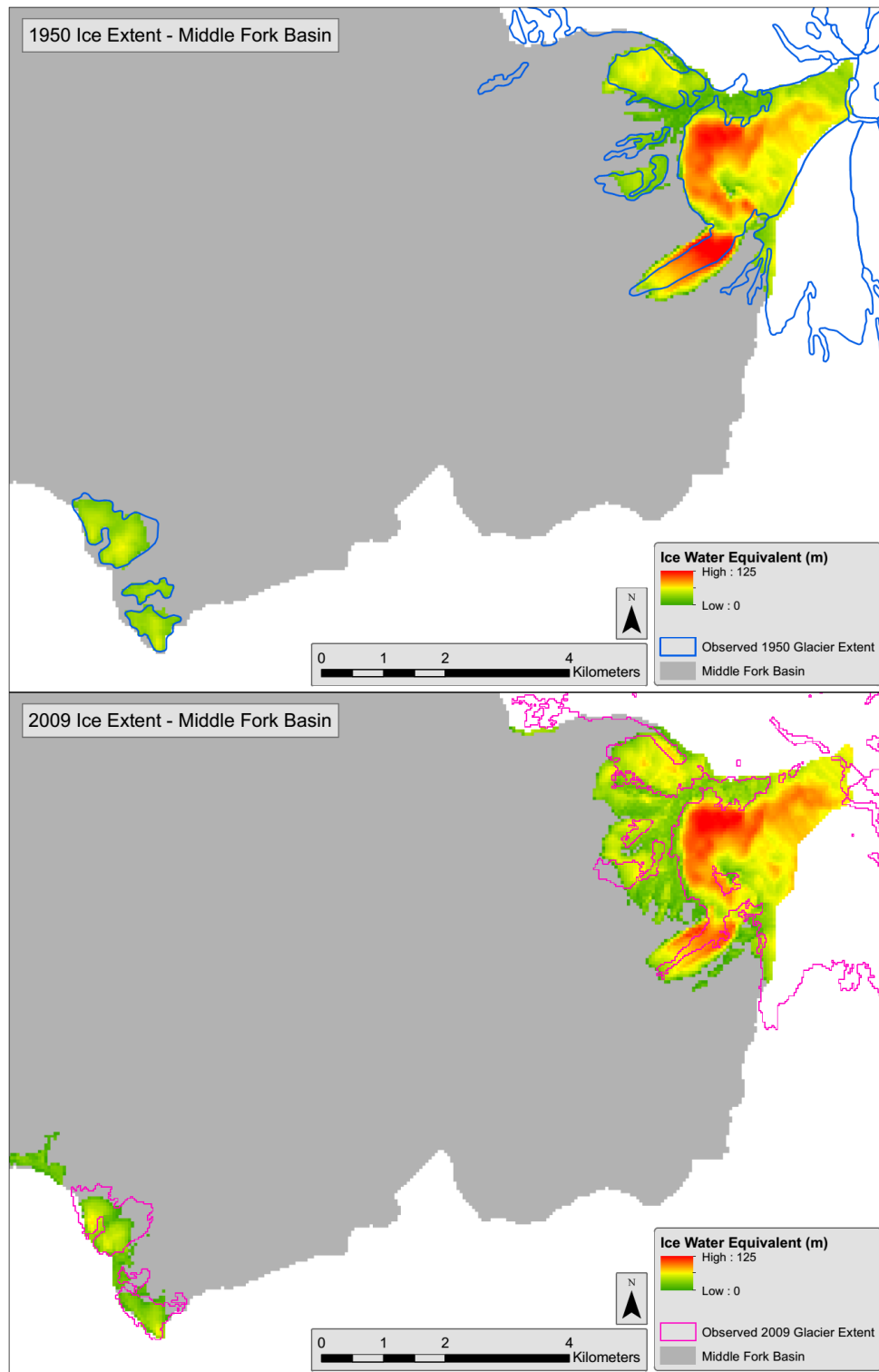


**Figure 7.** Top figure shows the initial ice extent and ice thickness for glaciated areas of the Middle Fork basin for year 1950 after model spinup. Estimated 1950 ice extent is indicated by the blue outline. Bottom figure shows the estimated ice extent and ice thickness for September of 2009 after a model run from 1950-2009. Digitized observed areal extent is shown in pink.

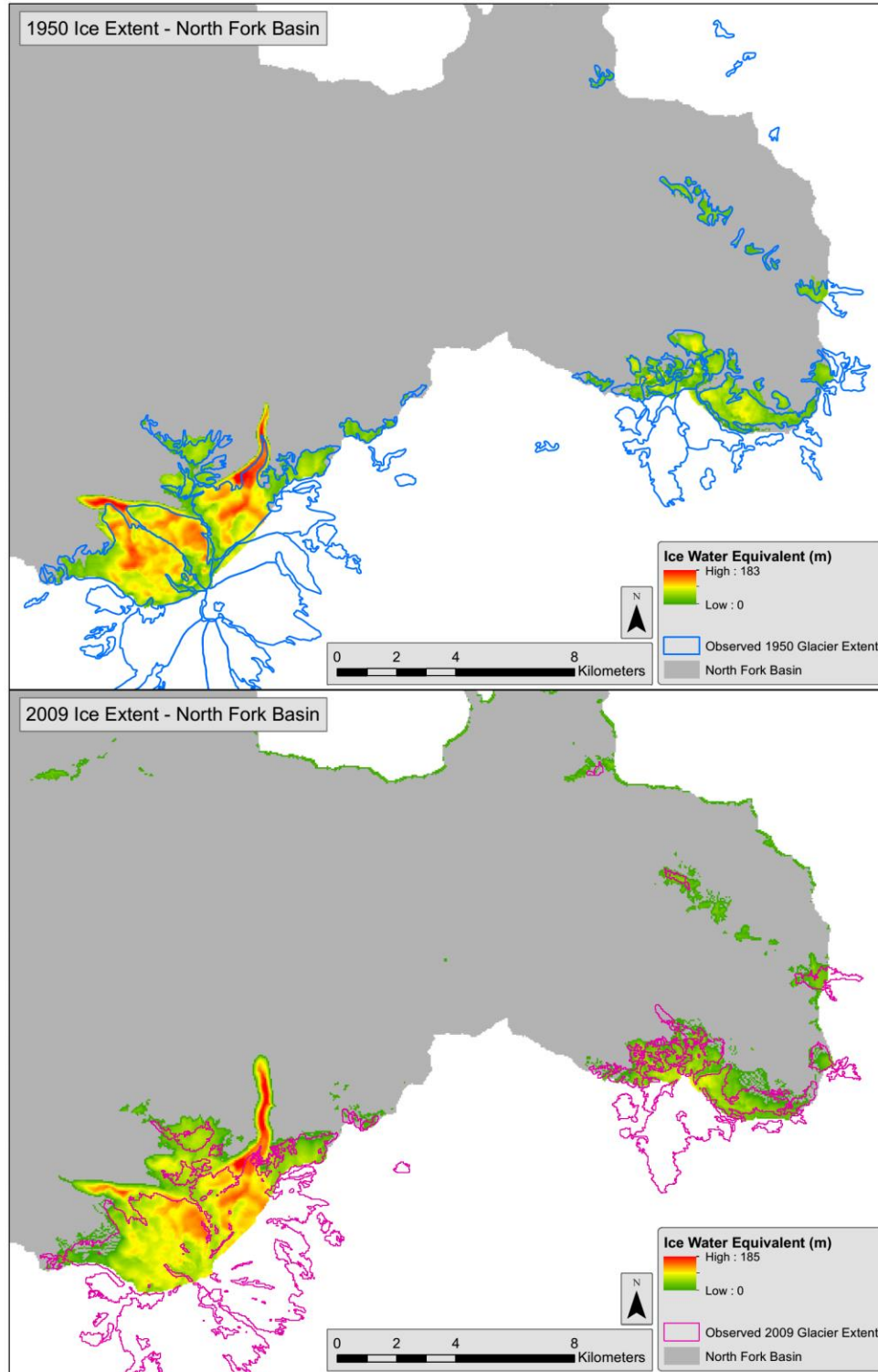


**Figure 8.** Top figure shows the initial ice extent and ice thickness for glaciated areas of the North Fork Nooksack basin for year 1950 after model spinup. Estimated 1950 ice extent is indicated by the blue outline. Bottom figure shows the estimated ice extent and ice thickness for September of 2009 after a model run from 1950-2009. Digitized observed areal extent is shown in pink.



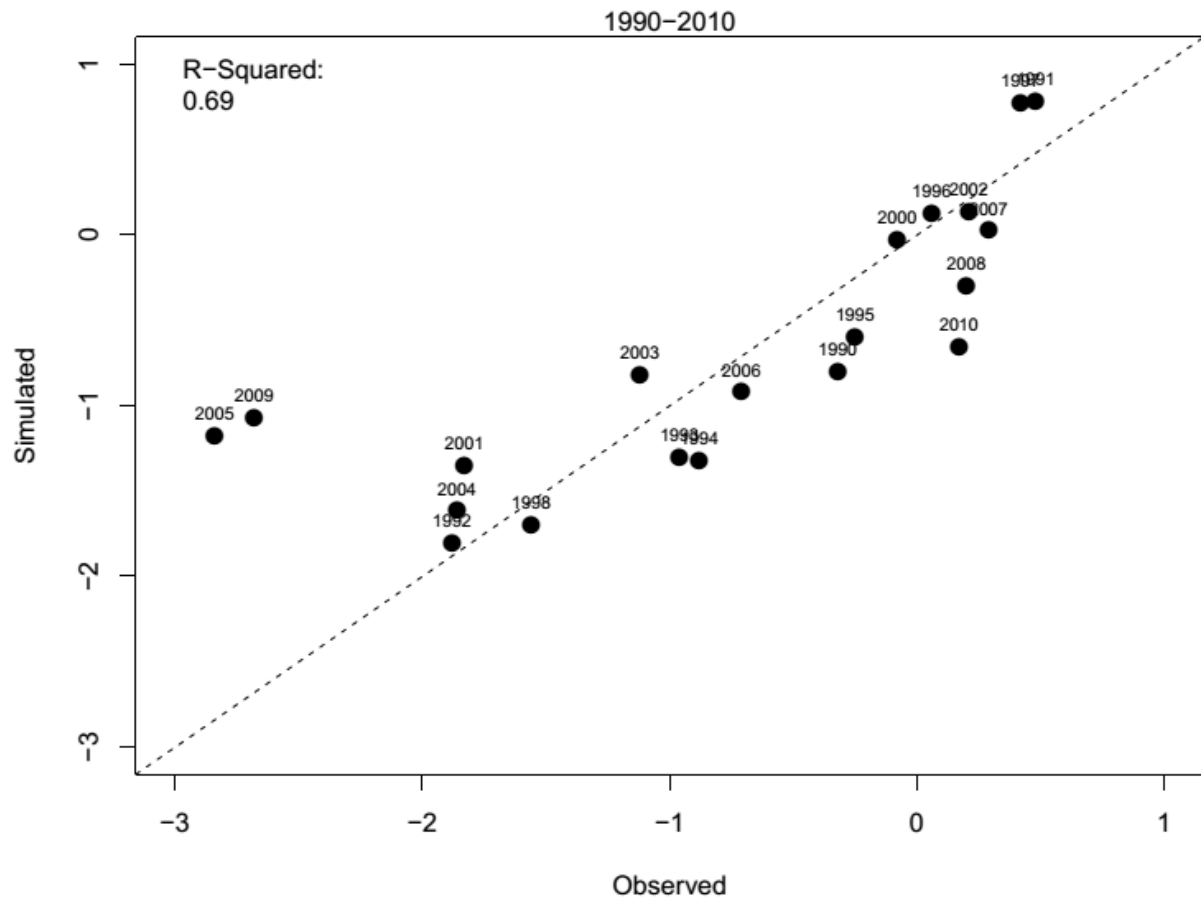


**Figure 9.** Comparison between simulated and observed annual glacier mass balance for the Sholes Glacier on Mount Baker in the North Fork Nooksack River basin for 1990 to 2010 (observations from Pelto and Brown, 2012).

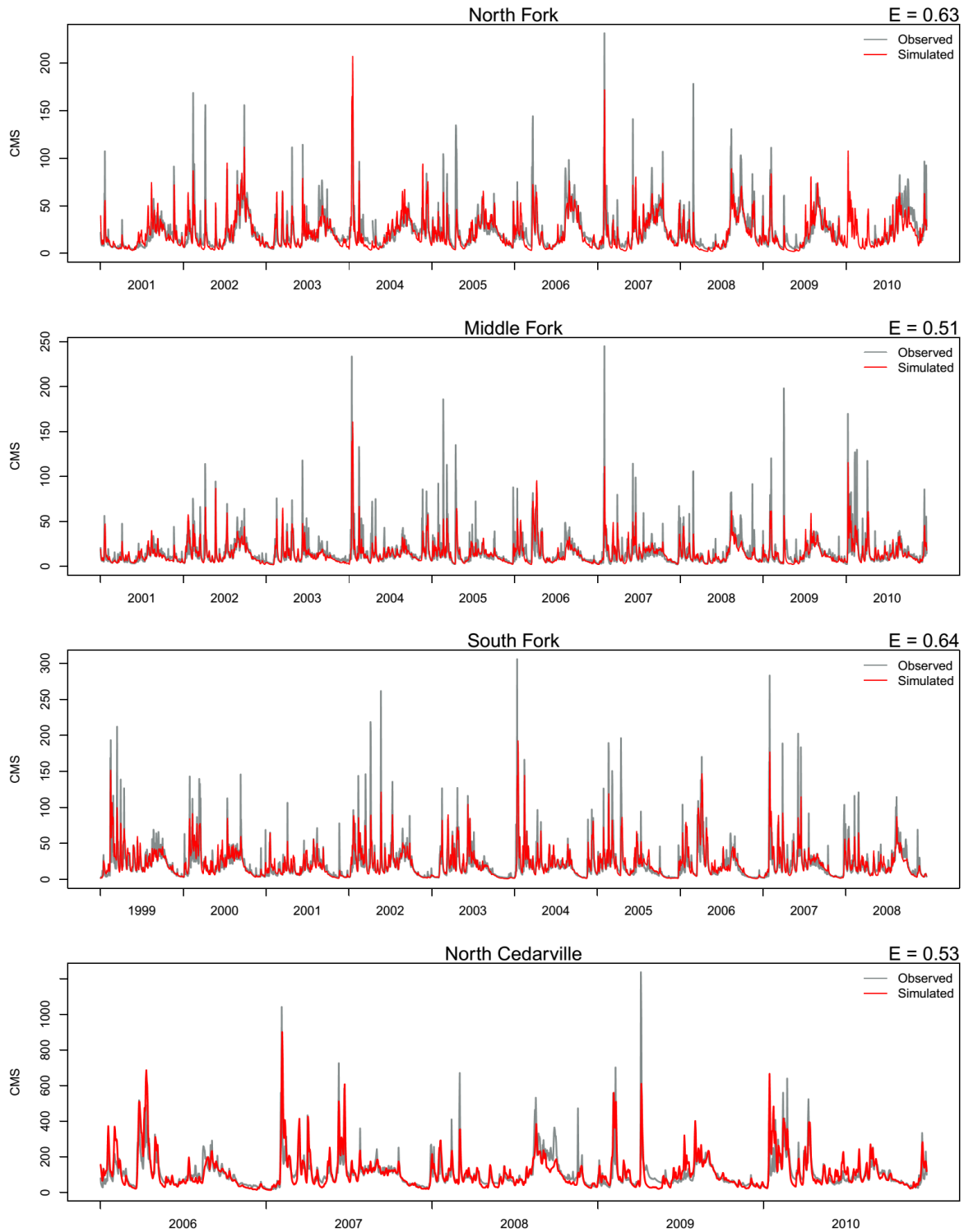


**Figure 10.** Daily streamflow calibration results at North Cedarville and the North, Middle, and South Fork basins of the Nooksack River at their respective USGS stream gauge locations. Nash-Sutcliffe efficiency scores are shown in the upper right corner of each plot. 2006 was the first year of consistent record for the North Cedarville gauge.

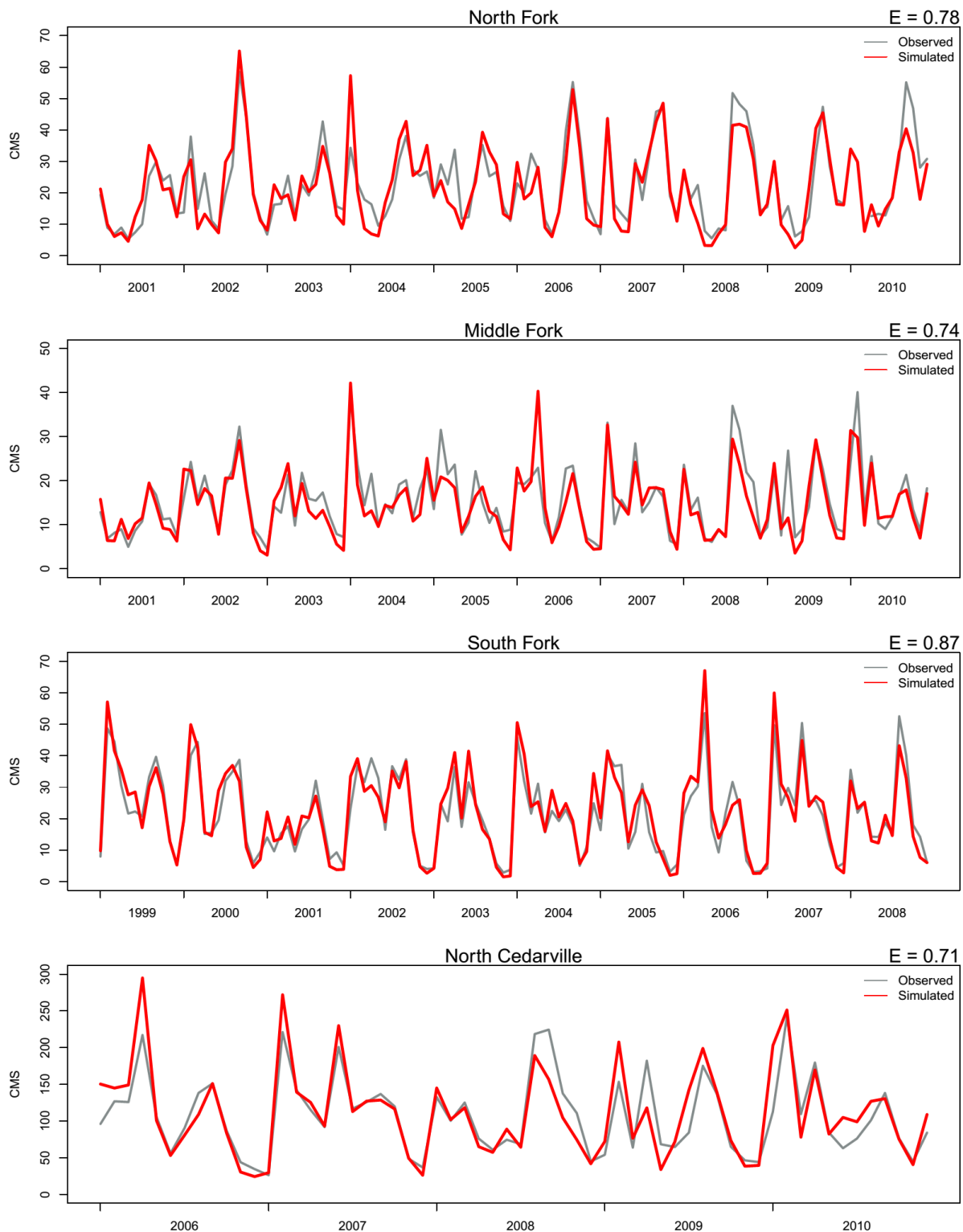


**Figure 11.** Monthly median streamflow calibration results at North Cedarville and the North, Middle, and South Fork basins of the Nooksack River at their respective USGS stream gauge locations. Nash-Sutcliffe efficiency scores are shown in the upper right corner of each plot.

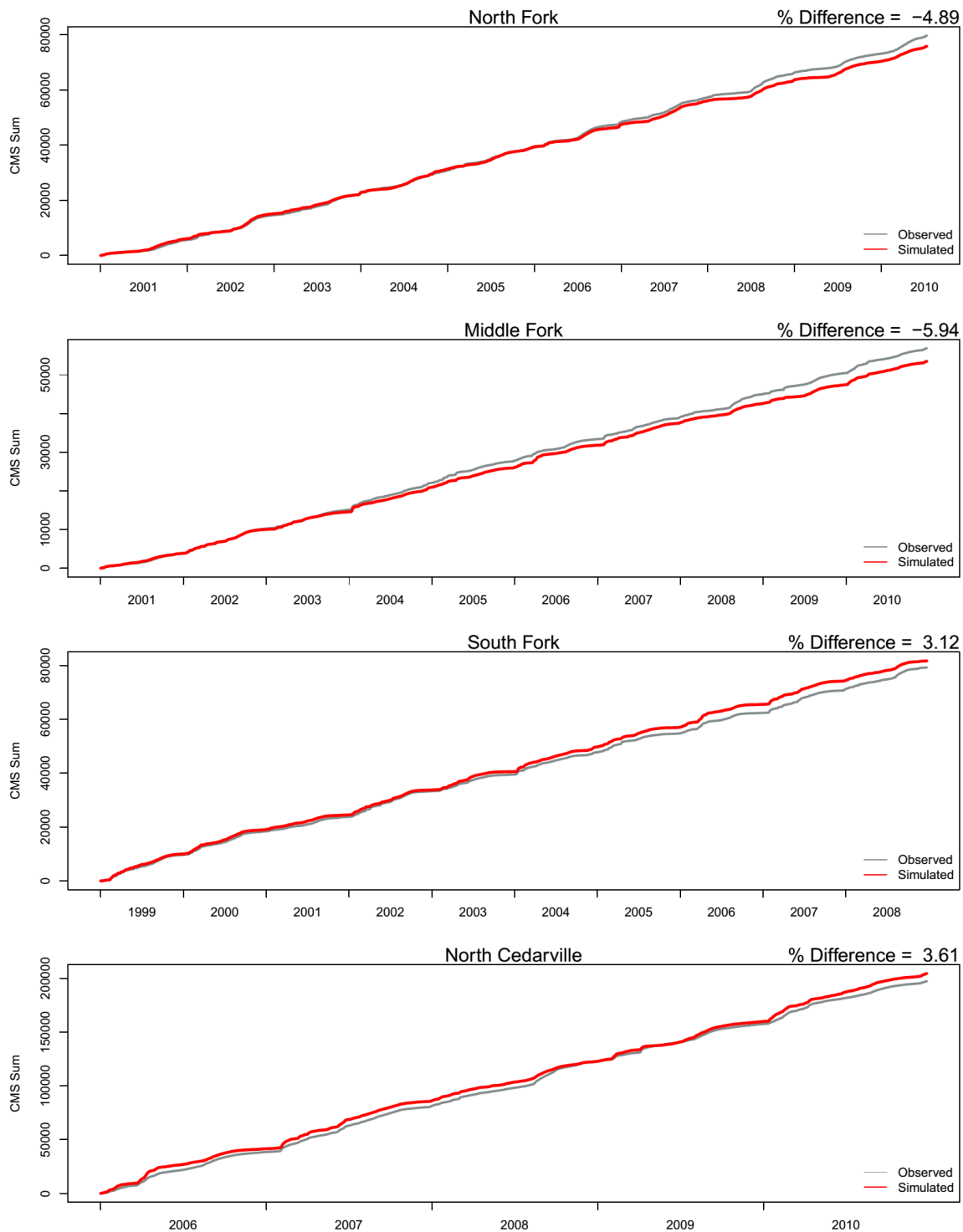


**Figure 12.** Modeled and Observed cumulative discharge (a summation of each time-step) at North Cedarville and the North, Middle, and South Fork basins of the Nooksack River at their respective USGS stream gauge locations. The discharge error of the model is shown at the top right of each plot. Positive error indicates an overestimation of flow while negative error indicates an underestimation of streamflow.

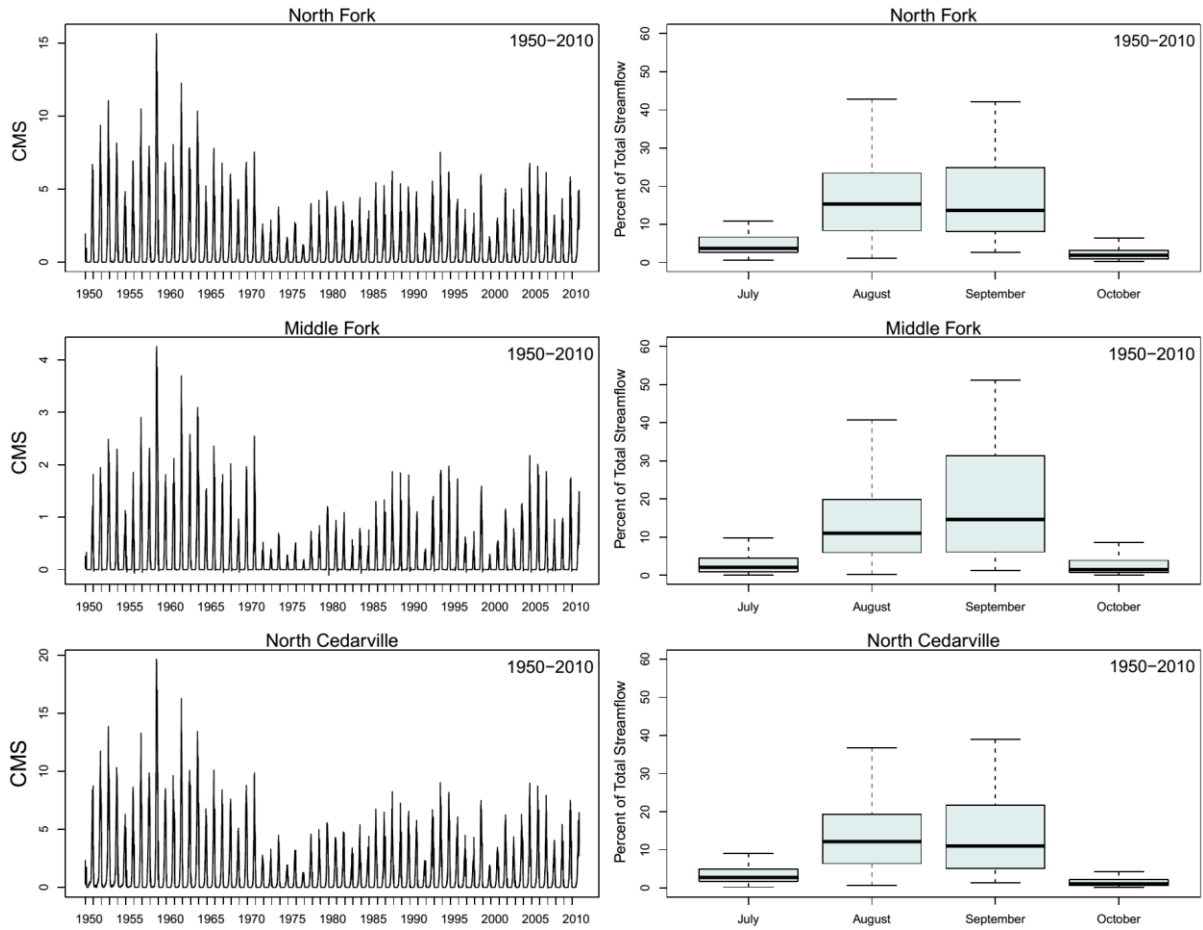


**Figure 13.** Modeled historic (1950-2010) glacier ice melt contribution to streamflow in daily magnitude (cms; left plots) and as a percent of total median monthly streamflow (right plots) for the North Fork and Middle Fork basins as well as the North Cedarville gauge location.

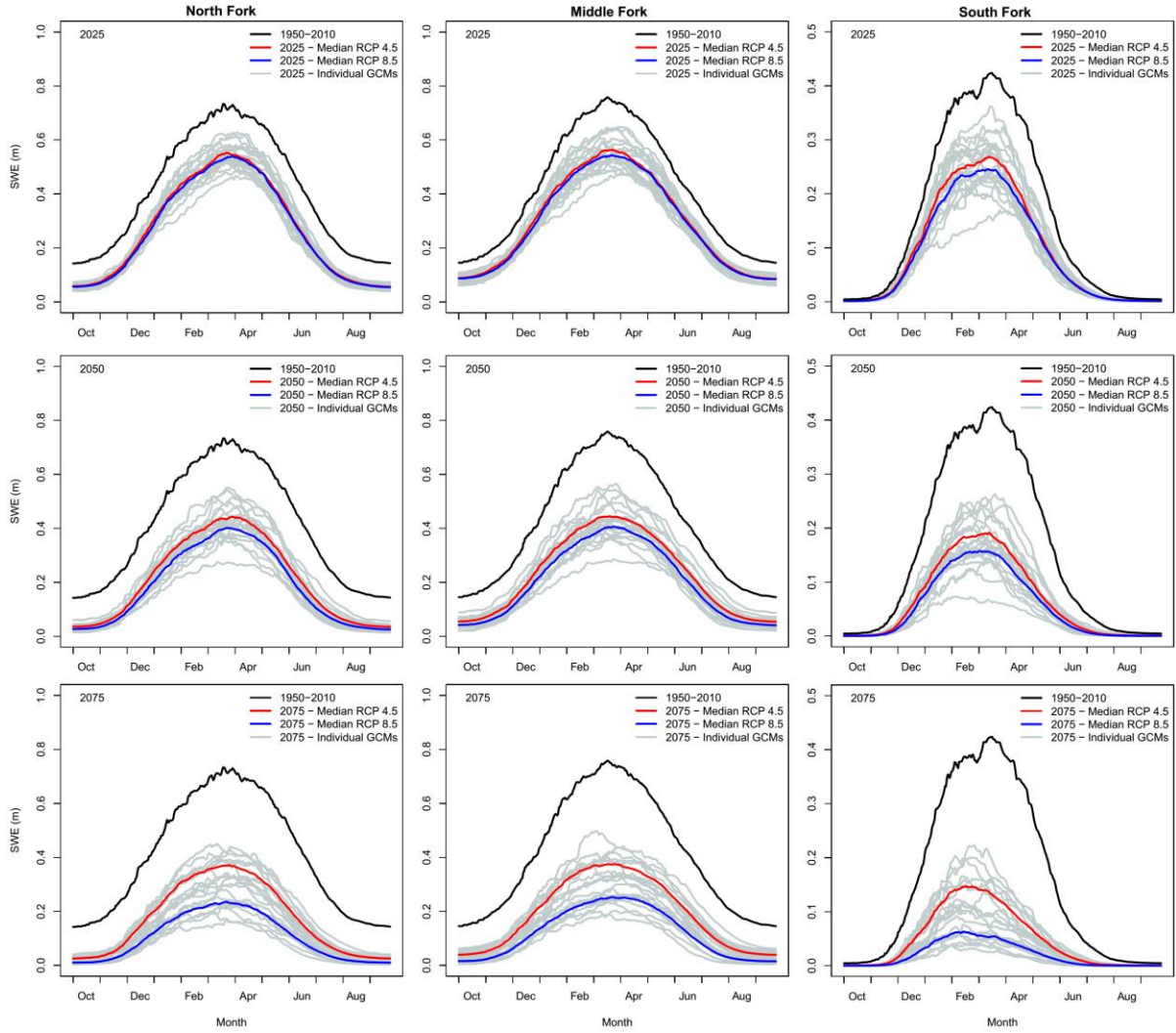


**Figure 14.** Modeled future daily median basin average SWE for the North Fork (left plots), Middle Fork (middle plots), and South Fork (right plots) basins for all 10 GCMs under RCP 4.5 and 8.5 scenarios. Historical flow line (black) represents a 60-year modeled median daily SWE magnitude (1950-2010) while each of the future scenarios (RCP 4.5 in red and RCP 8.5 in blue) represent 30-year median daily SWE magnitudes centered on their respective year (2025, 2050, or 2075). Gray lines each represent the median SWE from an individual GCM and RCP scenario over a 30-yr period.

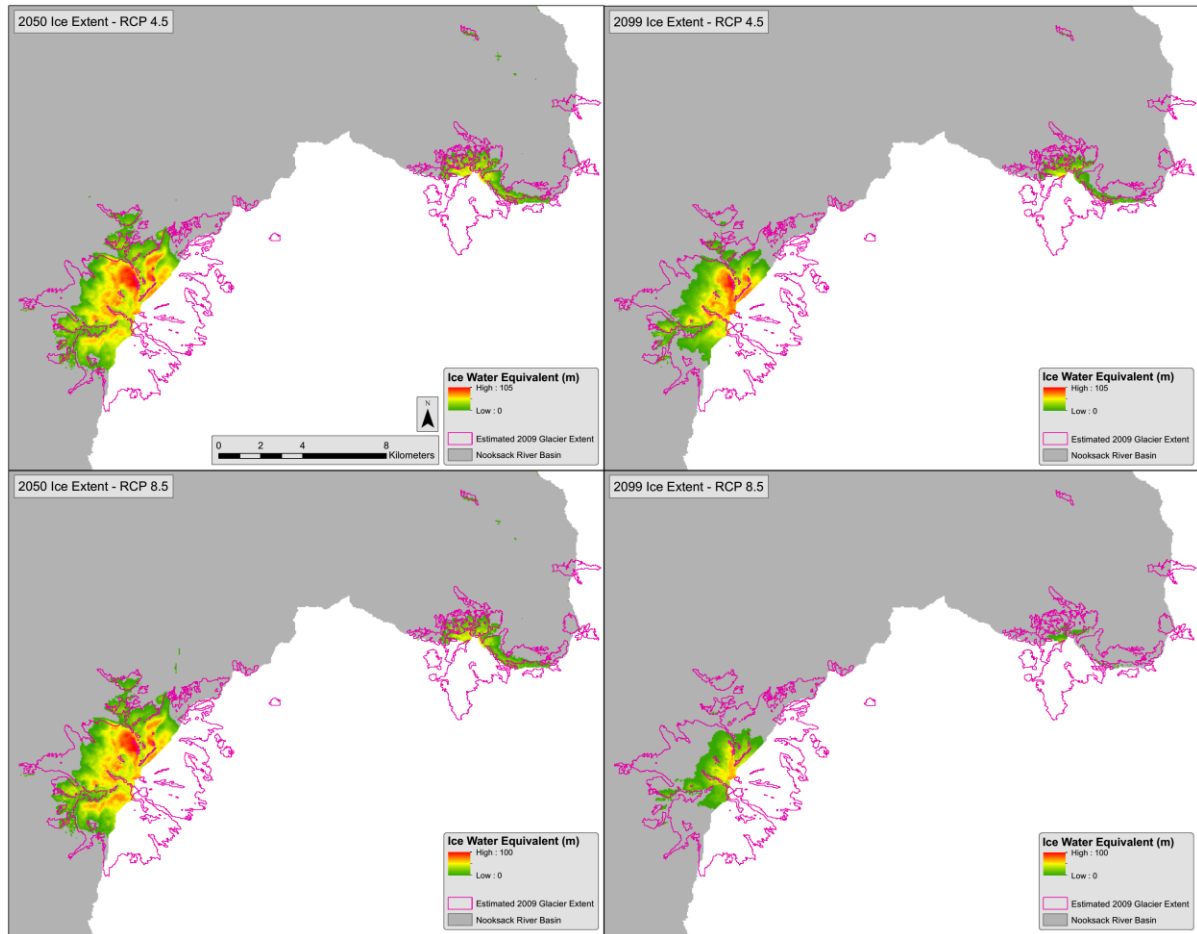


**Figure 15.** Modeled Nooksack River basin mean ice water equivalent and ice extent for the RCP 4.5 (top figures) and RCP 8.5 (bottom figures) GCM ensembles for 2050 (left figures) and 2099 (right figures). Each ice extent is the average of the 10 ice thickness rasters produced by the model throughout the 21<sup>st</sup> Century under each GCM. Estimated 2009 ice extent from Landsat imagery is outlined in pink.

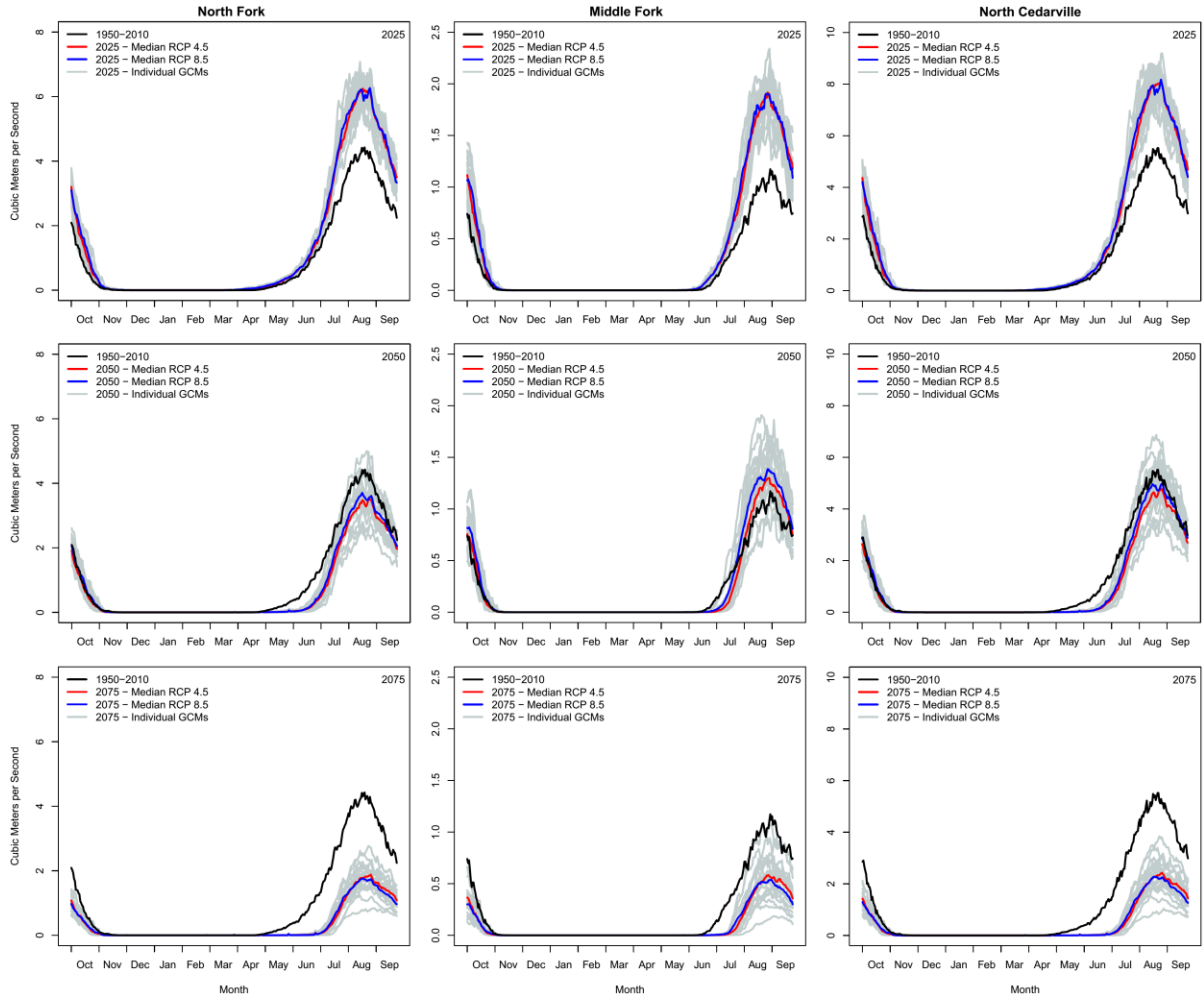


**Figure 16.** Modeled daily median glacier ice melt for the North and Middle Fork basins of the Nooksack River for 2025 (top row), 2050 (middle row), and 2075 (bottom row). Historical median flow (black line) represents 60 years (1950-2010) of modeled ice melt while each of the future scenarios represent 30-year medians of the RCP 4.5 (red) and RCP 8.5 (blue) GCM ensembles. Gray lines each represent the median daily melt from an individual GCM and RCP scenario over a 30-yr period.



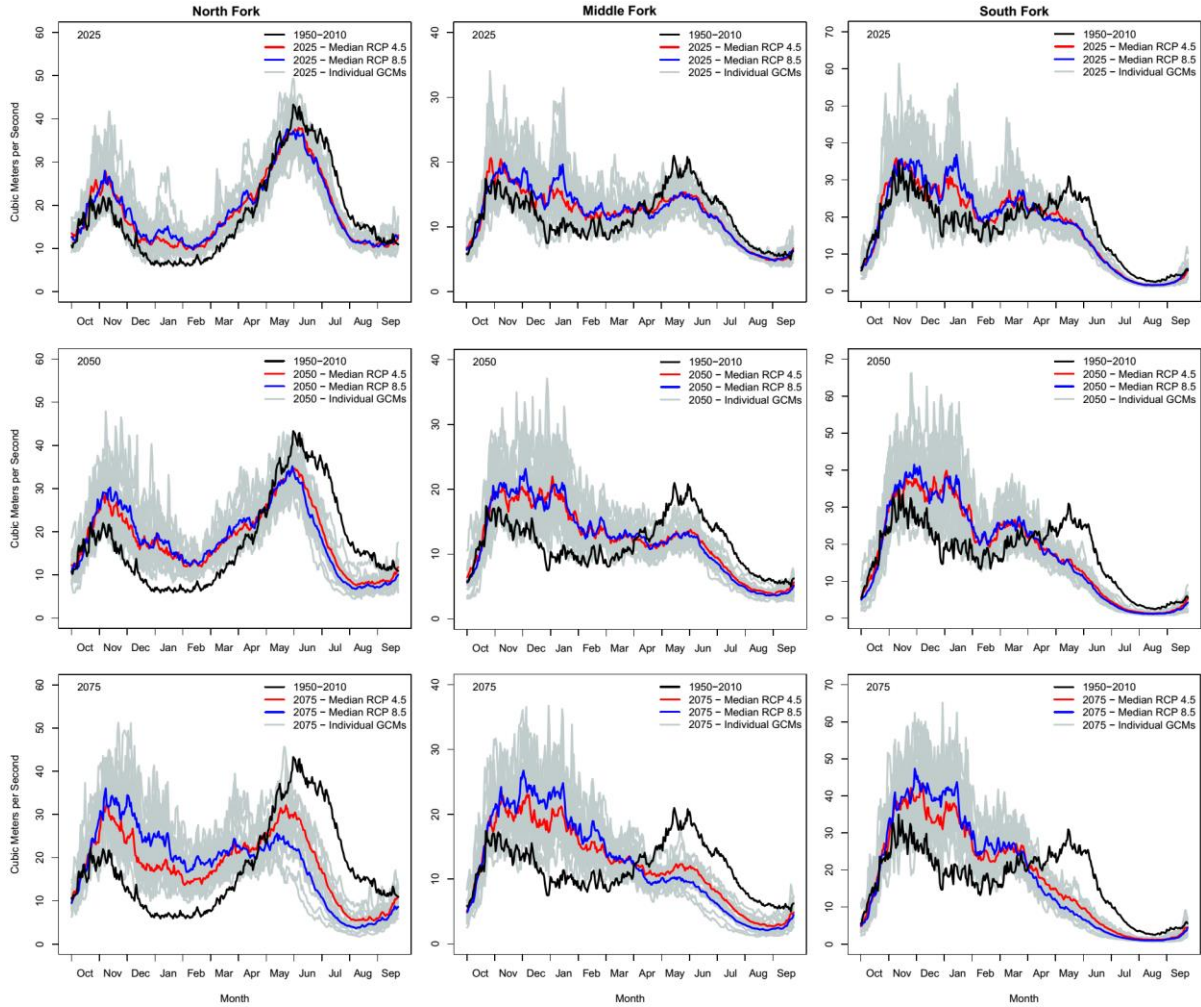


**Figure 17.** Modeled future daily median streamflows for the North, Middle, and South Fork basins for all 10 GCMs under RCP 4.5 and 8.5 scenarios. Flows for each basin are modeled at the location of the USGS gauge used for calibration. Historical flow line represents a 60-year median daily flow (1950-2010) while each of the future scenarios represent 30-year daily median flows centered on their respective year (2025, 2050, or 2075). Gray lines each represent the median flow from an individual GCM and RCP scenario over a 30-yr period.

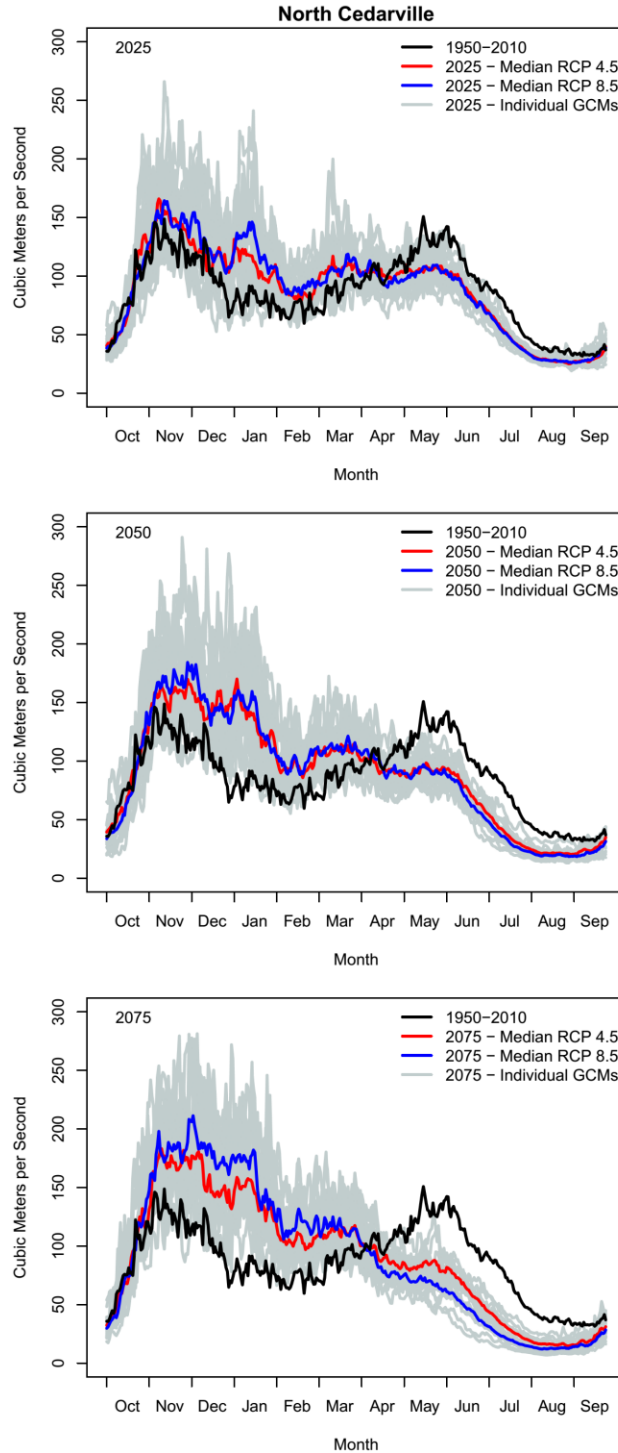


**Figure 18.** Modeled future daily median streamflow for the North Cedarville Nooksack River gauge location for all 10 GCMs under RCP 4.5 and 8.5 scenarios. Historical flow line (black) represents a modeled 60-year median daily flow (1950-2010) while each of the future scenarios represent 30-year daily median flows centered on their respective year (2025, 2050, or 2075). Gray lines each represent the median flow from an individual GCM and RCP scenario over a 30-yr period.

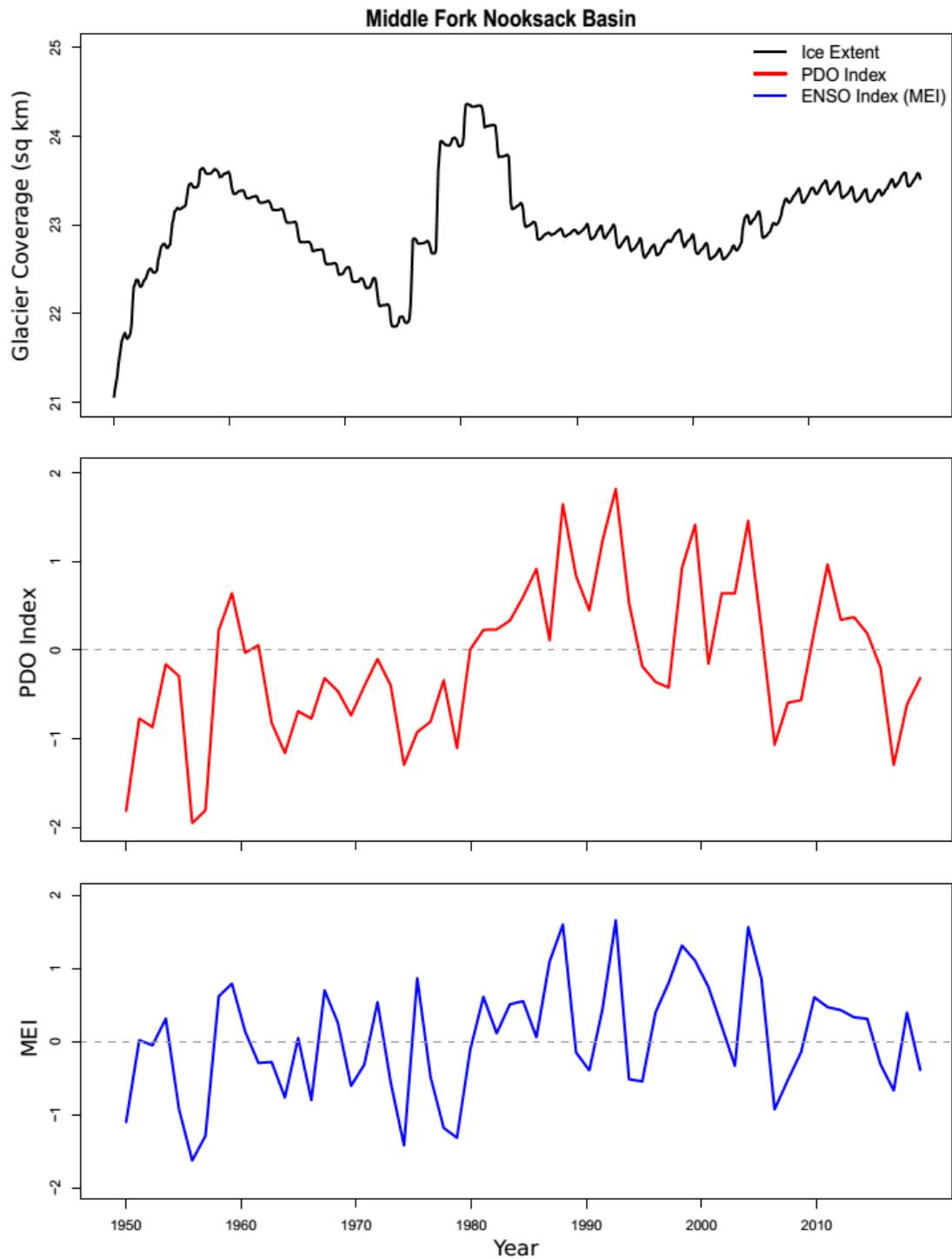


**Figure 19.** Modeled Middle Fork monthly glacier areal extent from 1950-2010 (top) and annual mean PDO index (middle) and Multivariate El Niño Southern Oscillation index (bottom) for the same time period.

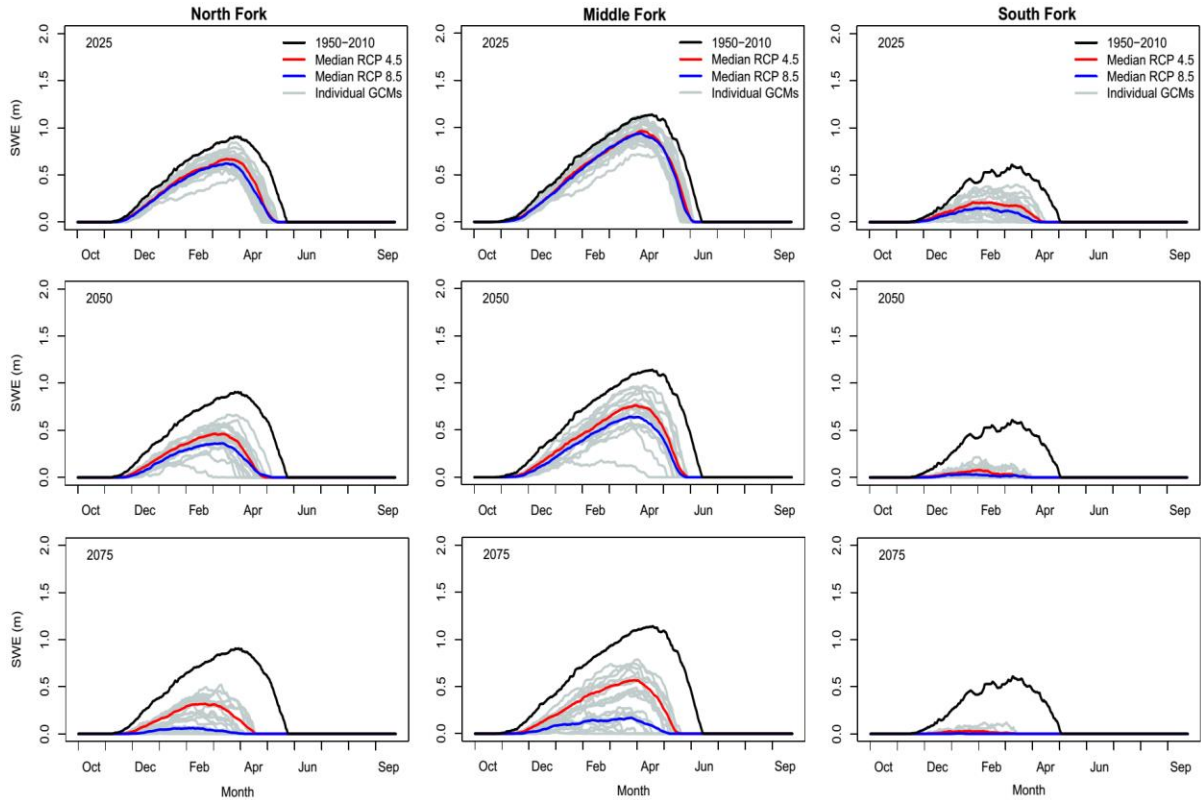


**Figure 20.** Modeled future median daily SWE at the Wells Creek (1228 m elevation), Middle Fork (1515 m elevation), and Elbow Lake (927 m elevation) SNOTEL gauge locations in the North, Middle, and South Fork basins respectively for 2025, 2050, and 2075. Historical flow line represents a 60-year median daily SWE magnitude (1950-2010) while each of the future scenarios represent 30-year median daily SWE magnitudes centered on their respective year (2025, 2050, or 2075). Gray lines each represent the median SWE from an individual GCM and RCP scenario over a 30-yr period.

## 9.0 Appendix A. DHSVM Setup

Much of this text was taken directly from a similar appendix in Carrie Donnell's Master's Thesis (2007) and in Susan Dickerson's Master's Thesis (2010). Additional comments and modifications were made by Ryan D Murphy (2015).

### 1.0 CREATE A DEM GRID

#### *1.1 Create a workspace.*

#### *1.2 Download and unzip Digital Elevation Models (DEMs).*

I used the following website, operated by the Washington State Geospatial Data Archive at the University of Washington:

<http://gis.ess.washington.edu/data/raster/tenmeter/byquad/index.html>

The projection of the DEMs are UTM, Zone 10, datum NAD 27, and units in meters. All the final grids will be in this projection.

#### *1.3 Convert DEM files to raster files.*

Open ArcMap→Arc Toolbox→Conversion Tools→To Raster→DEM to Raster

Input USGS DEM file: *your.dem*

Output raster: <select drive to save to> →OK

This will convert the DEM to a raster, and import the raster to ArcMap.  
All DEMs have to be converted to raster files individually.

#### *1.4 Mosaic DEMs.*

a. Access the Spatial Analyst toolbar: View/Toolbars/Spatial Analyst

Set analysis environment

From Spatial Analyst dropdown menu→Options

Or Right click in toolbox to set environments

Under general tab, Working directory: e.g., U:/ThesisGIS2/dems.

Under Extent tab, Analysis extent: Union of Inputs

Under Cell size tab, Analysis cell size: Maximum of Inputs

→OK

b. Mosaic the DEMs using Raster Calculator (or alternate method)

Open Spatial Analyst toolbar → raster calculator

Create the Mosaic expression in the text box:

<Nooksackdem>=mosaic ([deming], [CanyonLake], [etc.])

→Evaluate (this takes a long time)

b2. Alternate method: use the 'Mosaic to new raster' tool  
Open ArcToolbox→Data Management tools→Mosaic to new raster  
→Environments

Under general tab, Working directory: U:/ThesisGIS2/dems  
Under Extent tab, Analysis extent: Union of Inputs  
Under Cell size tab, Analysis cell size: Maximum of Inputs

c. Once DEMs are mosaic-ed, locate the new DEM in ArcCatalog and drag it into ArcMap.

### *1.5 Resample DEMs to 50 m by 50 m pixel resolution.*

a. Set analysis environment (very important)  
Open ArcToolbox→Data Management tools→Raster→Resample→environment

Under General Settings tab:

Current Workspace: U:/ThesisGIS2/dems

Scratch Workspace: U:/ThesisGIS2/dems

Output coordinate system: Same as layer "Nooksackdem"

Output Extent: Same as layer "Nooksackdem"

Under Raster Analysis settings tab:

Cell size: 50

Mask: None

→OK

b. Resample:

Input Raster: "Nooksackdem"

Output Raster: "dem50" (suggests an .img file extension, which I deleted)

Cell size: 50

Resampling Technique: Nearest

→OK

Once the mosaic-ed raster is resampled to 50m resolution, Nooksackdem (10 m resolution) can be removed from ArcMap.

## 2.0 CREATE A WATERSHED MASK

**Note: This is very important!** If using the coupled glacier dynamics model, the watershed mask must be the same as the glacier domain mask (see *Glacier Module Guide*). This means adding the glaciated area just outside of the watershed to the watershed mask produced in this tutorial. This will ultimately be the mask that every other spatial input will need to be clipped to and it must be the same (and have the same extent) as the glacier domain mask.

### *2.1 Create another folder within the workspace.*

I titled mine "setup".

### *2.2 Fill sinks to even out the DEM.*

Open hydrology/models toolbar→Fill Sinks  
Input surface: dem50  
Fill limit: <Fill\_All>  
Output raster: U:/ThesisGIS2/setup/fillsinks  
→OK (This takes a long time)

### *2.3 Perform flow direction on the filled DEM.*

This grid is necessary for determining the watershed boundary.  
Open hydrology/models toolbar→Flow direction  
Input surface: fillsinks  
Output raster: U:/ThesisGIS2/setup/flowdir  
→OK

### *2.4 Perform flow accumulation.*

This grid is also necessary for determining the watershed boundary.  
Open hydrology/models toolbar→Flow accumulation  
Direction raster: flowdir  
Output raster: U:/ThesisGIS2/setup/flowacc  
→OK

### *2.5 Set interactive properties to create a watershed boundary.*

Open hydrology modeling toolbar→Interactive properties  
Flow direction: flowdir  
Flow accumulation: flowacc  
→OK

### *2.6 Create the watershed boundary and mask.*

Click the watershed button from the hydrology modeling toolbar.

This is an interactive tool which will determine the boundary of the watershed based on the destination cell. I selected the point downstream of the North Cedarville USGS gauging station and ArcGIS determined which cells would eventually drain water to that point. I had to repeat the process a few times before I was satisfied with the watershed boundary.

When a watershed is created, it is a temporary file. Make it permanent, right-click on the watershed grid in ArcMap table of contents→Make Permanent→set source to the current workspace (U:/ThesisGIS2/setup/nf). This raster file will be used as the “mask” input for DHSVM.

If you need to erase rasters from one another (to isolate sub-basins for example), the raster calculator can be used. Note: the “Erase” tool only works on polygons, so unless you want to convert everything to polygons, erase, then convert back to rasters, the raster calculator is the best option.

To use the Raster Calculator to erase one or more rasters from another, open the Raster Calculator tool (Spatial Analyst→Map Algebra→Raster Calculator) and enter:

```
SetNull(~(IsNull([Erase Raster])),[Original Raster])
```

*Note: For ArcMap version 9.X.X, replace “~” with “Not”*

Where *Erase Raster* is the raster/area that will be taken out and erased from the *Original Raster*. If you need to remove more than one raster from a larger raster, simply type the above command, add a space, type “&” (without the quotations), then type the same command but input the other *Erase Raster*.

*2.7 Once the watershed mask is created, it can be used to clip the DEM and hillshade (optional) to the watershed.*

The polygon of the watershed can also be used to clip other grids to the watershed, but be careful that the polygon was not simplified, because the final mask needs to have the same number of rows and columns as each of the clipped coverages.

Open ArcToolbox→Spatial Analyst Tools→Extraction→Extract by Mask

Input raster: U:/ThesisGIS2/dem/dem50

Input raster or feature mask data: nook

Output raster: U:/ThesisGIS2/setup/nookdem

→OK

Alternatively, you can use the raster calculator for this step (or any extraction step).

*2.8 Extract a clipped DEM with filled sinks.*

This will be needed for running the AML (see below).

Open ArcToolbox→Spatial Analyst Tools→Extraction→Extract by Mask

Input raster: U:/ThesisGIS2/setup/fillsinks

Input raster or feature mask data: nook

Output raster: U:/ThesisGIS2/setup/nookdemf

→OK



I used an f at the end of a dem name to indicate that it is filled, and an flt to indicate that it had been converted to floating point (see below).

### 3.0 CREATE A LANDCOVER GRID

#### *3.1 Download landcover grid*

I used the 2006 NOAA landcover grid available publically. Additionally, I used an historical landcover grid developed for the lower Nooksack Water Budget (Bandaragoda et. al., 2012) to test the impact of landcover change on streamflow.

The NOAA landcover file was already an ESRI grid, so it does not need to be converted. The PCS may be different than that for the DEM, but ArcGIS should be able to project the grid on the fly.

#### *3.2 Resample grid to 50 by 50 m resolution.*

Open ArcToolbox→Data management Tools→Raster→Resample

Set the analysis environment (very important):

Under General Settings tab:

Current Workspace: (U:/ThesisGIS2/setup)

Scratch Workspace (U:/ThesisGIS2/setup)

Output coordinate system: Same as layer “nookdem”

Output Extent: Same as layer “nookdem”

Under Raster Analysis settings tab:

Cell size: 50

Mask: None

→OK to close environments setting

Input raster: landcover

Output raster: landcover50

Output cell size: 50

Resampling technique: nearest neighbor

→OK

#### *3.3 Clip landcover grid to watershed boundary.*

Open ArcToolbox→Spatial Analyst Tools→Extraction→Extract by Mask

→Environment

Working directory: U:/ThesisGIS2/setup

Analysis mask: nook

Extent: nook

Cellsize: 50

→OK

Input raster: U:/ThesisGIS2/setup/landcover50  
 Input raster or feature mask data: nook  
 Output raster: U:/ThesisGIS2/setup/nookveg  
 →OK

### *3.4 Reclassify NOAA vegetation classifications to DHSVM classifications.*

Open ArcToolbox→Spatial Analyst→Reclass→Reclassify  
 Set general and raster analysis environments  
 Input Raster: nookveg  
 Output Raster: reclassveg  
 Reclass Field: Value

Then:

NOAA Landcover classifications are different from the landcover classifications in DHSVM. Read the Coastal NLCD Classification Scheme and match land cover types with vegetation descriptions in the DHSVM configuration file as closely as possible. I used the following values for the reclassification:

NOAA	NOAA	DHSVM	DHSVM
11	Open Water	9	Water
21	Developed, Open Space	3	Developed
22	Developed, Low Intensity	3	Developed
23	Developed, Med Intensity	3	Developed
24	Developed, High Intensity	3	Developed
31	Barren Land (rock/sand/clay)	8	Rock
41	Deciduous Forest	4	Broadleaf
42	Evergreen Forest	1	Large Conifer
43	Mixed Forest	2	Large Mixed Stand
52	Shrub/Scrub	6	Shrubland
71	Grassland/Herbaceous	7	Sparse/Open/Agriculture
81	Pasture/Hay	7	Sparse/Open/Agriculture
82	Cultivated Crops	7	Sparse/Open/Agriculture
90	Woody Wetlands	10	Wetland
95	Emergent Herbaceous Wetlands	10	Wetland

These are the landcover reclassifications used by Ryan Murphy (2015) but may have to change if using a different landcover grid.

## 4.0 CREATE A SOIL TEXTURE GRID

Ryan Murphy (2015) used STATSGO soils from the USDA NRCS

### *4.1 Download soil texture coverage*

STATSGO for the study area can be downloaded from one of the following sites:

<http://websoilsurvey.sc.egov.usda.gov/App/HomePage.htm>  
[http://www.soilinfo.psu.edu/index.cgi?soil\\_data&statsgo](http://www.soilinfo.psu.edu/index.cgi?soil_data&statsgo)

#### *4.2 Convert file.*

This is a GIS export file that has to be converted in ArcCatalog.

Open ArcCatalog→Conversion Tools→Import from Interchange File

Input file: C:\MFdhsvm\soil\wa.e00\wa.e00

Output dataset: C:\MFdhsvm\soil\wa

The file will now appear in ArcCatalog and can be dragged into ArcMap.

The PCS may be different than that for the DEM, but ArcGIS should be able to project the grid on the fly.

#### *4.3 Convert soil polygon to raster.*

Open ArcToolbox→Conversion Tools→To Raster→Feature to Raster

Set analysis environments by clicking on the Environments button

Under General Settings tab:

Current Workspace: (C:/MFdhsvm/soils)

Scratch Workspace (C:/MFdhsvm/soils)

Output coordinate system: Same as layer “Nooksackdem”

Output Extent: Same as layer “Nooksackdem”

Under Raster Analysis settings tab:

Cell size: 50

Mask: None

OK to close environments setting

Input features: wa polygon

Field: MUID

Output raster: C:\MFdhsvm\soil\wa.e00\wa\soilgrid

Output cell size: 50

→OK

Remove wa polygon from ArcMap

#### *4.4 Clip soil grid to watershed.*

Set analysis environment:

Click Spatial Analysts toolbar→ Options

Working directory: C:/MFdhsvm/soils

Analysis mask: watershedpoly

Extent: watershedpoly

Cellsize: 50

From Spatial Analyst dropdown menu→raster calculator

Type the expression: soilshed=soilgrid

→Evaluate

Soil classifications are as follows:

MUID	Description	MUID	Description
1	Sand	10	Sandy Clay
2	Loamy Sand	11	Silty Clay
3	Sandy Loam	12	Clay
4	Silty Loam	13	Organic (as loam)
5	Silt	14	Water (as clay)
6	Loam	15	Bedrock
7	Sandy Clay Loam	16	Other (as SCL)
8	Silty Clay Loam	17	Muck
9	Clay Loam	18	Talus

Dickerson (2010) notes the following problems and possible solutions:

Although the hydrology of the Nooksack River basin is not likely to be highly sensitive to soil types due to relatively shallow soil depths on steep, mountainous slopes, I found a few problems with the above methodology, and chose to use a soil type dataset derived specifically for hydrology modeling. First, the association of the map unit identification (MUID) with the “value” is eliminated during the clipping process. The MUID numbers in the table, above, are actually value numbers. To retain the MUID, you must use “Joins and Relates” to join the two attribute tables based on Value. The MUID is the link to all information in the STATSGO database including the comp table and the layer table (which are included in the download of the wa.e00 file). Each map unit has up to 21 components with no spatial resolution (e.g. 24% of a map unit is one soil composition, but there is no spatial information about the distribution), and each component can have up to 7 layers, all of which are linked in attribute tables via the MUID (USDA/NRCS, 2001). The classification scheme, above, which relates a Value to a Soil Type appears to be from the Wiley and Clancy Washington soil dataset that I use, described below, rather than a direct usage of the STATSGO database. In applying the above classification scheme to the STATSGO data and then comparing the soil types to the Wiley and Clancy data for the same area, there were conflicting soil type classifications.

An alternate method could be to use the surface texture (“SURTEX”) characteristic associated with each map unit, or to use the dominant texture grid from the CONUS database on the STATSGO website:

[http://www.soilinfo.psu.edu/index.cgi?soil\\_data&conus&data\\_cov&texture&datasets&geo](http://www.soilinfo.psu.edu/index.cgi?soil_data&conus&data_cov&texture&datasets&geo)  
(the CONUS coverage is a large file (10 Mb) because it covers the entire United States).

## 5.0 CREATE SOIL DEPTH AND STREAM NETWORK GRIDS

I created the soil depth and stream network grids using Arc (Arc is a command line version of ArcGIS, and accessible through the ArcInfo Workstation menu options).

To get to Arc: Start->ArcGIS->ArcInfo Workstation->Arc (command line prompt pops up)

Helpful Arc commands:

(more available from “ArcDoc” accessed through the ArcInfo workstation):

workspace	lists current workspace
listgrids	lists grids in current workspace
quit (or q)	leave grid session and back to Arc prompt, or end Arc session

### *5.1 Reclassify the watershed mask (e.g. nook).*

The watershed mask values must be defined as inbasin=1 and outside basin=NODATA. Otherwise the AML will create a stream network for the entire raster. You can check the values in ArcMap by opening the DEM properties dialogue.

Open ArcToolbox→Spatial Analyst Tools→Reclass→Reclassify

Input raster: U:/ThesisGIS2/setup/nook

inbasin=1 and NODATA (outside basin)=NODATA

Output polygon features: U:/ThesisGIS2/setup/Reclass\_nook

→OK

### *5.2 Create a workspace.*

Create a new folder: C:/yourname\_dhsvm/nook/streams

The AML only works for me when I run it directly from the hard drive rather than a networked drive or an external hard drive. Also, there is much discussion on the DHSVM archive about the finicky nature of the createstreamnetwork aml; tips gleaned from that website include: close ArcCatalog and ArcMap before running the AML (so that the needed files are not open or being accessed), and always begin with a new, completely empty folder for each AML run so that you do not inadvertently carry over files that were created during the previous run of the AML.

*Note: I had issues with incorrect outputs when using the AMLs from the newest DHSVM tutorial (version 3.1). Using an older AML version worked.*

Obtain the AML scripts from Bob Mitchell or the DHSVM tutorial online

(<http://www.hydro.washington.edu/Lettenmaier/Models/DHSVM/index.shtml>) (To do this, download tutorial.tar.gz (save, not open), Find the file in the windows folder; double click, “I

agree” when winzip pops up, select all and “extract”; AML scripts are in the arcinfo folder that is created by extracting the files.)

In ArcCatalog: Copy the reclassified mask, the filled, clipped dem (nookdemf) and amlscripts from the DHSVM tutorial into the “streams” folder.

Check the computer to ensure that it has a Java Runtime Environment (JRE). If it doesn’t, download Java software from [www.sun.com](http://www.sun.com).

To check for JRE, open Arc and type:

Arc: &sys java -version

If the JRE is installed, you should get:

Java version “1.6.0\_11” (I used 1.4.2\_05, on Bob Mitchell’s lab computer)

Java [TM] SE Runtime Environment, Standard Edition (build 1..6.0\_11-b03)

Java HotSpot[TM] Client VM (build11.0-b16, mixed mode, sharing).

### *5.3 Check file paths for AML.*

If you are using a folder that is titled something aside from “streams”, make sure to change the filepath for AddAat2.class within the createstreamnetwork AML, before running the AML.

The scripted is coded to look in the streams folder, so if this step is skipped, the AML will encounter an error, but will continue to run anyway. It will produce zeros within the streamnetwork.dat for slope, segorder, etc. and DHSVM cannot use this file.

To change the filepath, open the AML as a text file (e.g., using Wordpad) and use the ‘find’ tool (find “AddAat.2”) to locate the path and changed the path to your soildep folder instead:  
&sys java -classpath ../soildep/amlscripts/AddAat2 %streamnet%

### *5.4 Convert filled dem to floating point and run the AML*

Open ARC. Type:

ARC: &workspace C:/Susan\_dhsvm/nook/streams

ARC: grid

GRID: nookdemflt = FLOAT(nookdemf)

GRID: q

ARC: &watch aml.watch

ARC: &amlpath C:/Susan\_dhsvm/nook/streams /amlscripts

ARC: &run createstreamnetwork nookdemflt nook\_mask nooksoildep1 nookstreams1

MASK 220000 0.76 1.5

Where ‘nookdemflt’ is the clipped, filled dem converted to floating point; ‘nookdemf’ is the clipped, filled dem; ‘nook\_mask’ is the reclassified raster mask; ‘nooksoildep1’ and ‘nookstreams1’ are the names I chose for output files.

The last three numbers are variables representing the minimum contributing area before a channel begins, the minimum soil depth, and maximum soil depth (in meters). I used a 1 at the end of each of the output files to distinguish them from future files, when the AML is run again with different soil depths (e.g. nooksoildep2 may range from 0.76 to 2.5 m).

This process takes a long time (approximately 45 min for Middle Fork 388x514 pixel grid). Just before the script finishes running it will ask you if you want to continue. Answer 'y' for yes, and it will finish the process.

Output from this step includes: soil depth raster (nooksoildep), a stream network feature class, stream.map.dat, and stream.network.dat (note that the two .dat files only appear when the folder is viewed with Windows, not in ArcCatalog. Open stream.network.dat with Wordpad to check whether the AML has run properly; if it has, there will be a variety of numbers in the last two columns rather than all zeros.

I ran this step multiple times – for each basin that I created and then changing the soil depth for calibration of the model. Each time I renamed the “streams” folder (e.g., to streams\_1.5), and then created a new stream folder by copying in the needed inputs. This is because the program will overwrite the files that are named the same way every time the AML is run (e.g., stream.network.dat)

## 6.0 CREATE A SERIES OF SHADING MAPS

### *6.1 Create a workspace.*

Create a new folder: C:/Susan\_dhsvm/northfork/shadow

Copy the clipped dem and watershed mask into this folder using ArcCatalog.

The solar AML (process\_solar or process\_solar1) and 3 “C” files, make\_dhsvm\_shade\_maps.exe, skyview.exe, and average\_shadow.exe are available from Robert Mitchell; they are not available in the amlscripts folder in the DHSVM tutorial. Carrie Donnell compiled these using the ‘lcc’ compiler in the Computer Science department with the help of Matt Paskus. Copy the amlscripts folder with the aml, and the .exe files into the ‘shadow’ folder. Note that the three .exe files should be in the shadow folder directly, rather than in the amlscripts folder. In addition, make sure that a copy of cygwin1.dll is located in the shadow folder as well. Arc cannot find the .dll otherwise and it is needed in order to run the skyview.exe.

### *6.2 Run the AML*

Arc: &workspace C:/Susan\_dhsvm/northfork/shadow

Arc: &watch aml.watch

Arc: &amllpath C:/Susan\_dhsvm/northfork/shadow/amlscripts

Arc: &r process\_solar nook nookdem 3 0.0

Arc: q

The watershed mask is nook, and the dem is nookdem. The last two numbers represent the model timestep (I used 3 hours) and GMT offset, respectively. Robert Mitchell's previous DHSVM set-up instructions have noted that Matt Wiley (formerly of UW, currently of 3Tier in Seattle) usually uses 0 as the GMT offset; it's a little confusing, in that the time stamp on the model runs is then off by 8 hours, for example the warmest part of the day is at 8:00 pm, but that works better when using daily data with the met record creation programs, and avoids the confusion of daylight savings time, times zones etc.

At the end of the session Arc will state that the AML command "rm" is not recognized in Windows; however, it produced the needed output (which are 12 shadow maps and a skyview file, all of which are .bin files and will not be visible in ArcCatalog). Transfer the shadow maps to Horton, and rename each file (ex: 'Shadow.01.hourly.bin' is renamed 'shadow.01.bin').

*Note from Ryan Murphy (2015): I had some issues with this process producing incorrect shading maps. Ultimately, I used a shell scripting method in Linux which gave more control over some of the commands. This seemed to work and did not involve the need for compiling code on the Windows machine. The scripts needed to do this are available within the tutorial available on the DHSVM website. There is a lot of hardcoded stuff in some of the scripts (number of maps to produce, etc) so look for that.*

### 7.0 CONVERT DEM, SOIL TYPE, SOIL THICKNESS, VEGETATION, AND WATERSHED FILES TO ASCII GRIDS

I created a new file for each conversion and copied the GIS grid to be converted into the file. I then convert all the NoData values in the grids to something that DHSVM recognizes (e.g., water=14) and converted the grids to ascii format.

For DEM, Soil Type, Soil Thickness, and Vegetation:

Example:

For the nooksack DEM, Type:

Arc: &workspace U:\ThesisGIS2\setup

Arc: grid

GRID: nookdem.asci = gridascii(con(isnull(nookdem),14,nookdem))

Repeat for all dem, soil type, soil thickness, and vegetation grids.

GRID: q

ARC: q

NOTES:



- the term before the equal sign is the new file name; the “.ascii” is just to remind me that it is an ascii file.
- there is no space between & and workspace
- there is a space on either side of the equal sign, the function will not work if you have a space in the wrong place.
- the new file will not appear in Arc Catalog, but a “projection” file will be created along with it that ArcCatalog will see; the new file can be viewed in Windows via “My Computer”.

#### For the Mask:

Use the re-classified watershed raster. Use 0 rather than 14 for the no data values

GRID: nook\_mask.ascii = gridascii(con(isnull(nook\_mask),0,nook\_mask))

### 8.0 TRANSFER ASCII GRIDS FROM WINDOWS TO A UNIX SYSTEM

All of the ascii files need to be transferred to Luna, the Unix system in Robert Mitchell’s laboratory. The transfer requires a secure shell (e.g. WinSCP or SSH); the address for Luna is:

luna.geol.wvu.edu

Transfer the ascii files to the Input directory. Additionally, transfer stream.network.dat and stream.map.dat (stream.network.dat and stream.map.dat were created by the aml in Step #6), the twelve shadow maps, skyview file, and the meteorological input file to the Input directory.

### 9.0 CONVERT ASCII GRIDS TO BINARY (on Horton)

Open the ascii Files using EMACS (a UNIX word processing program), and read/record first six lines (# of rows, columns, etc.), and then delete them. The files can also remain in your PC workspace for future reference of the first six lines. Check that each ascii file has the same number of rows and columns – a difference in the size of the grids will prevent DHSVM from running.

Convert the ascii grids (e.g. nookdem.ascii) to binary files using “myconvert” (a program available from Robert Mitchell) in the Input directory.

The correct variable type for each grid is:

mask, landcover, soil type: uchar

dem, soil depth: float

Example (for mask, land cover, soil type):

```
horton > ./myconvert ascii uchar nookmask.asc nookmask.bin 366 430
```

Example (for dem, soil depth):

```
horton > ./myconvert ascii float nookdem.asc nookdem.bin 366 430
```

Where:

```
horton> ./myconvert source_format target_format source_file target_file number_of_rows  
number_of_columns
```

### 10.0 CREATE A FINAL STREAM MAP AND STREAM NETWORK FILE

Use the program “assign” (a program available from Robert Mitchell) to create a final stream map and stream network. stream-net.dat and stream-map.dat are the final map and network files.

Example:

```
horton>./assign stream.network.dat stream.map.dat stream-net.dat stream-map.dat
```

I used the hyphen to indicate that the file that has been “assigned”.

### 11.0 Locate the stream gauge for DHSVM calibration.

The stream gauge location in DHSVM is based on the location of the end of a stream segment generated in the stream network aml, not the actual location of the gauge. Open ArcMap and add the stream network Arc to the map if needed. Locate the position of the stream gauge using the coordinate indicators in the lower right corner of the screen, or plot the location of the stream gauge using “Tools” and “add X Y data”. The output segment is the segment that terminates the closest to the stream gauge location. Stream discharge is not at a pixel, it is at the end of a selected stream segment. After the stream gauge is located, click on the stream segment nearest the gauge using the “INFO” button to determine the stream segment ID #. Record the segment number/value. On Horton, open the final stream network file using EMACS, and type ‘SAVE’ next to the appropriate stream segment.

Then, copy the final stream files (stream-net.dat and stream-map.dat) into the state directory.

### 12.0 Locate the PIXELs for SWE OBSERVATIONS.

Determine coordinates for pixel dumps that will be used for SWE calibration. Exact locations of SNOTEL stations are available by contacting NRCS (the locations on the website are intentionally vague). Use ArcMap to locate the pixel, and check the elevation, aspect, and land cover for that location. If necessary, move the SNOTEL location to a nearby pixel that has the correct characteristics, or reclassify the pixel. For example, for

accurate simulation of SWE the pixel must not have over-story vegetation (i.e., it should be classified as urban, bare, or grassland).

### 13.0 SET INITIAL CONDITIONS FOR DHSVM CALIBRATION

#### *13.1 Create initial channel state files:*

In the State Directory, type:

```
horton> awk '{print $1, 0.1}' stream-net.dat> Channel.State.09.30.2005.23.00.00
```

The Channel.State file should be named for the day and last time step before the water year you will simulate (09.30.2005.23.00.00 for simulating WY 2006).

#### *13.2 Create model state files*

First:

Edit InitialState.txt (available from Bob, or from the dshvm tutorial): change the starting date (e.g 9-30-05-23 for running a simulation of water year 2006, which begins on 10/1/05), and the number of rows and columns in the grids (previously deleted from the ascii files).

Then:

Run the MakeModelStateBin program with the following syntax:

```
horton> ./MakeModelStateBin InitialState.txt
```

This creates the initial Interception, Snow, and Soil state files for the date that is specified in the InitialState.txt file. The date indicates the beginning of the model simulation.

### 14.0 SET UP INPUT FILE

Edit the DHSVM configuration file using EMACS, including specifications for: start and end dates and times, UTM coordinates for extreme NW corner of mask, pixel size, names of binary inputs (e.g., soil, soil depth; note that file names are case sensitive), location of meteorological station, location of pixel dumps (e.g., SNOTEL stations), soil parameters, temperature and precipitation lapse rates, and other parameters.

### 15.0 RUN THE MODEL

From the main directory (horton/dickers/dhsvm/nooksack/nook>)

```
horton> DHSVM input.nook (note: DHSVM command is case sensitive)
```

or

```
horton> time DHSVM input.nook
```

Where DHSVM is the command, and input.nook is the configuration file (a text file); the addition of “time” to the beginning of the command will print the elapsed time at the end of the simulation.

Another useful command is:

```
horton> nohup DHSVM input.nook &
```

This will allow DHSVM to run in the background without terminating when you “hang up” the connection by logging off Horton or powering off your remote PC.

### 16.0 RE-RUN THE MODEL with NEW INITIAL CONDITIONS

Create initial conditions using the steps above, run the model for a year or more (the “spin-up” period), and then use the output conditions from the first simulation as the initial conditions to re-run the model for the same year. To do this, copy the output states (in the Output directory) to the State directory and rename them to be consistent with the first date and hour of the next simulation.

## 10.0 Appendix B. Glacier Model Setup

September 2015

*This document was created by Ryan Murphy (Master's candidate at Western Washington University) and is based on the DHSVM Glacier Model Tutorial (dated 3/19/2014) from Chris Frans (University of Washington) and personal communications with Chris Frans and Christina Bandaragoda (University of Washington).*

### DHSVM Coupled Glacier-Hydrology Model Options

To calibrate and run the glacier dynamic glacier model for use with the DHSVM version 3.2 (as of this document's creation) is a multi-step process requiring iterative runs of the model under different settings. DHSVM has four glacier model run options:

1. NO\_GLACIER = Runs DHSVM routine without simulating glacier ice. Snow that reaches the density of ice is removed.
2. GLSPINUP = Runs glacier model independently (i.e. with no DHSVM) with annual average mass balance forcing at an annual time step for 1000 years to “grow glaciers” to steady state (need to specify Glacier Mass Balance File in input configuration file)
3. GLSTATIC = Runs DHSVM simulation representing a glacier ice layer (Surface Topography Input – Bed Topography Input), however no glacier flow dynamics are included (ice is static and does not flow cell to cell; mass is finite)
4. GLDYNAMIC = Runs DHSVM simulation representing glacier ice and glacier ice dynamics (ice flows cell to cell based on glacier ice physics)

### General Outline for Setting up and Running the Glacier-Hydrology Model:

1. Estimate bed topography
2. Estimate Mass Balance Field
3. Run “GLSPINUP” with mass balance field to grow steady state glaciers
  - a. Iterate by perturbing mass balance field until glacier outlines match historical extent estimate
  - b. Once satisfied with simulated extent, use ice thickness and bed topography to create surface topography field
4. Use surface topography field as input to initialize glacier states (Glacier Ice = Surface Topography – Bed Topography) in coupled glacier-hydrologic simulations (GLDYNAMIC, GLSTATIC)

In order to run the coupled glacier-hydrology model properly, several steps must be taken. A representative mass balance field for the domain, as well as a surface topography field must be estimated. The DHSVM is used to estimate these parameters under the GLSTATIC and GLSPINUP glacier options. Once these files have been created, the dynamic model can be run and the static model can be run with more confidence.

### Necessary Inputs:

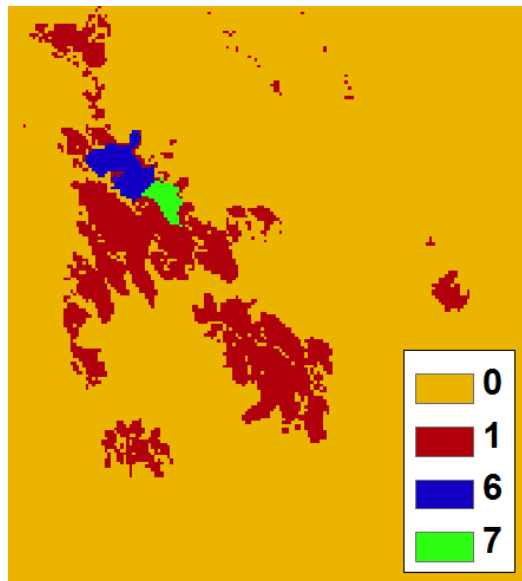
All inputs for the glacier portion of the model can be created or altered in ArcMap. The user should first decide which years they would like to model the glacier (i.e. starting with current glacier extent vs starting with the extent from the year 1950 for example). Typically the oldest observed glacial extent is used. This will largely depend on what GIS datasets (NOCA, GLIMS, etc.) are available. Make sure to specify the correct cell size and extent for you rasters. The grid spacing and number of rows/columns must match the other inputs to the model (DEM, mask, landcover, etc.).

Note: Pixels with no data should have values of 0 rather than -9999.

#### *Glacier Mask File*

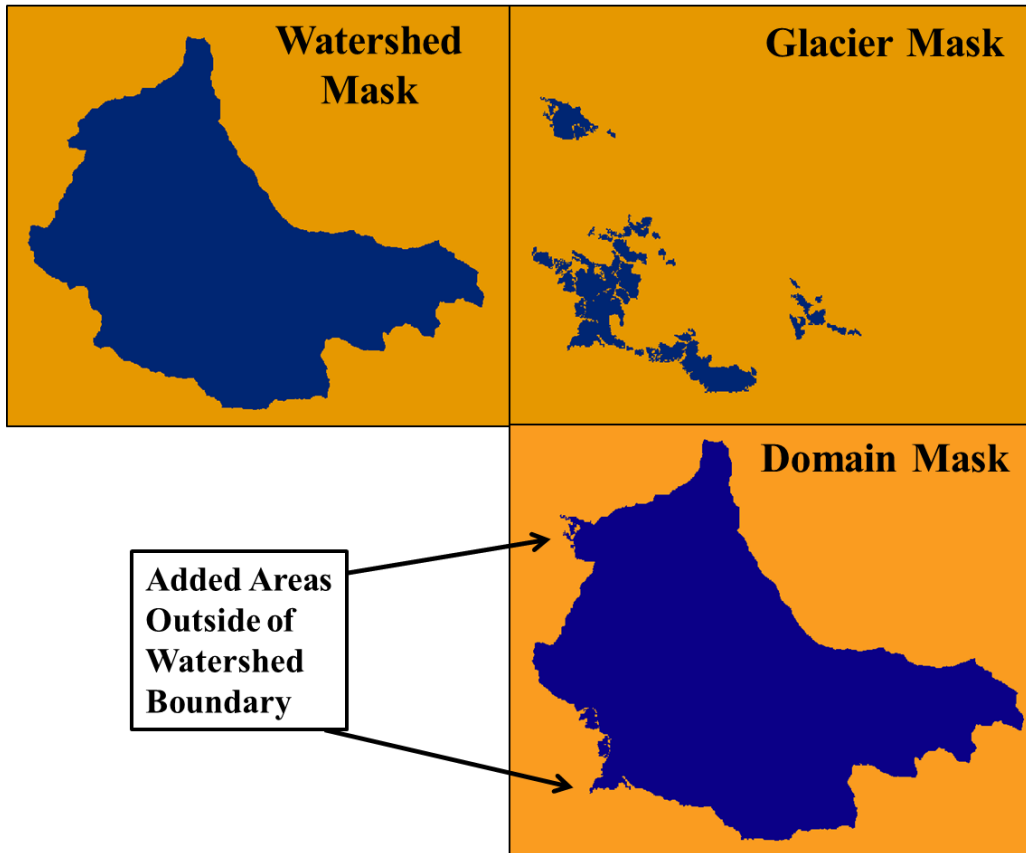
After obtaining the historical glacier GIS dataset, isolate the glaciers that have at least part of their extent within the watershed of interest. Glaciers directly adjacent to the study area watershed should also be selected. Create a subset layer with just these glaciers. Do not clip to the watershed boundary. Include the entire glacier in the new layer even if only part of it enters the watershed. If this layer is a polygon, convert to a raster using the polygon to raster tool.

Reclassify the raster so that non-glaciated pixels have a value of 0. Currently, the code is set up to output glacier mass balance and area for two individual glaciers, which should be reclassified with integer values 6 and 7. All other glaciated areas should have a value of 1 (see below for example).



#### *Glacier Domain Mask*

Similar to the watershed mask, this file identifies an area that includes all the glacial bodies connected to the watershed. Glacier flowsheds do not always correspond to watershed boundaries. Because ice at watershed boundaries can flow into and out of the watershed, this larger mask is required for the glacier model. This domain should be large enough to include all of the ice bodies that have portions that flow into the watershed. Glaciers directly adjacent to the study area watershed should also be included (the same ones as in the glacier mask). See figure below.



The domain should not have any holes in it. If necessary, buffer the glacier extent to remove any “NoData” pixels within the domain.

This can be created using the Mosaic to New Raster tool in ArcMap using the watershed mask and the glacier mask file as inputs.

#### *Glacier Bed Topography*

This file is the elevation field of the entire domain, and represents the topography under the current glacier extent. Simply stated, this file is equal to the DEM outside of the glacier and is less than the DEM under the glaciated areas. The methods *Clarke et al. 2012* have been used to estimate bed topography in past applications.

Unless ground penetrating radar or other data are available for the study area, the basin domain DEM is used. This likely provides a good estimate where glaciers are relatively small. I used a DEM clipped to the entire rectangular extent, not just the basin mask, since there were some glaciated areas outside of the basin.

#### *Glacier Surface Topography File*

This file is an estimate of the initial ice thickness. This file cannot be created until the SPINUP mode is run, but there are several steps before that can happen. A run using the GLSTATIC option must be

performed, which is necessary to estimate mass balance which is needed for the surface topography file. These steps are outlined below in the “*Running the Model*” section.

One DEMs is needed for the first GLSTATIC run and one DEM is needed for calibration:

1. Create a grid file that represents a thick layer of ice across the entire domain. This can be done by adding 1000m to the domain DEM of the entire area using the Raster Calculator. This layer will ultimately help track changes in mass balance over time (explained more in the “*Running the Model*” section).
2. Create a DEM that represents a thick layer of ice across only the glaciated areas. Do this by adding 1000m (or some large number) to the glaciated areas. This can be done in a number of ways. I extracted the glaciated DEM area using the Extract by Mask tool with the original DEM being the input file and the glacier mask being the “mask” file. I then used the Raster Calculator to add 1000 to the newly created DEM of just the glacier area. The Raster Calculator can then be used again to add the glacier area DEM plus 1000m layer to the original DEM. This layer will ultimately help determine how much streamflow is coming from the static glaciated areas (explained more in the “*Running the Model*” section). This can be used in the calibration process. Note: this is not strictly necessary but does help to get baseline glacier melt results during calibration.

#### *Basin Mask File*

This is the same as the watershed mask.

#### *Glacier Mass Balance File*

This file will be created by the DHSVM after the GLSTATIC mode is run. An output file called “balance\_sum.bin” will be produced. Convert this file from binary to ascii, add in the basin header (six lines containing the spatial information, gid size, and NoData values), and import back into ArcMap using the ASCII to Raster tool. This file represents the cumulative mass over time and needs to be divided by the number of years in the simulation run (using the Raster Calculator) to get the mean annual mass balance (explained more in the “*Running the Model*” section).

#### *Running the Model*

##### *Model with No Glacier*

To run the model without any glacier component (no glaciers are simulated, static or otherwise), set the glacier option under the constants section to NO\_GLACIER. This will produce a simulation for basin hydrology that does not include glacier melt. Under this mode type, snow that reaches the density of snow will be removed by the DHSVM.

##### *Dynamic Glacier Modeling*

To run the dynamic glacier model, two simulations must be performed first to estimate the mass balance and glacier ice thickness. Note: this is a general procedure for setting up and running the dynamic glacier model and does not include all of the steps for the initial glacier calibration. For more detailed calibration procedure/recommendations, see the “*Calibration*” section.

1. Run the DHSVM with the glacier component option set to GLSTATIC. This step will estimate the mass balance field for the area. Input files are as follows:



- **Domain Mask File** = the file generated in the *Glacier Domain Mask* step above
  - **Glacier Mask File** = the file generated in the *Glacier Domain Mask* step above
- In this case, the full domain is used instead of the glacier mask for calibration purposes.

Typically DHSVM can have a habit of accumulation of snow/ice in areas where glaciers do not exist. This phenomena is really small when the model is well parameterized and calibrated, but can be large when not. The problem when running future warmer climate scenarios is that this ice will eventually melt, in turn simulating a future source of water that should not be there. Therefore, the mass is removed as it accumulates. So, prior to imposing this constraint where ice outside of the glacier mask is removed, what I have done, and what I recommend, is that when doing initial model calibration and testing, set the glacier mask to be the same as the domain mask. This way ice can accumulate and the glaciers can flow anywhere they want. In the end when you have a good calibration, the glaciers should stay close to where they are observed to be, and only a minimal amount of ice will accumulate outside the mask. At this point you can go ahead and use the glacier mask file reflecting real historical glacier outlines and you can run your simulations without the worry of generating small artificial ice reservoirs that will melt in the future.

- **Glacier Bed Topo File** = basin DEM from the *Glacier Bed Topography* step above
- **Glacier Surface Topo File** = use the DEM that represents a thick layer of ice across the entire domain (DEM+1000m everywhere).
- **Basin Mask File** = watershed mask
- **Glacier Mass Balance File** = not required. I use a placeholder such as the glacier surface topo file

Change the input file for the DHSVM. I recommend saving a new input file for the GLSTATIC model run. This simulation should be run for a time period of 10 years or more to get an accurate measure of mean annual mass balance.

After the model finishes, an output file called “balance\_sum.bin” will be produced. This represents the mass balance for the simulation period. The annual mass balance is calculated by tracking the changes in ice and snow water equivalent through time. Having a thick layer of ice everywhere is required so that negative mass balances can be tracked at elevations outside of the current ice extent.

Convert this file from binary to ascii using “MyConvert,” add in the basin header (six lines containing the spatial information, gid size, and NoData values), and import back into ArcMap using the ASCII to Raster tool. This file represents the cumulative mass over time and needs to be divided by the number of years in the simulation run (using the Raster Calculator) to get the mean annual mass balance.

Convert the mean annual mass balance layer to ascii, transfer to the Unix machine, convert into binary using “MyConvert.” This file will be used as the Glacier Mass Balance file for the SPINUP run.

Temperature and precipitation fields have also been used with a temperature index model to generate the annual mass balance field; however, using DHSVM to generate the field includes the representation of energy balance terms as well as the effects of topography (shading, skyview, etc.).

2. Now that the bed topography (the DEM) and mass balance fields have been created, you must estimate initial glacier ice thickness. This requires running the model for a spin-up time period so that the ice thickness profiles are physically realistic and mathematically stable. Change the glacier mode to SPINUP. Executing the model with this option will run the glacier model independently at an annual time step for 1000 years using the annual mass balance field that is specified as an input (Glacier Mass Balance File). Input files should be as follows:

- **Domain Mask File** = the file generated in the *Glacier Domain Mask* step above
- **Glacier Mask File** = the file generated in the *Glacier Domain Mask* step above
- **Glacier Bed Topo File** = basin DEM from the *Glacier Bed Topography* step above
- **Glacier Surface Topo File** = not required. I use the DEM that represents a thick layer of ice across the entire domain (DEM+1000m everywhere) as a placeholder.
- **Basin Mask File** = watershed mask
- **Glacier Mass Balance File** = mass balance file created from the previous model run (GLSTATIC) that was divided by the number of simulation years.

Change the input file for the DHSVM. I recommend saving a new input file for the SPINUP model run. This will output the ice thickness file (h\_spinup.bin). Surface topography of the watershed including the glaciers can be calculated from this file.

Import h\_spinup.bin into ArcMap using the steps outlined in the previous section. Visualize the simulated glacier extent at end of spinup period and compare with the observed extent. If the mass balance field does not accurately represent the forcings that control the glaciers' current extent, the mass balance field may need to be iteratively altered so that the glaciers will grow to appropriately match the observed extent. For example, if the mass balance field was generated from recent meteorological forcing data that was much warmer than the historical time period, the mass balance field is likely too low to grow glaciers of size comparable to what is observed.

Once satisfied with the simulated glacier extent from the spinup time period, use the raster calculator in ArcMap to add the ice thickness (h\_spinup) to the DEM. This will serve as the calculated glacier surface topography (ice thickness + bed topography) as an input for the coupled model simulations (GLDYNAMIC).

3. To run the dynamic coupled glacier-hydrology model, change the input file for the DHSVM and set the glacier mode to GLDYNAMIC.
- **Domain Mask File** = the file generated in the *Glacier Domain Mask* step above
  - **Glacier Mask File** = the file generated in the *Glacier Domain Mask* step above
  - **Glacier Bed Topo File** = basin DEM from the *Glacier Bed Topography* step above
  - **Glacier Surface Topo File** = Use the ice thickness + DEM layer that was created in the

SPINUP.

- **Basin Mask File** = watershed mask
- **Glacier Mass Balance File** = not required.

### *Calibration*

Calibrating the glaciers before calibrating the hydrology is recommended.

Recommended glacier calibration procedure:

1. Run the simulation for just glacier areas and SNOTEL locations under the GLSTATIC option to calibrate the model for accumulation and ablation processes. This is done in ArcMap by altering the domain mask by setting the parts of the watershed that you want to run (i.e. glacier extent and SNOTEL areas) to 1 and the other areas to 0. You can run this for the entire watershed, but the computational efficiency will improve if only the areas of interest are used in the domain. Since the model is set to the static glacier option, the glaciated cells are independent of each other (for the glacier component of the DHSVM) and the entire watershed mask is not needed. Compare mass balance model results to where observations are available. Ideally you would want to compare with accumulation on the glacier because glaciers are at higher elevations than SNOTEL sites, but you have to work with what you have.

**sensitive parameters:** temperature lapse rate, precipitation lapse rate, maximum snow albedo, glacier albedo

Note: make vegetation class at SNOTEL locations bare, as most of these locations are in clearings

2. Now that you have an accurate simulation of mass balance processes, calculate mean annual mass balance across the entire domain with this calibration (running the model with 1000+ meters of ice everywhere) using the GLSTATIC option. The model will output a mass balance file, which needs to be divided by the number of years in the simulation.
3. Use the mean annual mass balance field to force the spin-up (GLSPINUP option). Since the mass balance reflects current climate which is warmer, the glaciers will not likely grow to historical extent.
4. Iteratively adjust the mass balance field to grow the glaciers to the historical extent. You can do this by adding or subtracting a small amount (e.g. 1 or 2 or 3) to the mass balance field using the raster calculator or by altering parameters within the DHSVM and rerunning the static glacier model to produce a new mass balance output. This will force the model to accumulate more ice, better reflecting historical glaciation. If the glacier is producing too much ice, iteratively decrease the mass balance field until satisfied with the glacier extent.
5. After the glacier calibration is complete, the DHSVM can be calibrated to hydrology.

Calibration notes:

- Using the static glaciers option (GLSTATIC), glaciers that have finite mass and cell to cell ice flow is not simulated. Over short timescales of 1-10 years this is a valid assumption depending of the watershed location, relative glacier cover, and drainage area. This will allow the user to calibrate watershed properties (soil, vegetation, temperature, precipitation lapse rates) and have some contribution of glacier melt

included. For this application, a surface topography file will need to be created that reflects ice mass with the glacier masked area (e.g., Surface Topography = 100m (or more) + Bed Topography in areas located within the glacier mask.

- In snowmelt dominated basins, most of the hydrograph will be related to snowmelt. Using the NOGLACIER option, watershed calibration can also be conducted as long as it is recognized that in months where glaciers are expected to contribute the most, streamflow will be biased low.
- Later calibration efforts to match glacier rates of recession and glacier mass balance observations will be conducted with the GLDYNAMIC run option.

### Calculating Contribution of Glacial Melt to Streamflow

The easiest way to determine the contribution of glacial ice melt to streamflow is to run the calibrated and validated model using the NO\_GLACIER mode and then run it again using the dynamic glacier mode. The melt contribution to streamflow is the difference between the streamflow outputs of the two model runs.

### Glacier Model Output

*gl\_sn\_cov.txt*

Reports snow and glacier extent (km<sup>2</sup>) and ice volume (m<sup>3</sup>) at monthly timesteps.

*gl\_cov\_glac6\_7.txt*

Reports glacier area and volume for 2 individual glaciers denoted in the glacier mask file with integers 6 and 7.

*balance\_glac6\_7.txt*

Reports specific net balance at a monthly time-step for 2 individual glaciers denoted in the glacier mask file with integers 6 and 7.

*balance\_sum.bin*

Grid of cumulative mass balance across the simulated domain. This can be used to calculate mean annual mass balance field for the SPINUP run.

*h\_spinup.bin*

Grid of ice thickness at the end of the glacier ice spin-up run

### Additions to existing DHSVM output files

Glacier ice water equivalent and glacier melt have been added to the Mass.Balance and Aggregated files. Maps of glacier ice water equivalent can be dumped (variable ID #705). IceRemoved is variable included in the calculation of mass balance to track ice mass that is removed from the simulation with NO\_GLACIER option.

### Miscellaneous

1. Estimated bed topography: the method suggested above, among others in the literature, require multiple inputs (e.g., thinning rates, distributed mass balance) and the applicability of these methods are limited by the resolution and accuracy of the DEM and size of the glaciers

being simulated. Experiments in areas where glacier masses are relatively thin with respect to the DEM resolution, suggest that using the DEM as bed topography does not yield significantly different results than using bed topography estimated using a more complex method.

Comparing the effects of using estimated bed topography and a DEM as inputs for bed topography in the model spinup step in the Bow River Basin (Naz et al., 2014), demonstrated that using the estimated bed topography yielded 10% more glacier volume, and almost no difference in glacier area. The glaciers in the Bow River Basin were estimated to be up to over 300 m thick.

Steady state glacier thicknesses from this spinup method may not be representative of the current/historical transient state of the glaciers. If the glaciers in the couple simulation do not initially recede but do lose mass (and the actual glaciers were observed to recede) it is likely that the glaciers are actually in a thinner transient state. To thin the glaciers to a transient state from the steady state condition one can run the model with current climate forcings, thinning the glaciers without changing their area. The amount of years required to do this is an iterative procedure and is validated when rates of recession are well simulated.

## 11.0 Appendix C. MACA Downscaling Methodology

Researchers at the University of Idaho (UI) have made available a variety of downscaled gridded datasets for the western United States by employing the Multivariate Adaptive Constructed Analogs (MACA) method. The MACA statistical downscaling method utilizes the daily results from 20 different GCMs of the CMIP5 and users may select which downscaled GCM outputs they would like from the MACA webpage ([maca.northwestknowledge.net](http://maca.northwestknowledge.net)). The MACA method is unique in that it incorporates a training dataset (the Livneh 2013 gridded dataset used in model calibration) to match spatial patterns in GCM output and remove historical biases. Due to the scarcity of meteorological stations prior 1950, only the Livneh data for years 1950-2011 are used as a training set for downscaling. The MACA method is a six step process (from Abatzoglou and Brown, 2012):

1. Observational data and results from GCMs are interpolated to a common grid at 1 degree lat/long resolution
2. Using a 21-day, 31-year running mean, seasonal and annual trends are calculated at each grid point for both the observational data and GCMs and are removed
3. The cumulative distribution function (CDF) for a 15-day window for all years of data is calculated at each grid point for both the GCM and observational data. The CDF of the historical GCM and future GCM is mapped to the CDF of the observational data. Quantile differences between the historical and future GCM data are preserved.
4. By identifying days in the observational record that have similar spatial patterns to the target GCM day, a best fit approach is applied. The best 100 patterns are

selected based on the lowest root-mean-square error to the target pattern. A linear model is constructed based on coefficients for each spatial pattern. These same coefficients are then applied to the fine-scale (1/16 degree lat/long) observational data to create the downscaled GCM grid.

5. Adjustments removed from step two are reintroduced. This ensures consistency with GCM outputs.
6. A final bias correction to ensure compatibility with the observational dataset is performed.

The downscaled datasets are available publically from the UI MACA website and are downloadable in a network common data form (.nc file) or as text files which can be used in the DHSVM once disaggregated into 3-hr timesteps and converted into a binary form. Disaggregation was carried out with the VIC model (Liang et al., 1994). To maintain consistency with the calibrated model, all bias corrections and lapse rate changes that were applied to the historical Livneh meteorological grid were applied to the MACA downscaled GCM grids.

## **12.0 Appendix D. Collaboration and Deliverables to Funding Agencies**

This project was part of a larger scope of work that was overseen by the Nooksack Indian Tribe to assess the water resources of the Nooksack River. The scope of the project aimed to evaluate the effects of climate change on hydrology, glacier recession, and fish habitat as well as provide methods to help reduce potential impacts on the salmonid species present in the Nooksack River. The predicted impact of changes in late summer streamflows on fish habitat will be evaluated at key Assessment Sites located throughout the upper Nooksack River and various tributaries. My model outputs were generated at WRIA 1 Assessment Sites in the South, Middle and North Forks (as listed in *WRIA 1 Data Integration of Hydrology, Fish Habitat and Hydraulics models*, Bandaragoda et al., 2014) to update existing hydrology-fish habitat relationships based on hydrologic modeling done in the Lower Nooksack Water Budget (Bandaragoda et al., 2012).